

AFOSR - TR - 77 - 0156

ADA037492

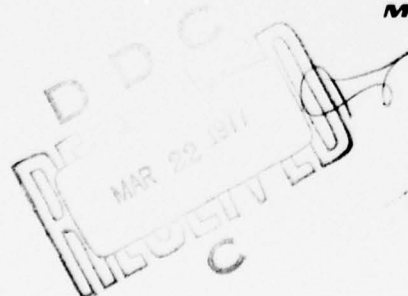
JANUARY 1977

(3)

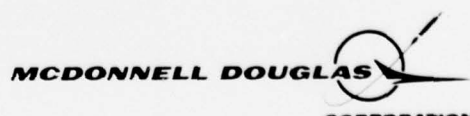
MAGNETOSPHERIC MAGNETIC FIELD MODELING

ANNUAL SCIENTIFIC REPORT FOR CONTRACT F44620-75-C-0033

DDC FILE COPY



MCDONNELL DOUGLAS ASTRONAUTICS COMPANY



Approved for public release;
distribution unlimited.

AIR FORCE OFFICE OF SCIENTIFIC RESEARCH (AFSC)
NOTICE OF TRANSMITTAL TO DDC

This technical report has been reviewed and is
approved for public release IAW AFN 190-12 (7b).
Distribution is unlimited.

A. D. BLOSE
Technical Information Officer

UNCLASSIFIED

SECURITY CLASSIFICATION OF THIS PAGE (When Data Entered)

REPORT DOCUMENTATION PAGE		READ INSTRUCTIONS BEFORE COMPLETING FORM
1. REPORT NUMBER <i>AFOSR-TR-77-8156</i>	2. GOVT ACCESSION NO.	3. RECIPIENT'S CATALOG NUMBER
4. TITLE (and Subtitle) MAGNETOSPHERIC MAGNETIC FIELD MODELING		5. TYPE OF REPORT & PERIOD COVERED Interim
6. PERFORMING ORG. REPORT NUMBER		7. CONTRACT OR GRANT NUMBER(s) F44620-75-C-0033 new
8. PERFORMING ORG. NAME AND ADDRESS McDonnell Douglas Astronautics Company 5301 Bolsa Avenue Huntington Beach, CA 92647		9. PROGRAM ELEMENT, PROJECT, TASK AREA & WORK UNIT NUMBERS 9751-05 61102F
10. CONTROLLING OFFICE NAME AND ADDRESS AFOSR/NP Bolling AFB, Bldg 410 Wash DC 20332		11. REPORT DATE Jan 77
12. MONITORING AGENCY NAME & ADDRESS(if different from Controlling Office)		13. NUMBER OF PAGES 97 103p.
		14. SECURITY CLASS. (of this report) UNCLASSIFIED
		15a. DECLASSIFICATION/DOWNGRADING SCHEDULE
16. DISTRIBUTION STATEMENT (of this Report) Approved for Public Release; Distribution Unlimited		
17. DISTRIBUTION STATEMENT (of the abstract entered in Block 20, if different from Report) <i>404 770</i>		
18. SUPPLEMENTARY NOTES		
19. KEY WORDS (Continue on reverse side if necessary and identify by block number) magnetosphere, magnetic field, charged particles, coordinate systems, electric field		
20. ABSTRACT (Continue on reverse side if necessary and identify by block number) A quantitative model of the magnetospheric magnetic field and associated procedures for accurately cataloging charged particle data out to and beyond geosynchronous orbit is developed. The magnetic field model incorporates all major magnetospheric current systems and is valid for all tilt angles; i.e., angles of incidence of the solar wind on the dipole axis. The model accurately represents the total magnetospheric magnetic field for conditions of low magnetic activity and to a geocentric distance of 15 earth radii or to the magnetopause. A new (B, I) coordinate system is developed to more accurately predict		

**MCDONNELL
DOUGLAS**

MAGNETOSPHERIC MAGNETIC FIELD MODELING

January 1977

Annual Scientific Report for Contract F44620-75-C-0033
Sponsored by the Air Force Office of Scientific Research

PRINCIPAL INVESTIGATOR: W. P. Olson

CO-INVESTIGATOR: K. A. Pfitzer

ACCESSION NO.		White Section <input checked="" type="checkbox"/>
NTIS	Balt. Section <input type="checkbox"/>	Black & White <input type="checkbox"/>
OFO	CLASSIFIED	
JUSTRIFICATION		
BY DISTRIBUTOR/AVAILABLE COPIES		
QTY	AVAIL. 500/M SPECIAL	
A		

MCDONNELL DOUGLAS ASTRONAUTICS COMPANY-WEST

5301 Bois Avenue, Huntington Beach, CA 92647

TABLE OF CONTENTS

	<u>Page</u>
1. INTRODUCTION	1
2. MAGNETIC FIELD MODEL	3
2.1 Model Assembly	4
2.1.1 The procedure	4
2.1.2 Tests in Construction	8
2.2 Model Features and Uses	14
2.2.1 Magnetic Field Representations	14
2.2.2 The Ordering of Charged Particle Data	24
2.3 Associated Induced Electric Field, E_I	28
3. THE B , \bar{L} COORDINATE SYSTEMS FOR PARTICLE DATA ORGANIZATION	38
3.1 Generalization to the Distorted Field	41
3.2 Tilt Effect in B , \bar{L}	45
4. SUMMARY AND CONCLUSIONS	47
5. APPENDIX A - COMPUTER CODES	50
5.1 Subroutine Description	50
5.2 Sample Output Description	53
5.3 Program Listing	55
5.4 Sample Program Output	79
6. APPENDIX B - COORDINATE TRANSFORMATIONS AND RELATED ANALYTIC DERIVATIONS	87
6.1 Coordinate Transformation	87
6.2 Time Derivation of the Tilt Angle	95
7. REFERENCES	97

• Section 1

INTRODUCTION

There are many reasons for DoD interest in the development of accurate quantitative representations of various environmental parameters. This is because the near earth space environment influences many military hardware systems. In many cases, these influences can be designed around but in others they cannot. In such cases, system performance can vary with the behavior of this environment.

In this report we review work performed at McDonnell Douglas Astronautics Company during the past year. The purpose of this work was to develop a quantitative model of the magnetospheric magnetic field, and associated procedures for accurately cataloging charged particle data out to and beyond geosynchronous orbit. The main reason for the development of this model and procedure was to provide a capability for mapping charged particle fluxes produced by natural and manmade sources of ionization. In particular, it had been found that attempts to accurately map charged particle fluxes from points above the earth's surface to geosynchronous orbit were not very accurate. One of the main sources of error was felt to be inaccuracies in the magnetic field model. Thus, one of the tests of the modelling exercises completed here will be comparisons made by DoD between model calculations and observed particle fluxes.

It is intended that this model and procedure will be used also for other purposes. The predecessor magnetic field model (Olson and Pfitzer, 1974) has been distributed to several dozen groups throughout the world and has been used for a variety of reasons that range from very practical (the location of the foot of the field line to various synchronous orbiting satellites) to other more basic studies that hopefully will shed light on the basic structure of the magnetosphere and its

physical processes. It has been the intent of the MDAC group to produce a set of quantitative environmental models that can be used together to accurately specify and/or predict several environmental parameters. In this role the magnetic field model described here will be used as an input in conjunction with other quantitative models of neutral upper atmospheric density and ionospheric electron density. This interaction between models will improve the density models since the corpuscular energy sources which influence both ionospheric and upper atmospheric parameters at high latitudes are constrained to move along magnetic field lines. A magnetic field model capable of describing variations in charged particle parameters associated with "tilt angle" changes and minor variations in magnetic activity should be helpful in locating such gross environmental features as the poleward edge of the mid latitude trough.

The reader of this annual report is cautioned that the results presented here are not to be considered the final description of the magnetic field model and the new B, \bar{L} coordinate system. Rather, it is intended that the magnetic field model together with its tests and suggested uses and the B, \bar{L} coordinate system will both be described in papers submitted to the Journal of Geophysical Research or a similar journal. Also, documentation on the computer programs generated during this contract will be described after further interaction with DoD personnel in a separate manual.

Section 2

THE MAGNETIC FIELD MODEL

In our previous magnetic field model (Olson and Pfitzer, 1974) all major magnetospheric current systems acting as sources to the total magnetospheric magnetic field were considered together for the first time. These current systems include the magnetopause current system, formed by the interaction of the solar wind particles with the total magnetospheric magnetic field, the tail current system produced by particles flowing across the tail of the earth's magnetosphere and returning on its boundary, and the quiet time ring current system produced by the motion of charged particles moving within the magnetosphere. The magnetopause current is formed by particles which interact with the earth's magnetic field and then return immediately to the magnetosheath. These particles interact with the current system only for fractions of seconds as they are deflected by the magnetospheric magnetic field. The particles flowing across the tail of the magnetosphere which form the tail currents remain part of that current system for as long as several days as they make their journey across the tail. The quiet time ring current system, however, is formed by particles trapped along magnetic field lines in the inner magnetosphere. These particles may contribute to the currents for as long as weeks or even months. Although the magnetopause currents flow only on a surface (on the magnetopause itself) both the tail current system and the ring current particles are distributed over a large region of space in the magnetosphere. This had previously posed a severe limitation on magnetic field models since typically scalar potentials were used to represent the magnetic field. A scalar potential representation cannot be used in the region of the source currents for the field. Thus, in the Olson and Pfitzer model (1974) the equivalent of a vector potential was used for the field representation. This allowed for the

first time the accurate representation of the currents flowing in a distributed fashion throughout much of the magnetosphere. That model, however, is limited to the case of perpendicular incidence of the solar wind upon the earth dipole axis. In order to extend the time of validity of the magnetic field model it is required that it be valid for all angles of incidence of the solar wind on the dipole axis ("tilt angles") and for all values of magnetic activity. In the current modelling exercise the first of these constraints has been removed. The model described below was developed such that it represents all major magnetospheric current systems and is valid for all tilt angles. It is believed that this model is capable of accurately representing the total magnetospheric magnetic field about 30-40 percent of the time - when magnetic activity is low.

2.1 Model Assembly

2.1.1 The Procedure

As with the 1974 model, a quantitative representation of the various important magnetospheric current systems was first developed. The ring and tail currents are initially represented in the form of wire loops. In Figures 1 and 2 projections of the wire loop onto the xz plane (in solar magnetospheric coordinates) are shown for tilt angles of 0 and 35 degrees. It is seen that in the inner magnetosphere there is a nest of three sets of wire loops used to represent the ring current. The tail currents flow almost linearly across the upper and lower boundaries of the plasmashell in the distant tail while close to the earth they curve around such that they are in close proximity to the ring current loops. The return path of the tail currents was constructed to flow approximately on the boundary of the magnetopause with the shape similar to that used in the determination of the magnetopause currents. A three-dimensional view of these current systems is shown in Figure 3.

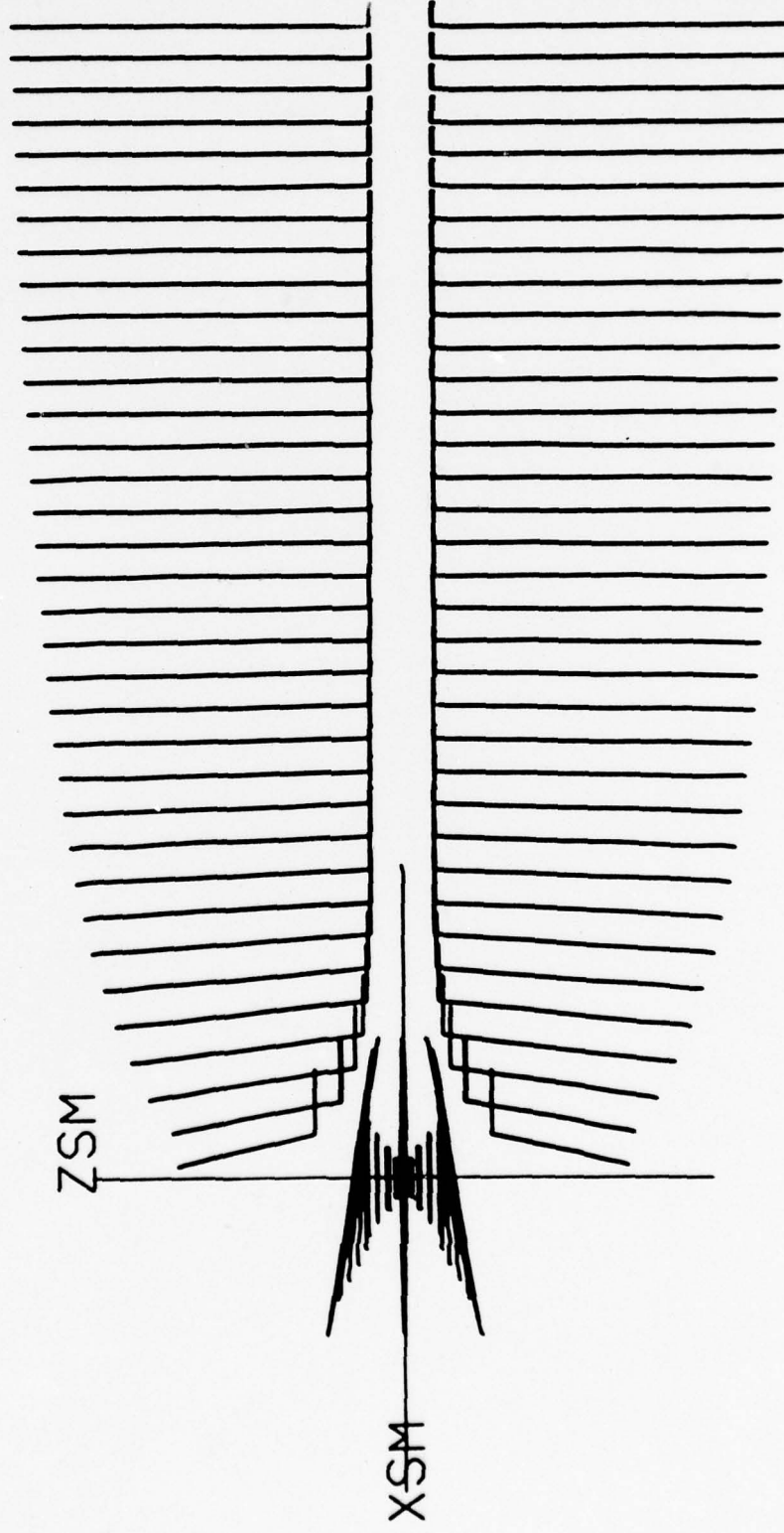


Figure 1. Projection of the current loops into the xz solar magnetospheric plane for tilt = 0° .

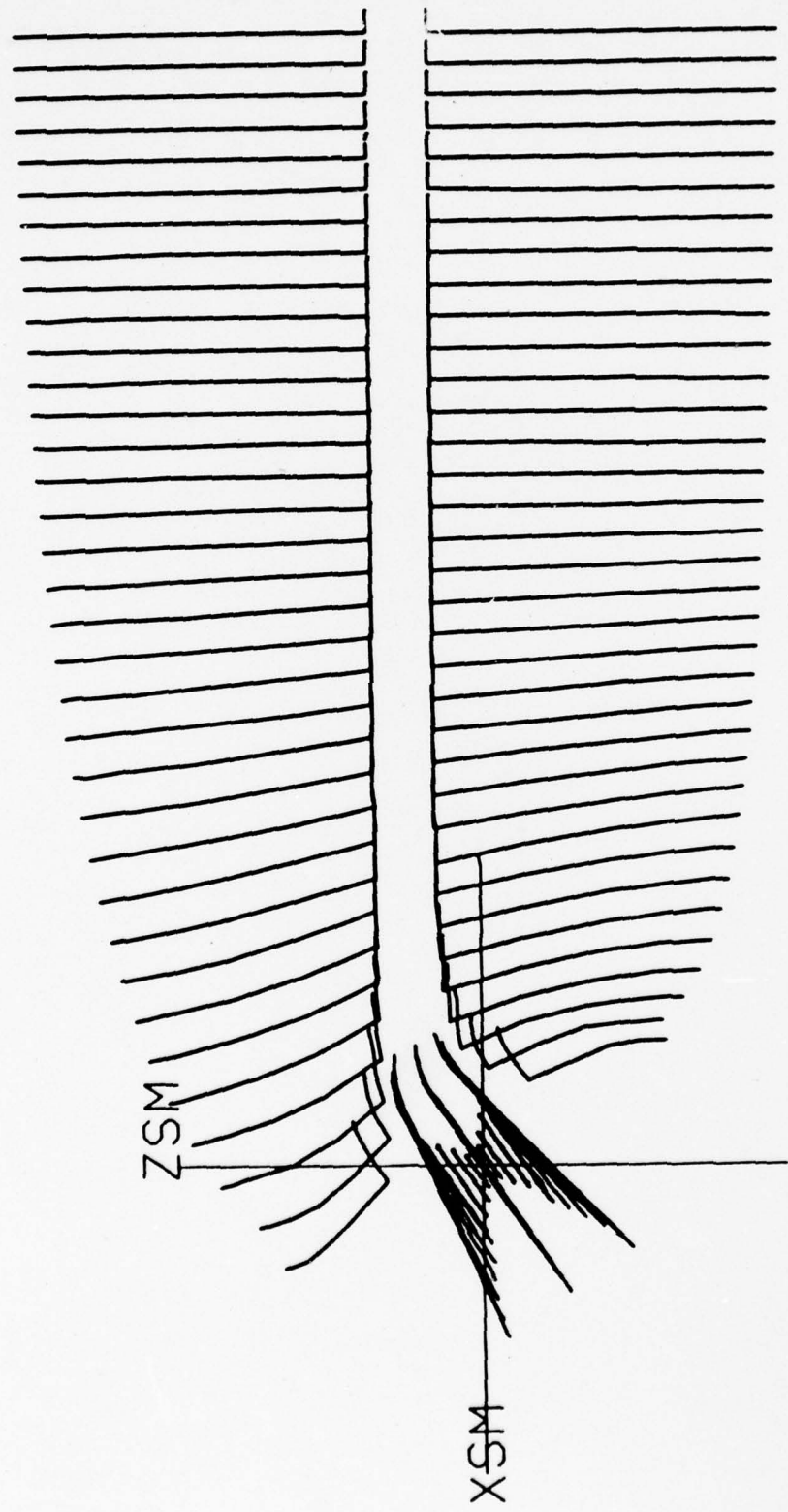


Figure 2. Projection of the current loops into the xz solar magnetospheric plane for tilt = 35° .

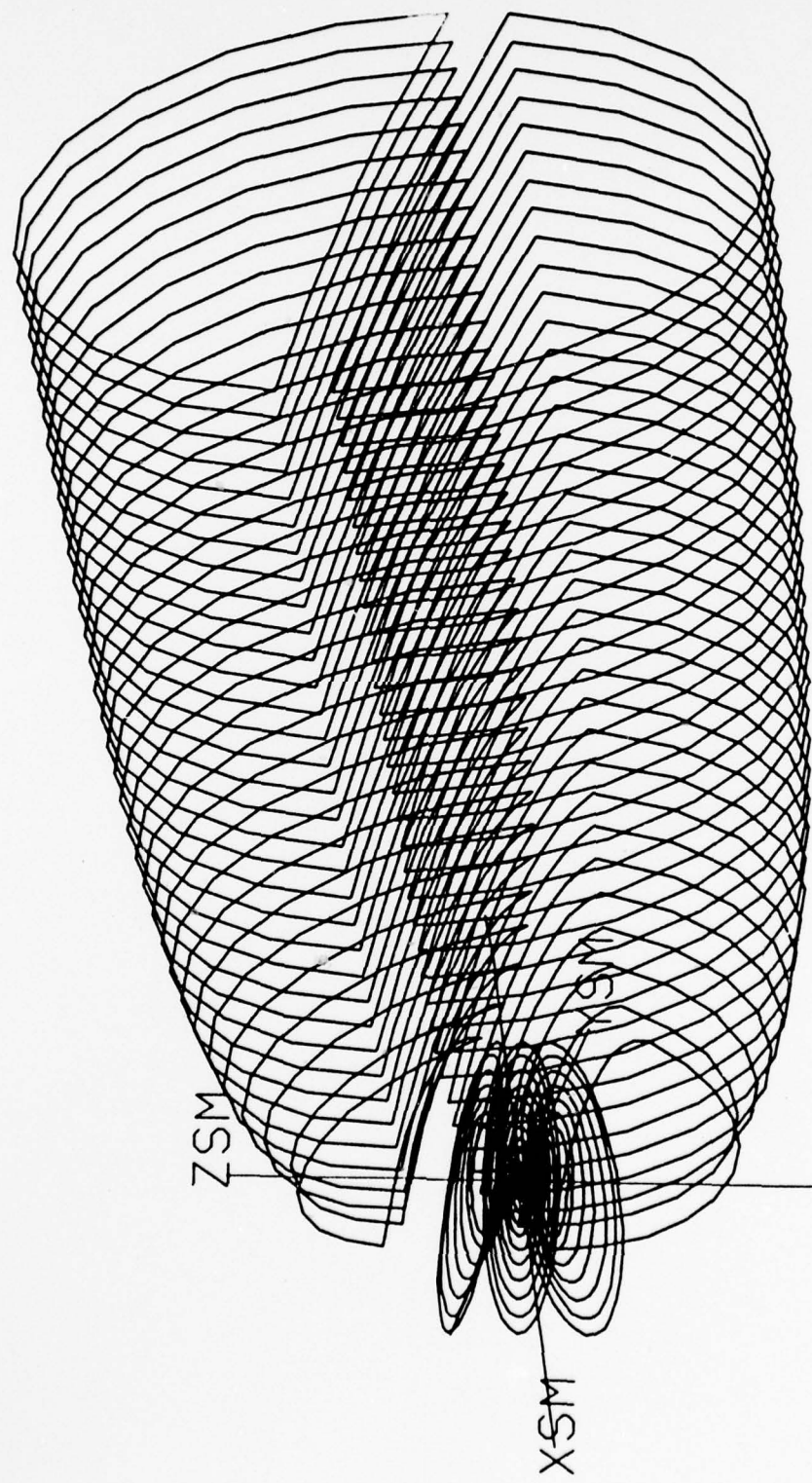


Figure 3. Three-dimensional view of the current system for tilt = 0° .

The currents flowing on the magnetopause and the associated magnetic field were determined using procedures similar to those developed by Olson (1969). This procedure permits the currents to be determined from a known magnetopause shape. Instead of using a self-consistent shape determined by the pressure balance condition, a more realistic shape based on observational data was used. The magnetopause was therefore represented as being more flared in the dawn dusk and tail regions and as having a flatter subsolar area. The magnetic fields from these current systems were then obtained using the Biot-Savart Law. Various primary tests were used once the magnetic fields were obtained to compare the results with observations of the magnetospheric magnetic field. Differences were determined and used to calculate changes in the locations and strengths of the various magnetospheric current systems. It is noted that the initial estimations of the placement of the wire loops was almost sufficient and little adjustment was necessary.

2.1.2 Tests in Construction

The purpose of this model was to provide an accurate representation of the total magnetospheric magnetic field out to and beyond geosynchronous orbit. For this reason we have determined the magnetic field only out to a geocentric distance of 15 earth radii. The model should not be used beyond that region as it was not constructed with tests valid outside of that region.

One of the most important tests of any magnetospheric magnetic field model is the comparison of model results with the observed magnetic field along the earth sunline. In Figure 4 the quantity ΔB is shown along the earth sunline. ΔB is the difference between the total observed field and the geomagnetic dipole field. It is that contribution to the total field produced by the magnetospheric

ΔB ALONG THE SUN-EARTH LINE

25744

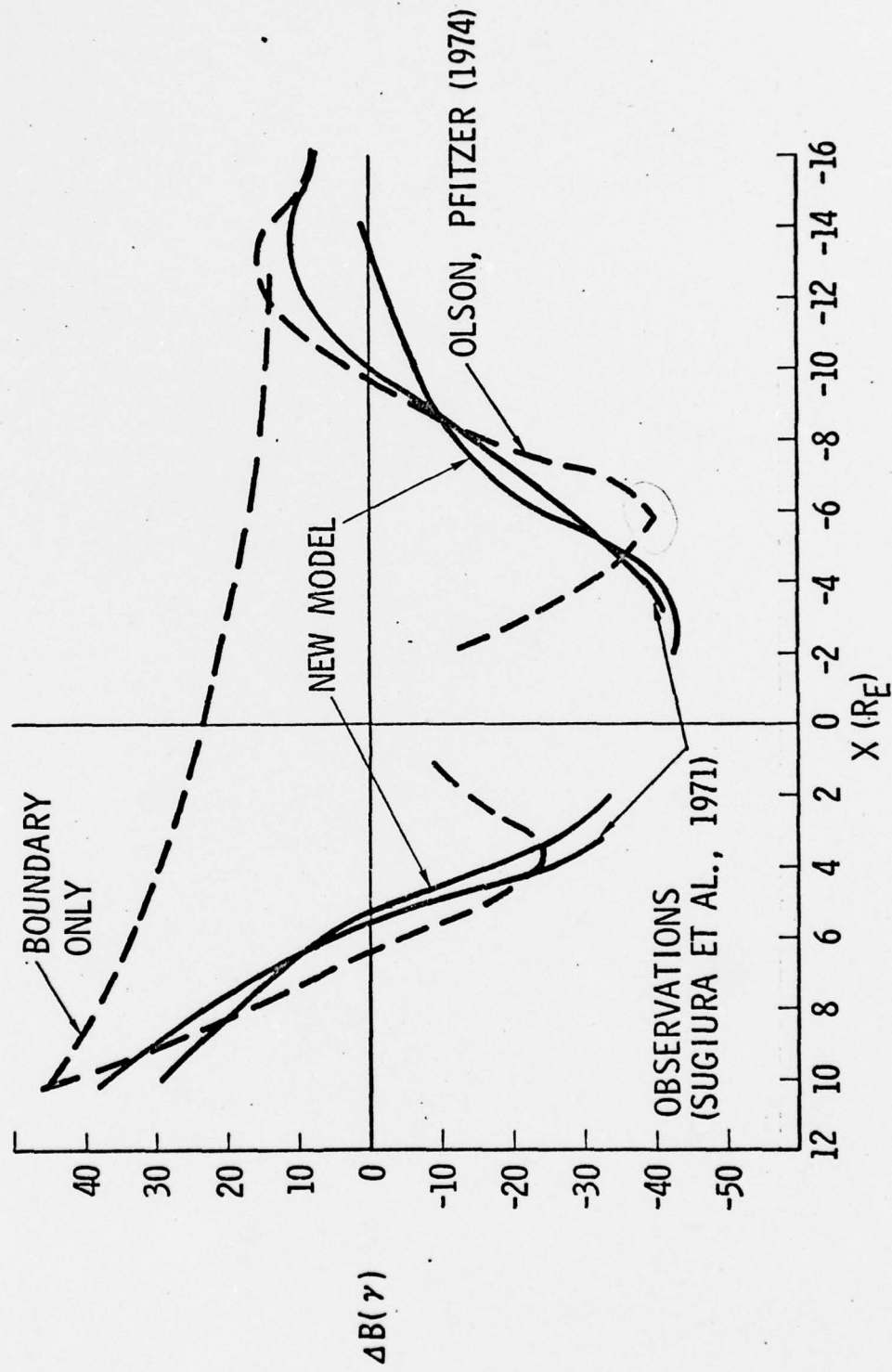


Figure 4

currents. It is seen that the observed field is quite structured in the inner magnetosphere. Older magnetospheric models containing only the magnetopause field are seen to not be capable of describing this structure. Indeed it is the field from the quiet time ring current that produces most of this structure. It is seen that the new model does an excellent job of representing the observed ΔB variations along the earth-sun line.

Note that the one discrepancy between these observations and our new model is in the tail region with $X_{SM} \approx 12$ earth radii (SM subscripts refer to solar magnetic coordinates). If contours of constant ΔB are plotted in the noon midnight peridian plane (the solar magnetic or solar magnetospheric xz plane) this apparent discrepancy can be accounted for. The model results are shown for a tilt angle of 0° in Figure 5. These results can be compared with the observed ΔB contours reported by Sugiura and his colleagues (1971) and reproduced in Figure 6. It is noted that there is excellent agreement in the placement of the $\Delta B = 0$ contours. In order to explain the apparent discrepancy mentioned in Figure 4 it must be pointed out that the $\Delta B = 0$ contour closes in the tail along the X axis at approximately -14 earth radii. In Figure 7 the $\Delta B = 0$ contour for the tilt angle of 35° is seen to cross the X axis at approximately -9 earth radii. This suggests that in data sets which contain data averaged over all tilt angles the $\Delta B = 0$ contour should lie somewhere near $X = -10$ earth radii as is seen to be the case in the observations reported by Sugiura, et al., 1971 shown in Figure 4.

Attempting to fit the ΔB contours reported by Sugiura, et al., led to an abnormally large field in the near earth portion of the tail in the Olson-Pfizer 1974 model. This problem has been brought to light in the present analysis and has been corrected in the present model, which for the 0° tilt case and all

ΔB IN THE NOON MID-NIGHT
MERIDIAN PLANE (TILT=0°)

25747

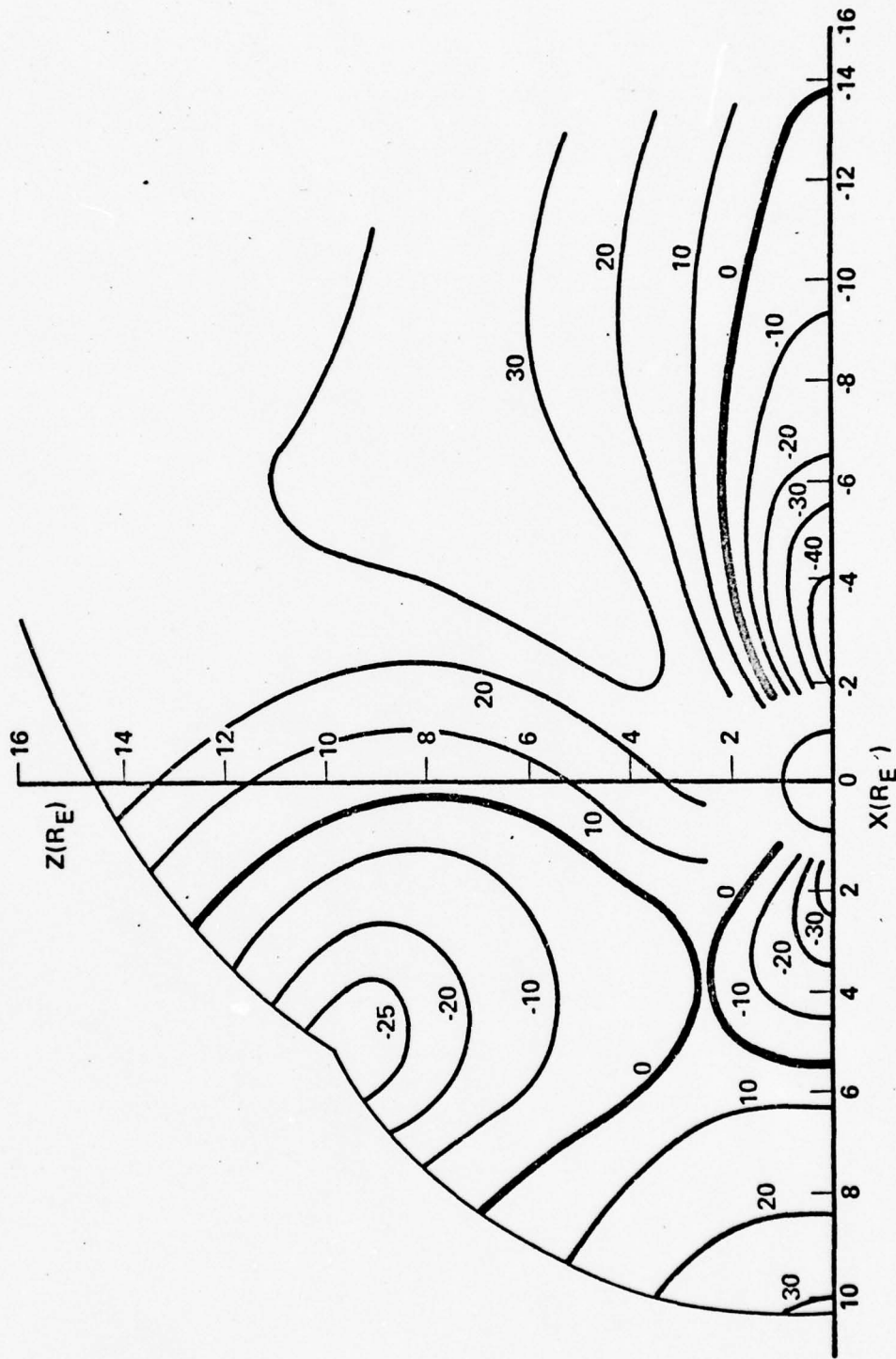


Figure 5

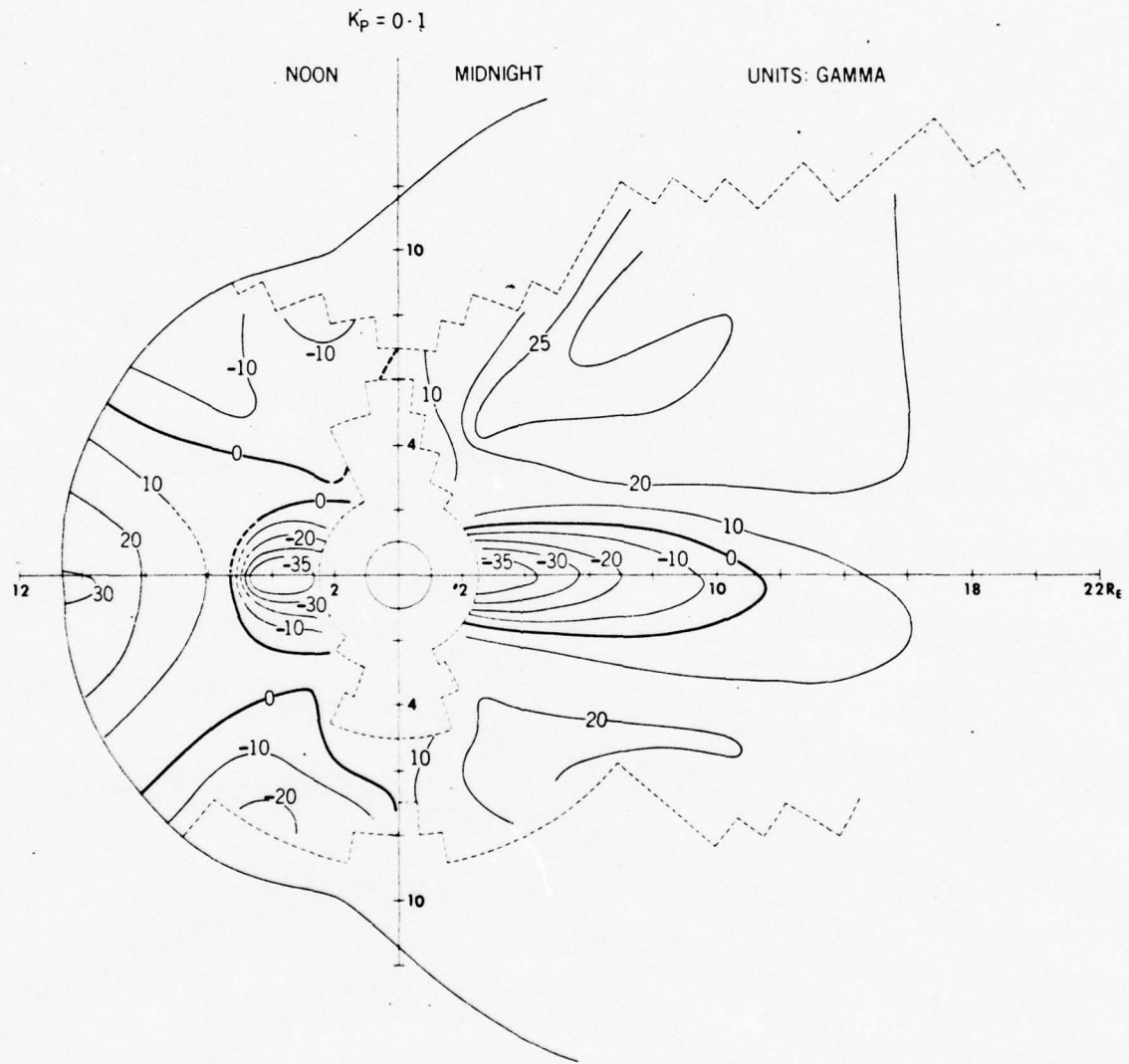


Figure 6. Experimentally determine values of ΔB in the noon midnight meridian plane ($\text{tilt} = 0$). (From Sugiura et al., 1971)

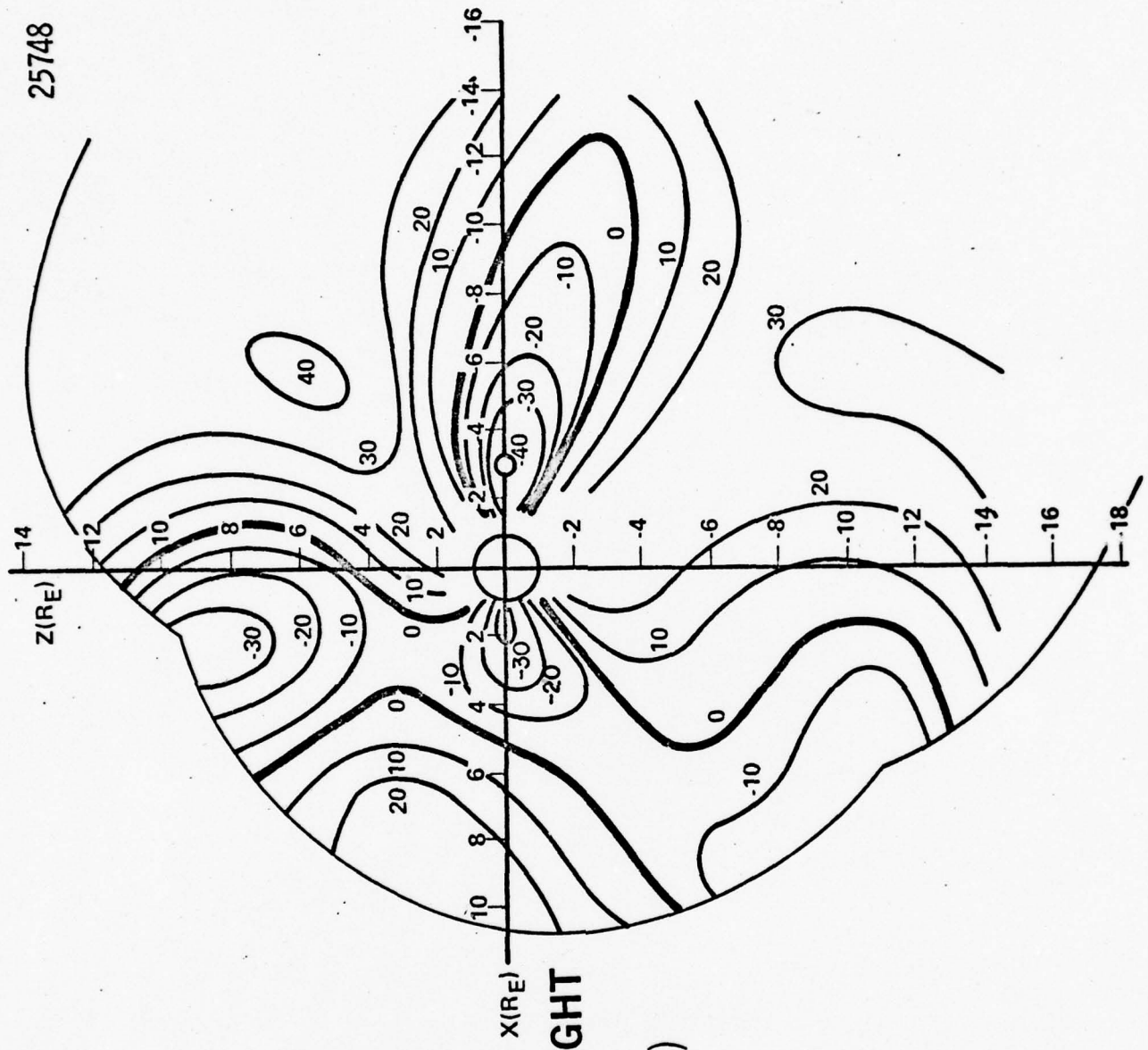


Figure 7

others better represents the average magnetospheric field configuration. Evidence of the abnormally large field in the model was pointed out by R. J. Walker in his review of magnetospheric field models (1976). This is most readily observed when the magnitude of the total magnetic field is plotted in the equatorial plane. Contours of constant total magnetic fields are shown in Figure 8. They are seen to vary smoothly in the tail region along the earth-sun line. Also, there is no buildup in field intensity near the subsolar region. These tests suggest that the 0° tilt version of the present model is now very close to the observed magnetospheric magnetic field in all ways capable of being tested with existing observational data sets.

2.2 Model Features and Uses

Having passed the preliminary tests discussed above, the model was used in two general ways to further test it and provide information on various magnetospheric magnetic field and particle population features.

2.2.1 Magnetic Field Representations

Field lines in the noon midnight meridian plane are shown in 2 degree intervals in Figures 9 and 10 for 0° and -35° tilt. Since some of the field lines on the nose of the magnetosphere penetrate beyond the magnetopause, there is some difficulty in assigning a value for the last closed field line. If the definition is the last line to return to the other hemisphere within the magnetopause, then the last closed field line has a latitude value of about 78° while for a tilt angle of -35° the latitude of the last closed field line is lowered to approximately 76° .

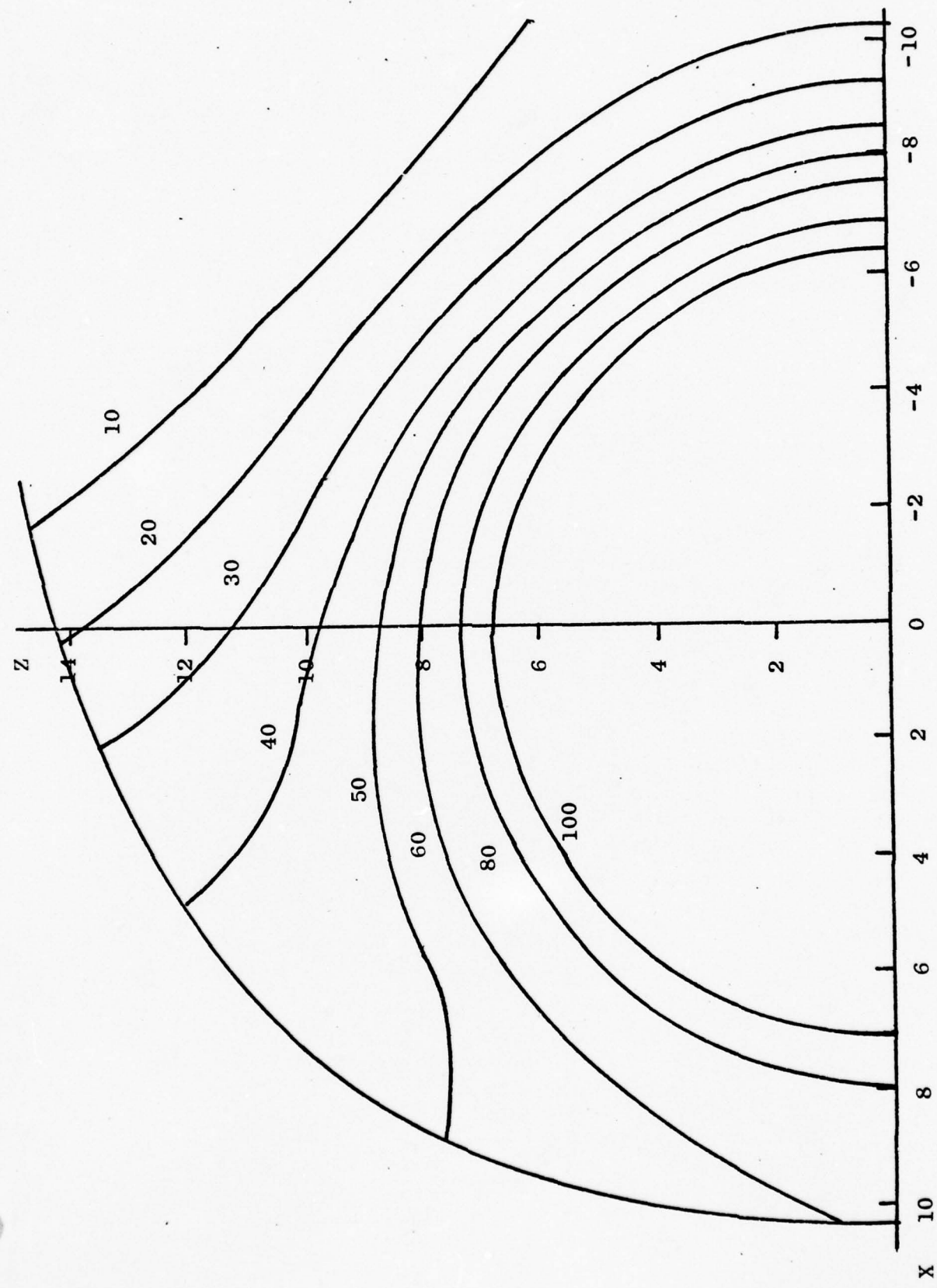


Figure 8. Contours of constant $|B|$ in the equatorial plane.

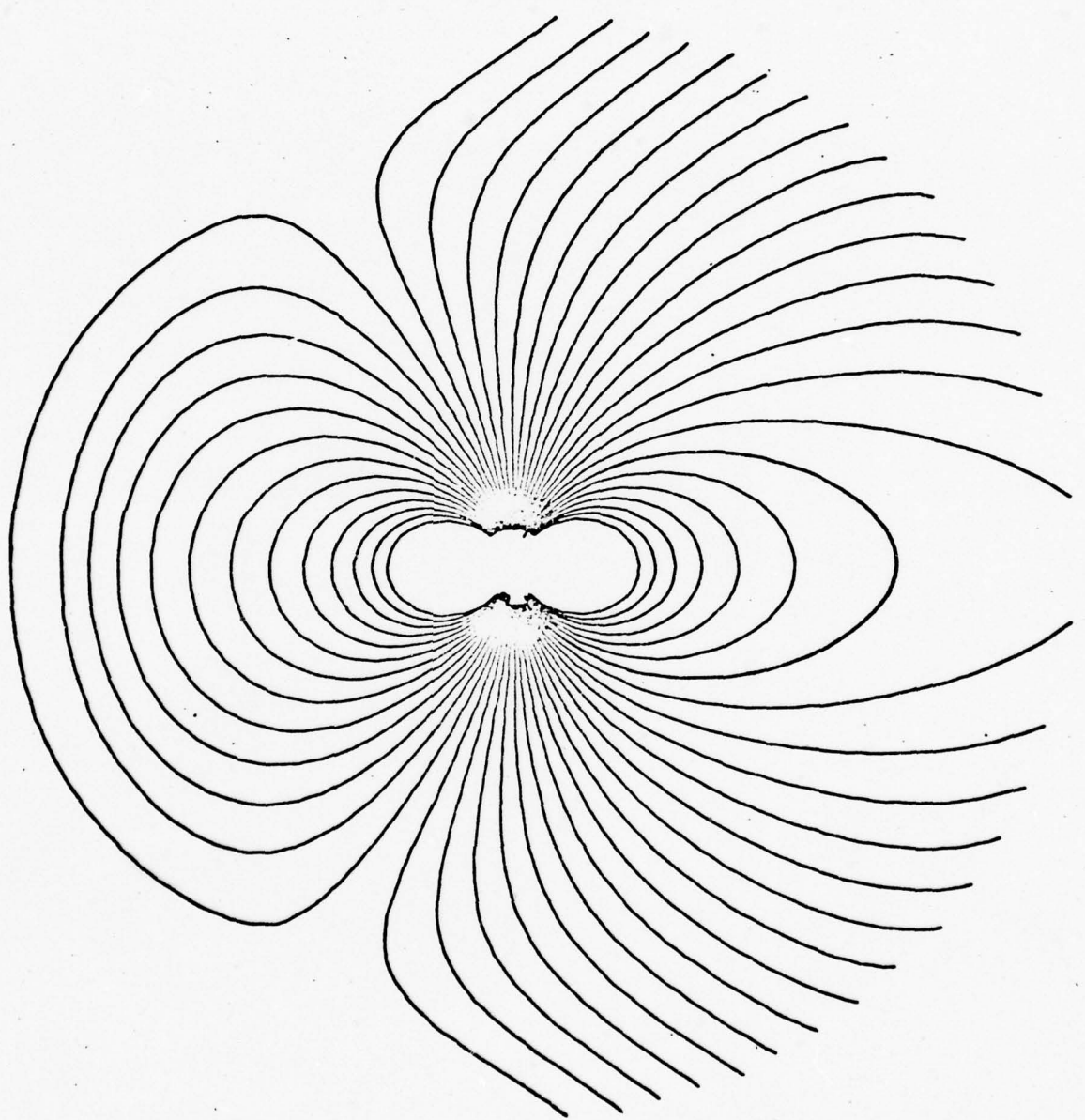


Figure 9. Field lines in the noon midnight meridian plane for tilt = 0° .

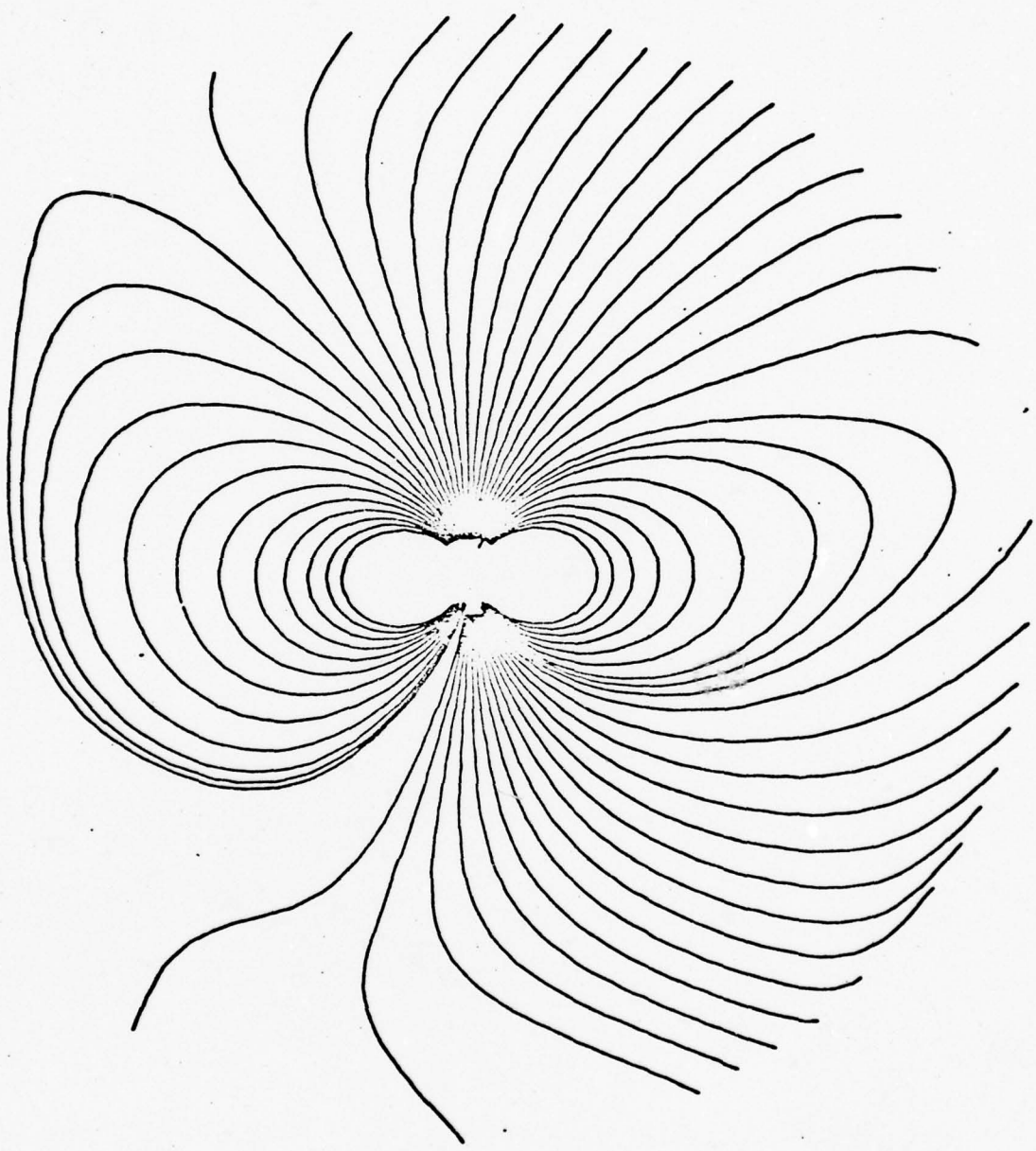


Figure 10. Field lines in the noon midnight meridian plane for tilt = 35° .

The extent of the field lines into the tail of the magnetosphere is also more pronounced than in all previous models. This is most clearly illustrated in Figure 11, taken from Walker's review paper (1976). Two curves have been added to his figure; that of the new model and the equatorial crossing of a pure dipole field. The figure gives the magnetic latitude as a function of the equatorial intercept of the corresponding magnetic field line. Thus, for example, the equatorial crossing of the field line from the magnetic latitude of about 75° at midnight is approximately $15 R_E$ for a dipole field while for our new model the field line originating at the earth's surface at approximately 70° magnetic latitude crosses at 15 earth radii in the tail. This feature, the extension of field lines far into the tail even during quiet magnetic conditions, is well documented observationally.

Another test of any magnetospheric magnetic field model is provided by several of the barium cloud releases that have been made in the magnetosphere. In Figure 12 one of those releases is shown and the magnetic field line illuminated by the barium is compared with field lines calculated from several models with the field location and initial direction given at one end of that portion of the line suggested by the location of the barium cloud. It is seen that the calculations using our new model perform significantly better than the older models and along the length of the optical track are well within the error bars for the position of field line.

One of the long awaited uses of accurate magnetospheric magnetic field models that include tilt angle effects is the variation in conjugate point locations that must occur even during quiet magnetic conditions. If the location of one foot of the magnetic field line is held constant over a 24-hour period the question of the location of the opposite end of that field line arises. In

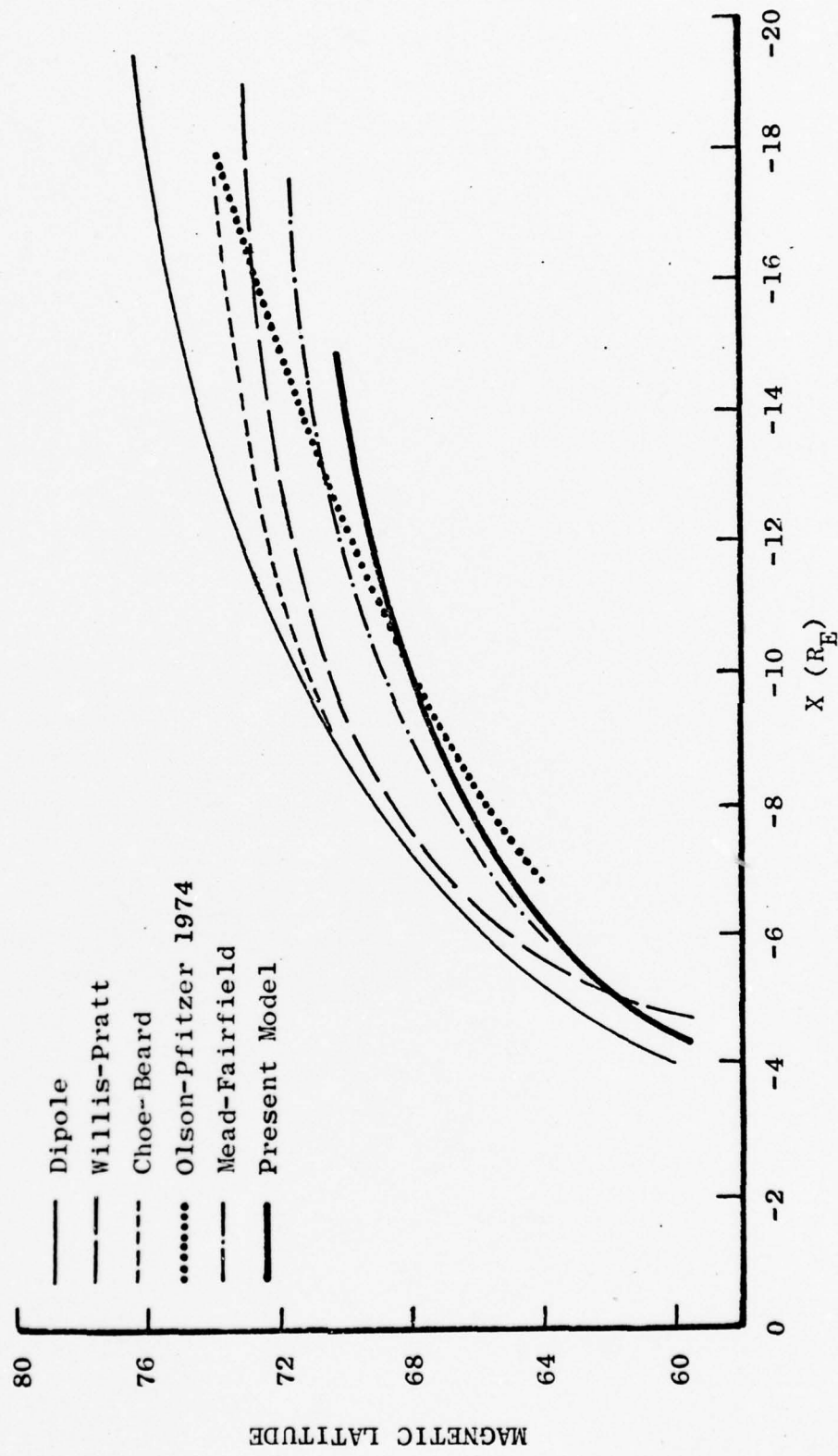


Figure 11. Magnetic latitude versus the equatorial intercept of the corresponding field line (tilt = 0°).

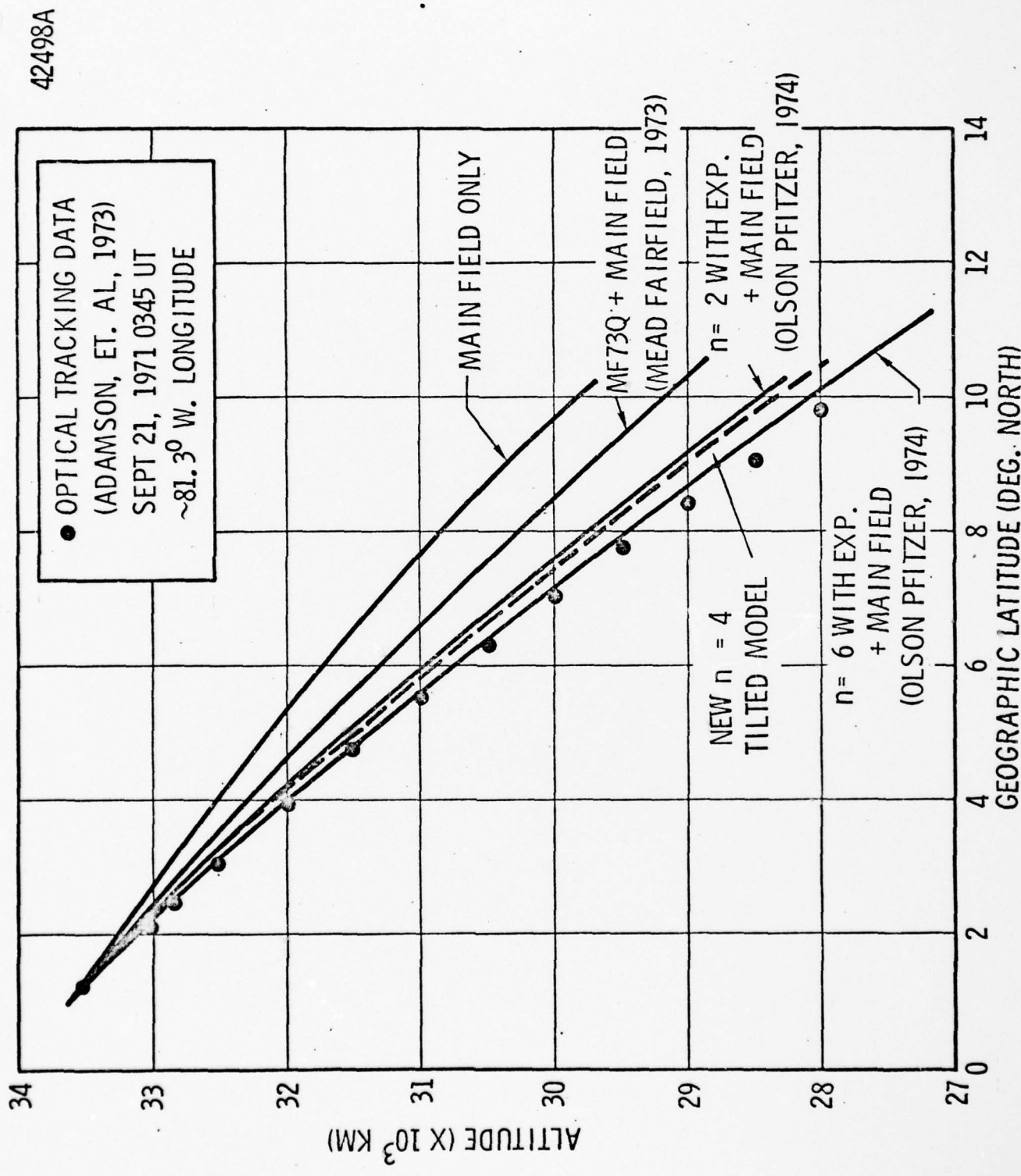


Figure 12. Comparison of model calculated field lines with barium cloud observations.

Figure 13 the variation in the conjugate point location of a particular field line is shown for winter and summer solstices and for spring equinox. It is seen that at summer solstice and near spring equinox, the conjugate point variation in the point is quite small. However, near winter solstice the variation becomes significantly larger. This is because near winter solstice this particular point is near the last closed field line location and considerable daily variations occur as is expected. Typically it appears that the conjugate point variations for field lines at auroral latitudes should be on the order of several tens of kilometers over a daily period.. However, sometimes, for field lines moving near the last closed field line location, the variations can be significantly larger. These are results predicted by the model. One additional check of this and other magnetospheric magnetic field models might be provided by the search for large conjugate variation during quiet magnetic conditions.

Another important use of accurate magnetospheric magnetic field models is the calculation of the intercept at the earth's surface of field lines extending through geosynchronous orbit. Such computations are necessary in order to coordinate particle and field work done simultaneously with ground based and synchronous satellite platform sensors. In Figure 14 the location of the foot of the field line through synchronous orbit is shown for a dipole only field and for three different tilt angle values as a function of local time. (Although the actual field line geometry does not vary in this manner, such a representation sheds light on the magnitude of the daily variations in field line intercepts with the earth's surface possible for various synchronous satellite locations.) First it is noted that the foot of the field line can be as much as 2° lower than that of a dipole only field. Early models that contained only the contribution from the magnetopause currents placed the foot of the magnetic field line

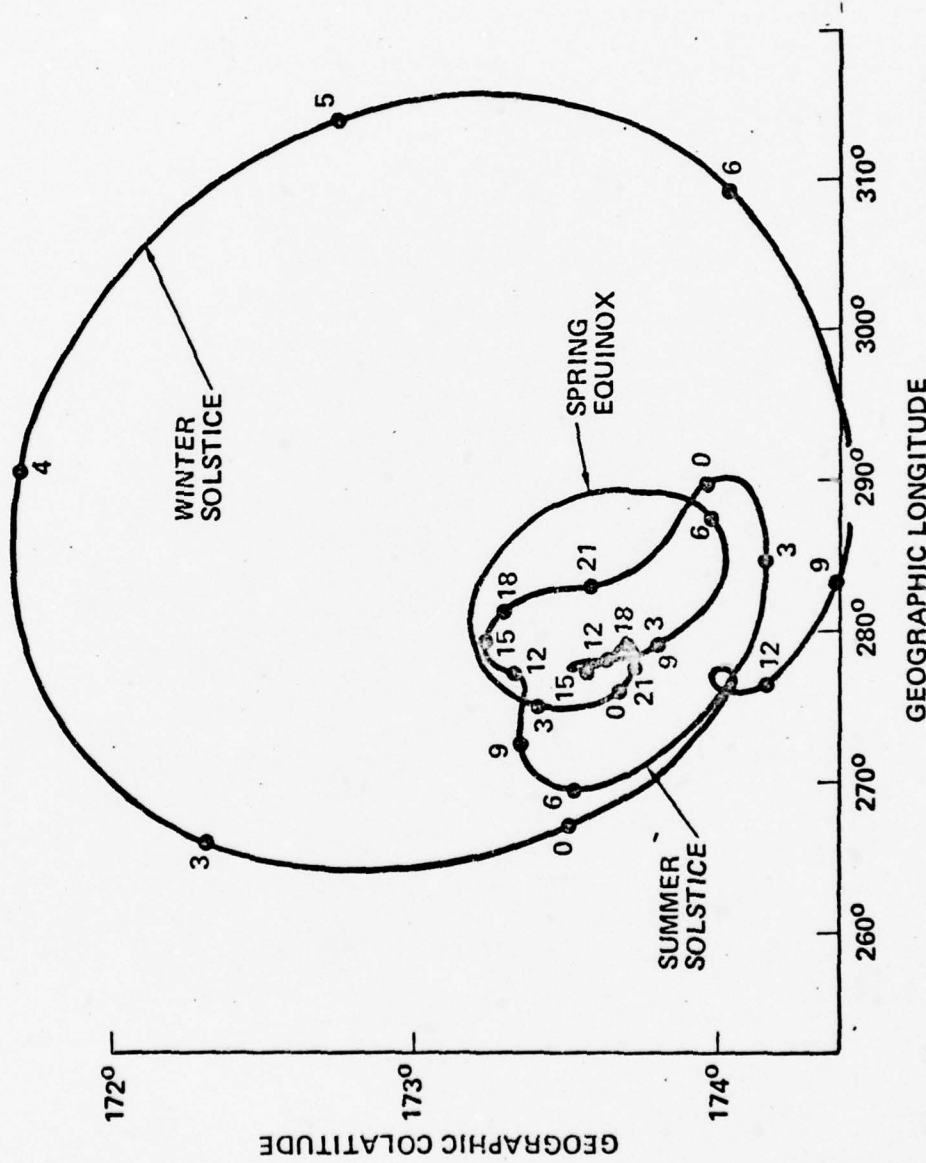


Figure 13

EARTH SURFACE FIELD LINE INTERCEPTS
FROM SYNCHRONOUS ORBIT

25745

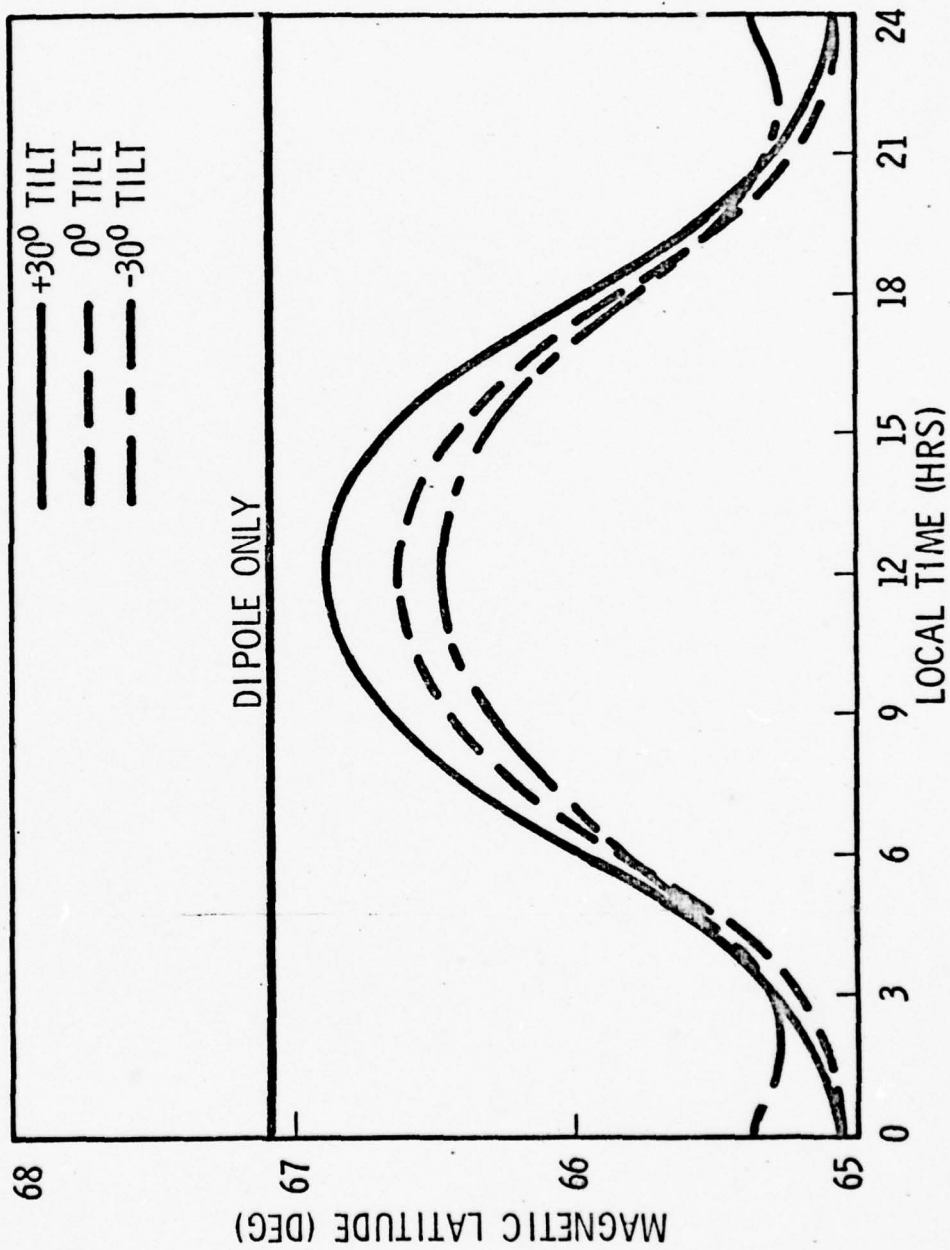


Figure 14

at a latitude higher than that of the dipole. The field line intercept from some actual synchronous orbit locations are shown in Figure 15. It is seen that the largest variation is near summer solstice at both geosynchronous longitudes. It is also noted that the daily variation can be as large as about 150 kilometers in latitude and a similar extent in longitude.

One final test of this tilted magnetospheric magnetic field is to compare model calculations of the daily variations in the components of the magnetic field at the location of the geosynchronous satellite ATS-1 with the daily magnetic variations observed at the location of the satellite. Such a comparison is shown in Figure 16 for the months of January and June where the values of the field at each hour were averaged for the 5 most quiet days during the month. It is seen that the variations agree quite well in both form and magnitude. Previous models do not come close to repeating the pattern of the observed variations.

2.2.2 The Ordering of Charged Particle Data

In addition to using the model directly to compute various magnetospheric magnetic field features of interest, it can be used together with the proper formalisms to study and organize both low energy and energetic charged particle data. The main purpose in the development of the magnetic field model was to use it together with adiabatic invariant theory to provide a more accurate means for organizing low energy charged particle data. This has resulted in the development of a new "coordinate" system, the B, \bar{L} coordinate system, it is described in detail in Section 3. This model and the previous Olson-Pfizer (1974) model have both been used very successfully to predict and interpret solar cosmic ray data. The 1974 model was the first magnetospheric magnetic field model capable of predicting

EARTH SURFACE FIELD LINE INTERCEPTS
FROM SYNCHRONOUS ORBIT

25746

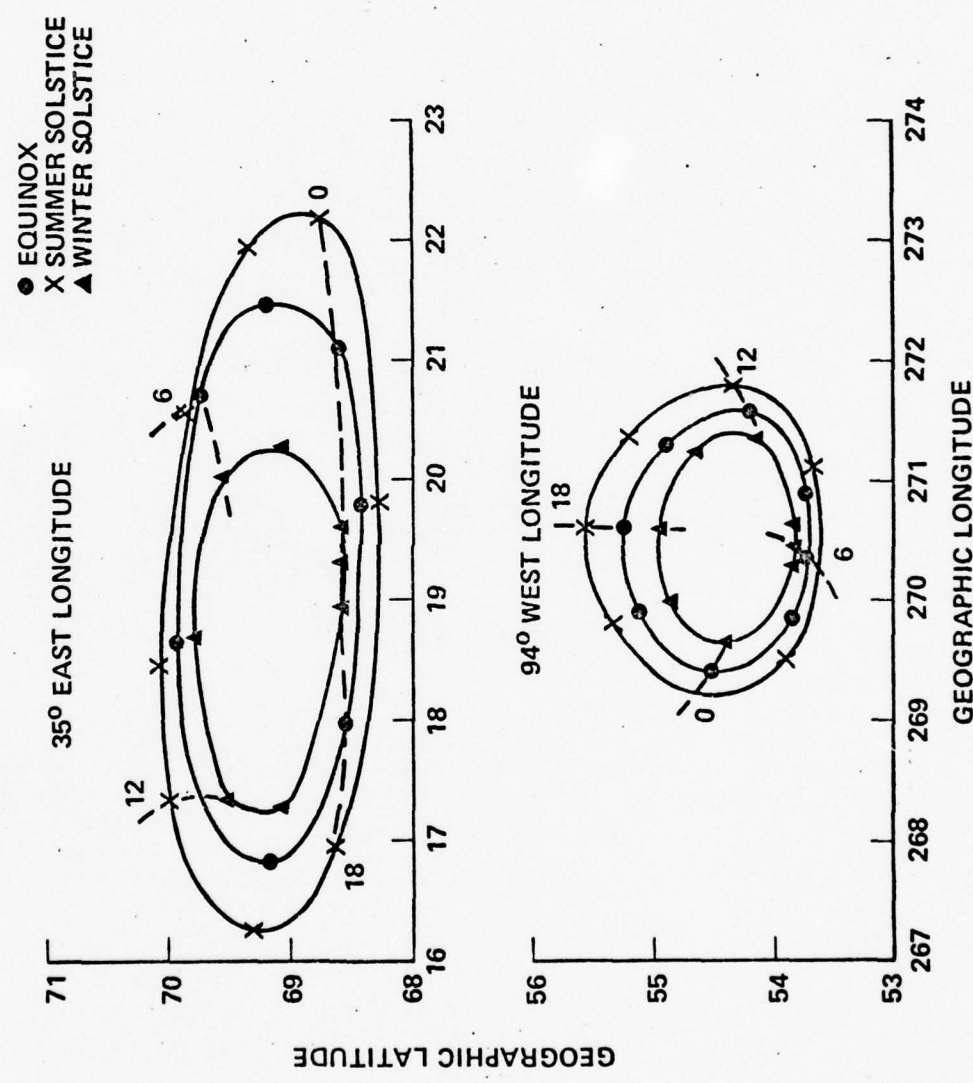


Figure 15

QUIET DAILY MAGNETIC VARIATIONS AT ATS-1

25741

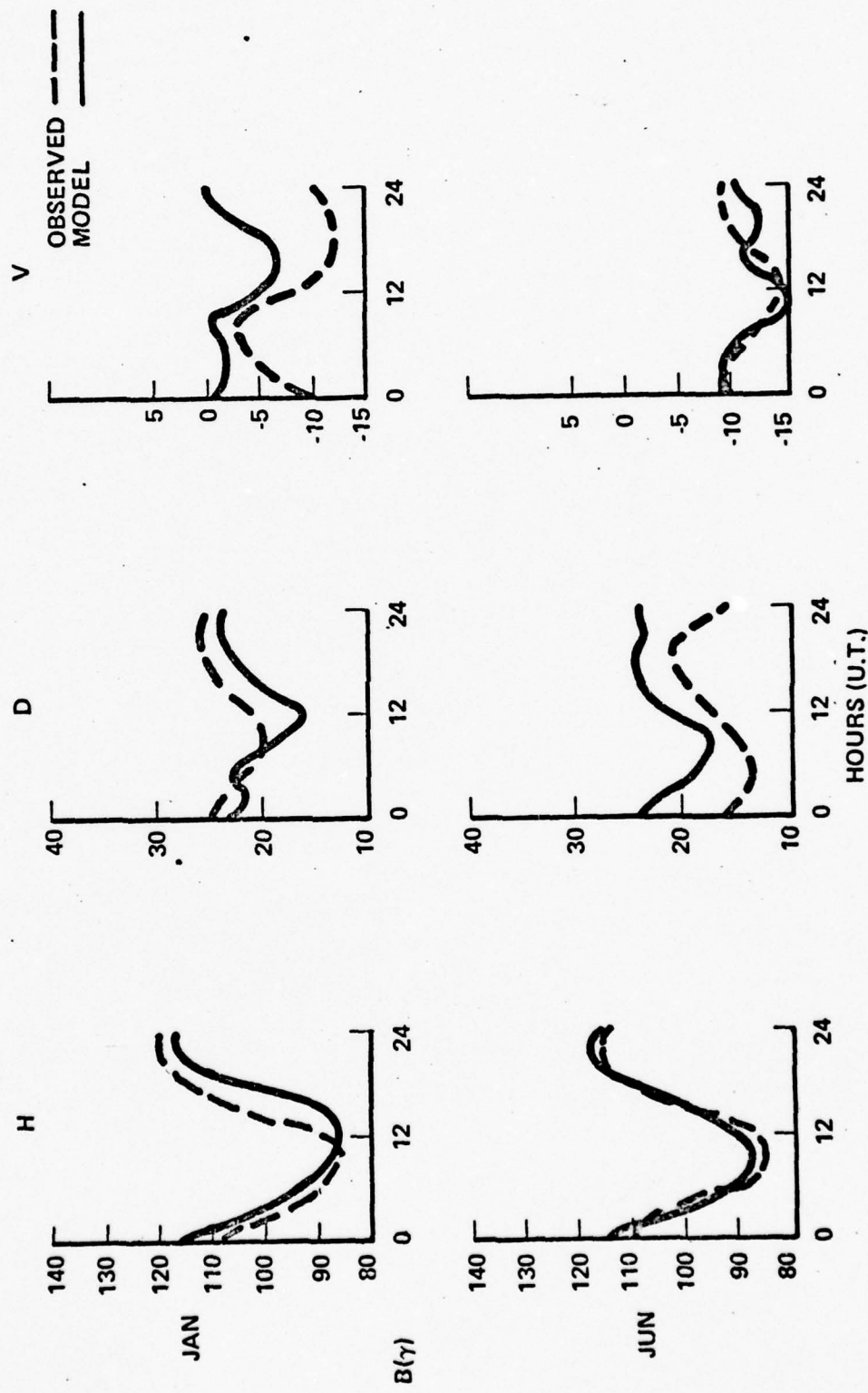


Figure 16

magnetic cutoff latitudes for the penetration of solar cosmic rays close to those observed. Prior to the introduction of this model many theories had been proposed to explain the discrepancy between the observations and older model predictions. In the present model some of the remaining discrepancies have been resolved.

One of the major successes of the Olson-Pfizer (1974) zero tilt model was the lowering of the cosmic ray cutoffs by over 4 degrees which brought experimental observations and theory into close agreement. The zero tilt model brought the noon and midnight cosmic ray cutoffs into complete agreement. However, a problem remained at dawn and dusk where the cutoffs predicted by the model were 3° - 4° too high. It was hypothesized that this discrepancy was the result of an excessively large field near the dawn dusk flanks of the magnetosphere.

The present model brings the magnetic field values near the magnetosphere boundaries into better agreement with observations, and is successful in lowering these cutoffs. Table 1 summarizes the cutoff calculations. The table shows that the observed and so calculated cosmic ray cutoffs are now in substantial agreement at all local times. Figure 17 shows a sample cosmic ray trajectory for a 5 MeV proton. The proton enters the daylit dawn side of the magnetosphere and enters the polar cap at a latitude of 68° . A survey of cosmic ray access using this model has shown that all particles which enter the polar cap within 3° - 4° of the cutoff enter the magnetosphere through the daylit dawn side. The particles which enter the center, or high latitude polar cap, either penetrate directly through the weak field region of the dayside cusps or arrive via the lobes of the tail field.

The data in Table 1 indicate a very small tilt dependence for the cutoff latitudes. The tilt dependence is less than a degree at dawn and dusk, a degree or two at

midnight and possibly as much as 3° at noon. These predicted effects are much smaller than the observed storm time variation of the cutoffs. Thus, to study the tilt dependence in the experimental data, the storm time dependence must first be removed. Masley (1975) has gathered a large set (over 500 observations) of cutoff values using data from the OGO-6 satellite. Here, orthonormal least squares fitting techniques were used to fit a parabolic surface in tilt and K_p through the data set. The function which gave the smallest rms errors is

$$\text{CUTOFF} = a_1 + a_2\mu + a_3\mu + a_4K_p$$

where μ is the tilt angle

K_p is the magnetic index and the

a_i are the least squares determined coefficients

Figures 18 and 19 show the comparison between theory and observation at $K_p = 1$. The small dots indicate the best fit line when $K_p = 1$, the large dots are the data for $0 < K_p < 2$ and the open circles are the tilt dependent cutoff calculations. There is good agreement between theory and experiment. The scatter of points for the noon data set is much larger indicating that the K_p dependence does not adequately remove the dynamic variations. Future studies must use other parameters such as D_{st} to remove this dependence.

2.3 The Associated Induced Electric Field, E_I

Any time-varying magnetic field has associated with it an induced electric field as given by Maxwell's equations. It is of considerable interest to determine whether or not the induced electric field associated with the time-varying magnetic

COSMIC RAY CUTOFFS

LOCAL TIME	MEASURED 060-6 (MASLEY, 1975)	OLD ZERO TILT MODEL	NEW TILTED MODEL		
			TILT = 0	TILT = +35	TILT = -35
NOON	69.9 ± .7	69	71	68	68
MIDNIGHT	66.5 ± .4	66	66	65	66
DAWN	67.6 ± .8	70	67	67	67
DUSK	67.3 ± .6	71	67	67	67

Table 1

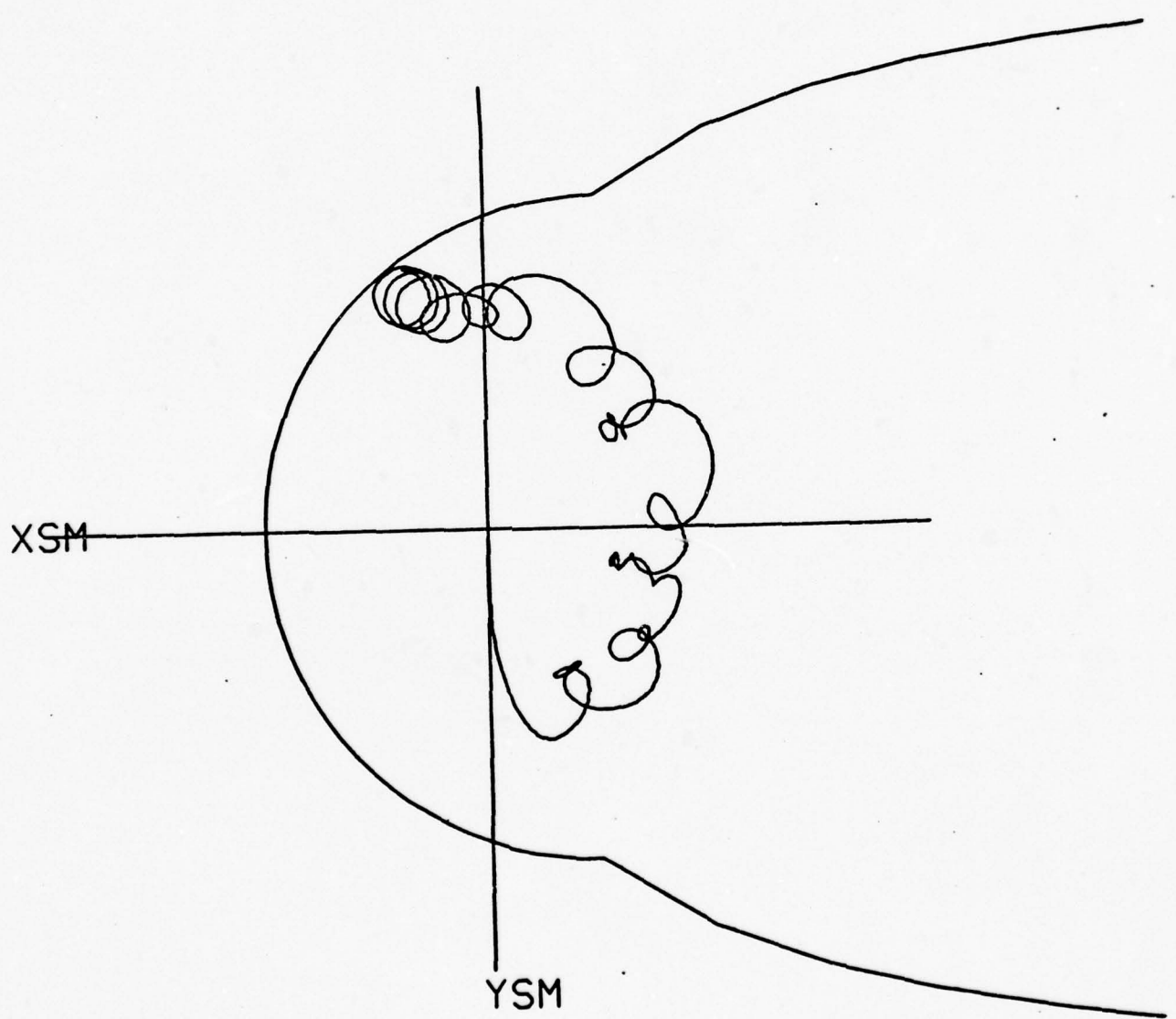


Figure 17. 5 MeV cosmic ray trajectory with a polar cap intercept latitude of 68° .

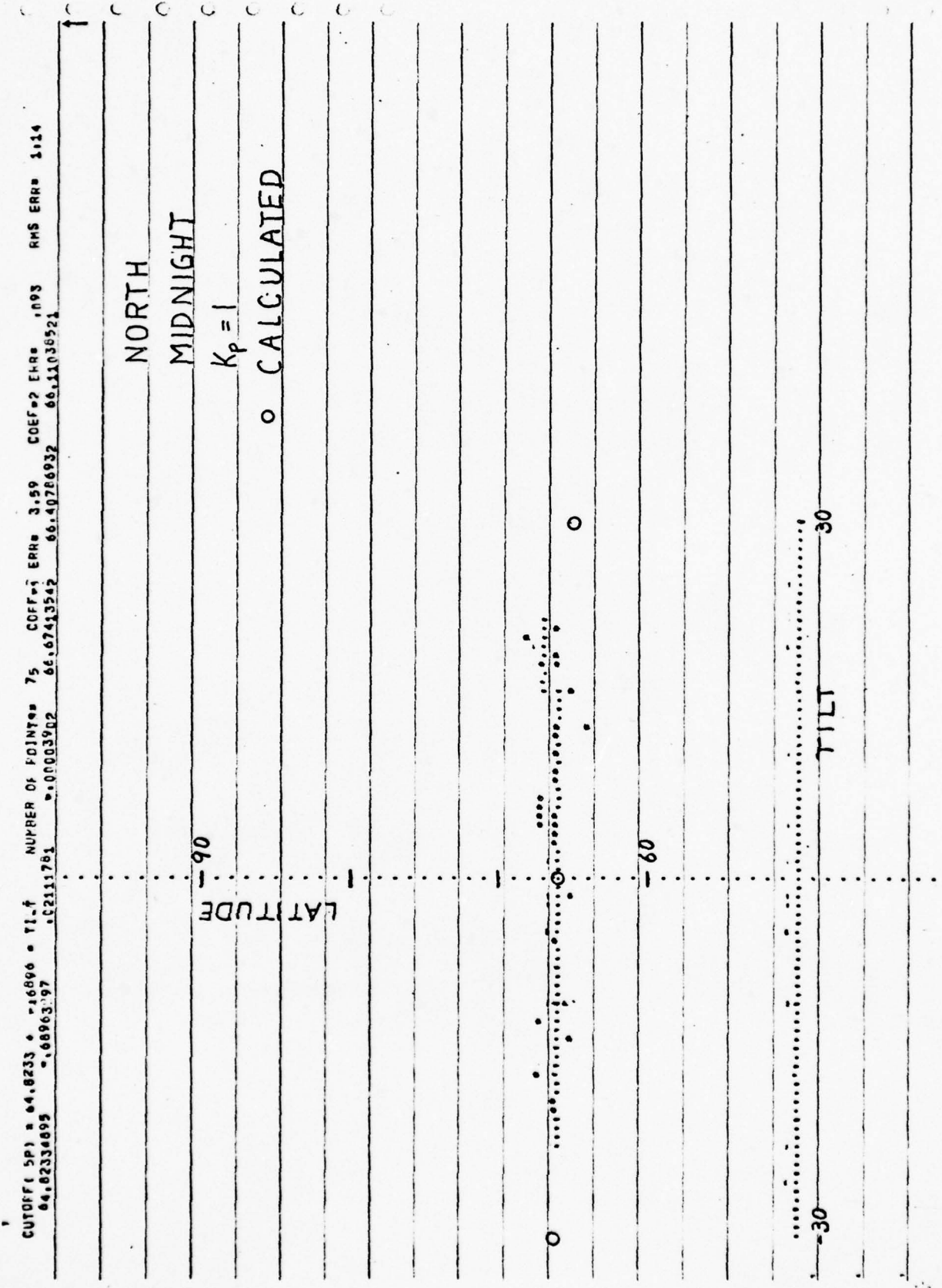


Figure 18. Tilt dependence of the cosmic ray cutoffs for the midnight meridian in the northern Polar cap.

CUTOFF SP = 48.9823 + 11.0364 * 11.4 NUMBER OF LINES = 50 COEFF ERR = 9.45 COEF = 72 ERR = 71.40106967 RMS ERR = 21.32
 48.98225833 -1.03642160 ,48524974 71.60309395 71.09725131

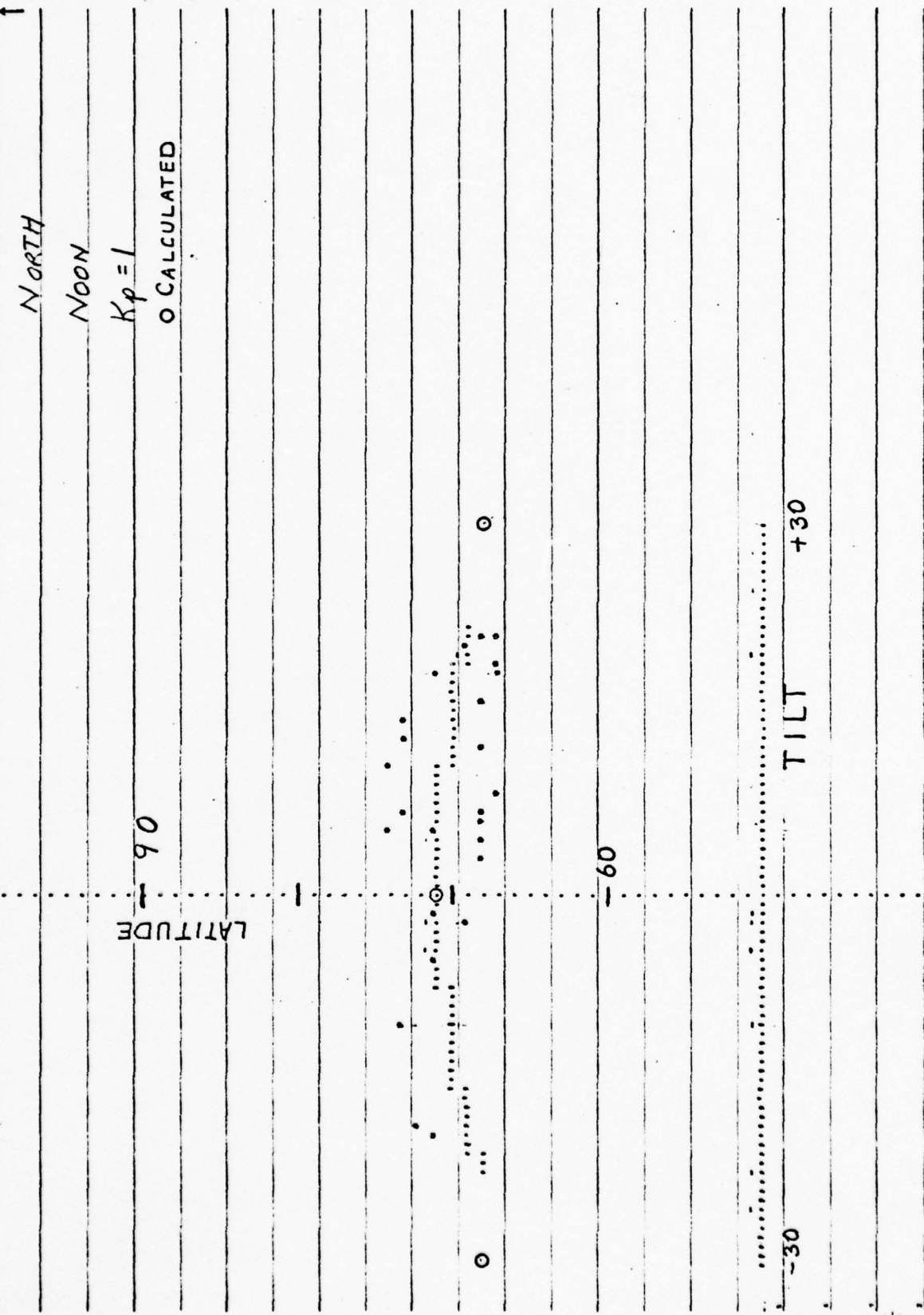


Figure 19. Tilt dependence of the cosmic ray cutoffs for the noon meridian in the northern polar cap.

field model described above is of importance for the motions of low energy charged particles in the magnetosphere. Although several sources of electric fields in the magnetosphere have been proposed, this is the first one that can be associated with an accurate quantitative model. This particular induced electric field is also of interest because its periodicity is so large. Other induced electric fields associated with magnetic storms and magnetospheric substorms have been discussed but their time constants typically range from several minutes to a fraction of an hour.

It is therefore with great interest that we report our preliminary findings of this induced electric field. Its magnitude and the strength of its components are shown over a 24-hour period at the location of the synchronous satellite ATS-1 at winter solstice in Figure 20. The magnitude of this electric field is found to be a large fraction of a millivolt per meter. Fields of this size are regularly assumed to be of importance to the plasma that fills the magnetosphere. Contours of constant induced electric field in the equatorial plane are shown in Figure 21 at winter solstice at universal time = 0. The field intensity peaks somewhere in the mid magnetosphere and then falls off again toward the magneto-pause.

The procedure for determining this induced electric field is now discussed. The induced electric field is most readily determined from the magnetic vector potential \vec{A} where $\vec{B} = \nabla \times \vec{A}$ and $\vec{E}_I = - \frac{\partial \vec{A}}{\partial t}$. Actually \vec{E}_I is determined from the product $\vec{E}_I = - \left(\frac{\partial \vec{A}}{\partial \mu} \right) \left(\frac{\partial \mu}{\partial t} \right)$. The values of \vec{A} were determined at the same time that the vector magnetic field was being constructed. Like \vec{B} , \vec{A} is given analytically in terms of the tilt angle, μ . The analytic formula for the time derivative of the tilt angle is given in Appendix B.

25742

INDUCED ELECTRIC FIELD AT ATS-1 AT WINTER SOLSTICE

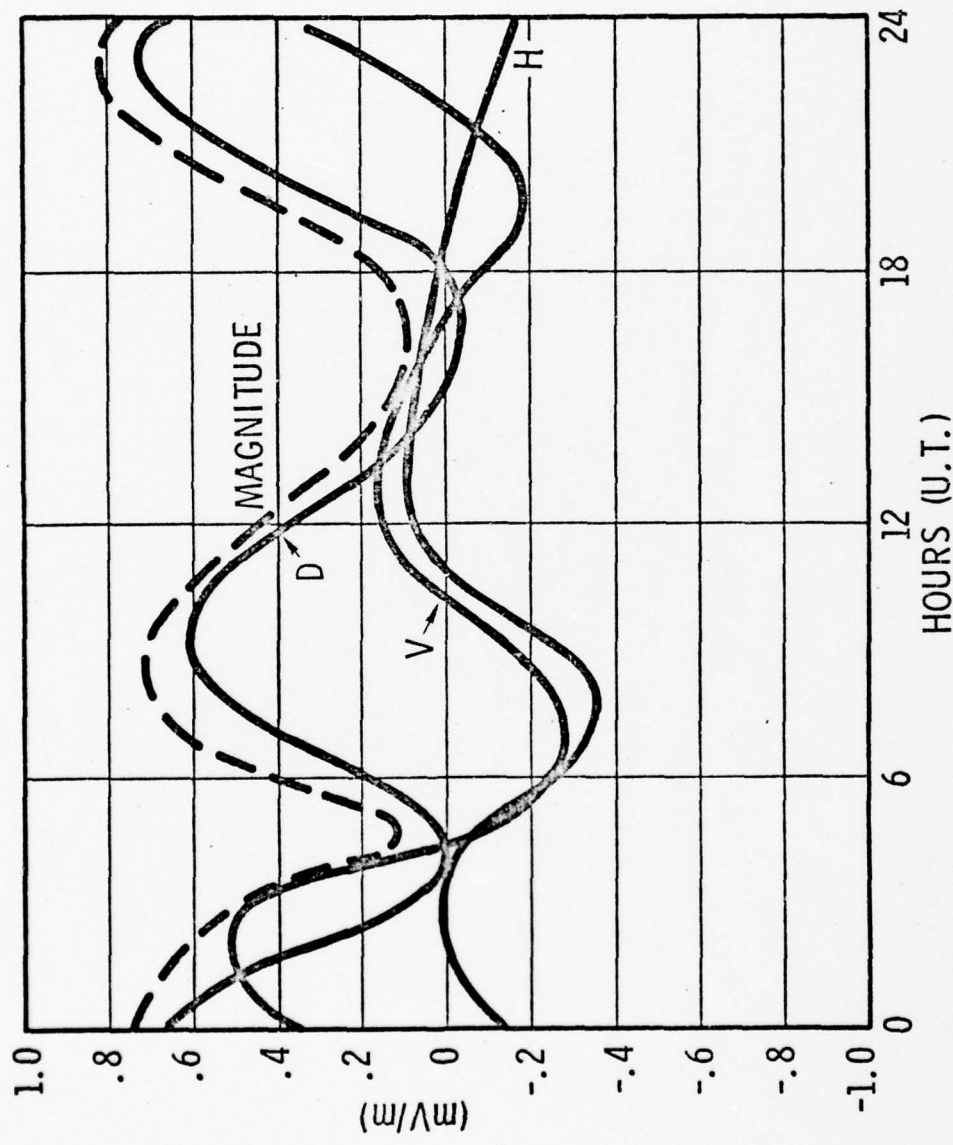


Figure 20

25740

CONTOURS OF CONSTANT INDUCED FIELD
INTENSITY AT WINTER SOLSTICE ($UT=0$) IN THE $Z=0$ PLANE

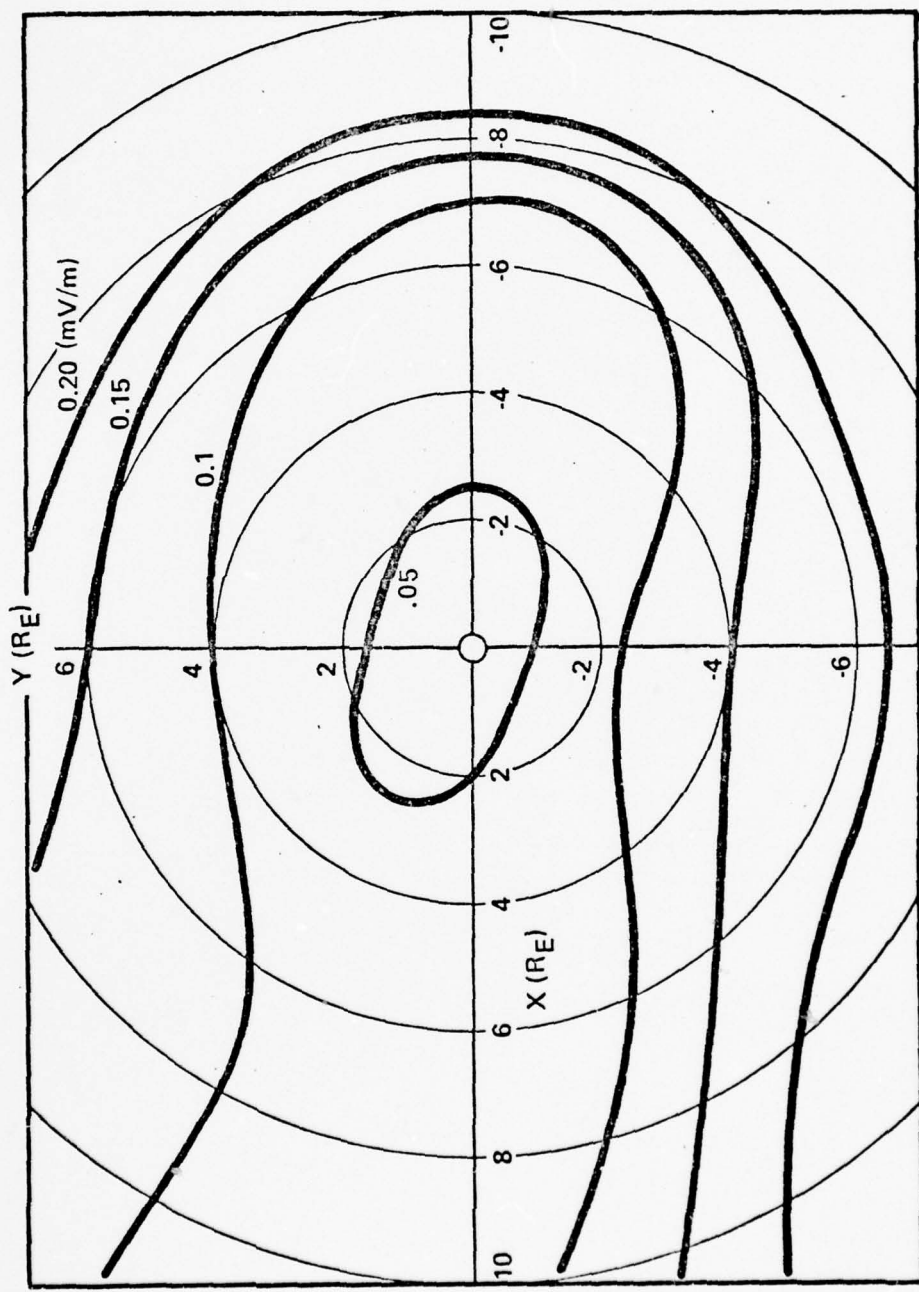


Figure 21

It must be pointed out that these results are preliminary and that the induced electric field \vec{E}_I is by itself only an estimate of the real electric field produced in the magnetosphere by the wobble of the earth's dipole axis with respect to the solar wind. A secondary electric field \vec{E}_S is produced by charge separation along magnetic field lines due to the plasma immersed in the magnetic field. This plasma tends to cancel an electric field along the direction of the magnetic field lines. Thus, the approximate condition, $\vec{E} \cdot \vec{B} = 0$, applies where \vec{E} is total magnetosphere electric field produced by the wobbling dipole. \vec{E} is therefore represented as having two sources (1) the induced field which is given in terms of the magnetic vector potential, and a second source that is derivable from a scalar potential and is produced by the charge separation along magnetic field lines, thus $\vec{E} = -\frac{\partial \vec{A}}{\partial t} - \nabla \phi$ where ϕ is the electric scalar potential. The $\vec{E} \cdot \vec{B} = 0$ condition then implies that $-\vec{E}_I \cdot \hat{B} = \nabla \phi \cdot \hat{B}$ or $-\vec{E}_I = -\frac{\partial \phi}{\partial s}$ where \hat{B} is the unit vector in the direction of \vec{B} and s is an element of length along \vec{B} . Thus, $E_{||}$ is known everywhere, if ϕ is known over some boundary it can then be found everywhere in the magnetosphere. A knowledge of ϕ and its gradients together with the values of the induced electric field suffice to actually determine the total electric field in the magnetosphere.

This problem was a biproduct of the present study and not investigated in detail. It is however called to the reader's attention in this report and it is felt it is an important problem basic to the study of magnetospheric physics. Its implications may be of considerable importance. First, the presence of such a field demands that magnetic field lines can no longer be considered as equi-potential surfaces. Indeed, this work has shown that the potential along the magnetic field lines extending to geosynchronous orbit can vary by as much as 7 or 8 kilovolts. The most important consequence of such a field, however, is

that it can accelerate charged particles in the magnetosphere locally. This is one of the key problems in magnetospheric physics, to understand how plasmas in the magnetosphere gain and lose energy. Such an electric field source should at least accelerate some of the particles some of the time. It would be expected that it would be those particles that drift around the magnetosphere with a period close to 1 day. The solar wind plasma with proton energies typically on the order of 1 kilovolt takes approximately 1 day to rotate around the magnetosphere at the location of geosynchronous orbit. The consequences of this induced electric field thus appear to be very exciting.

Section 3

THE B, L COORDINATE SYSTEMS FOR PARTICLE DATA ORGANIZATION

In order to properly utilize this magnetic field model to organize charged particle data it is necessary that the behavior of the particles in the magnetic field be properly understood. Adiabatic invariant theory has been used together with magnetic field models to develop "coordinate systems" for the meaningful representation of the particle data. Northrup and Teller (1960) discussed the use of adiabatic invariants in describing the motion of charged particles in a magnetic field. These invariants can be used to describe charged particle behavior when the change in the magnetic field over one cyclotron radius is very small, a condition that is satisfied by almost all charged particles trapped in the earth's magnetic field.

The first adiabatic invariant states

$$\frac{W_p}{B} = C = \text{constant.} \quad (3.1)$$

i.e., the component of energy perpendicular to the magnetic field, W_p , divided by the total magnetic field, B , is a constant. If α is the pitch angle of a particle (i.e., the angle that the velocity vector of the particle makes with the magnetic field vector) then $W_p = W \sin^2 \alpha$ where W is the total energy of the particle. Particles trapped in the earth's field bounce back and forth along field lines between two points called mirror points. The mirror points are the points where $\alpha = 90^\circ$ and $W_p = W$, and therefore the magnetic field at the mirror points, B_{mir} , is

$$B_{\text{mir}} = \frac{W}{C} = C' \quad (3.2)$$

That is for a particle of fixed energy B_{mir} , the field at the mirror points, is a constant and may be considered an alternate form of the first invariant.

The second invariant for a particle, the integral invariant, is defined as

$$I = \oint_{r' (B_{\text{mir}})}^{r' (B_{\text{mir}})} r' (B_{\text{mir}}) (1 - B_{\parallel}/B_{\text{mir}})^{1/2} ds \quad (3.3)$$

where ds is the differential path length along the line of force connecting the two mirror points r and r' and B_{\parallel} is the parallel component of the magnetic field. As adiabatic particles move in the earth's magnetic field they bounce back and forth between their mirror points and slowly drift perpendicular to the magnetic field in such a way that B_{mir} and I remain constant. In the earth's magnetic field the locus of points in space that have the same B_{mir} and I form a ring in each hemisphere and the field lines which connect these rings form a surface on which particles mirroring at B_{mir} are trapped. This surface is referred to as a drift shell. In general particles that mirror at different values of B along a line of force will not follow the same drift shell (shell splitting). McIlwain (1961), however, showed that when external magnetic field sources are neglected (he used the Jensen and Cain 512 term expansion to represent the earth's main field) this shell splitting effect is quite small. McIlwain made use of the fact that all particles which initially drift through a point will always be found on approximately the same shell and labeled these shells with a unique number, L , where L is approximately the radial distance in earth radii to the shell at the equator. Therefore, a coordinate system which identifies the shell (L) on which a particle moves and identifies where on the shell it mirrors (B_{mir}) uniquely identifies the particle.

In general L , the shell parameter, has the definition $L = f(B, I)$ but McIlwain showed that for a dipole field

$$\frac{L^3 B}{M} = f\left(\frac{I^3 B}{M}\right) \quad (3.4)$$

where M is the earth's dipole moment I and B are calculated using the full series representation of the earth's main field. The function f is evaluated using the dipole field expression at numerous points in space. An analytic expression for L in the real field is then obtained using least squares techniques. McIlwain used the function

$$\ln\left(\frac{L^3 B}{M} - 1\right) = \sum_{n=0}^{n=6} a_n X^n \quad (3.5)$$

where $X = \ln\left(\frac{I^3 B}{M}\right)$ and a_n are fitted by the least squares procedures.

The current version of McIlwain's (B, L) coordinate system considers only the internal magnetic field sources and thus is valid near the earth ($L \lesssim 3$) where the external field sources are negligible. At larger distances ($L \gtrsim 3$) one must include the external field sources in order to adequately describe the magnetic field. By including the external field sources in the definition of (B, L) the validity of (B, L) can readily be extended to about $L \approx 5$. For $L < 5$ the asymmetries of the field are small and the approximation that particles on a given field line will follow the same drift shell is valid. Roederer (1969) first showed that at large geocentric distances ($L > 5$, where the field distortions become large) particles of different pitch angle should follow different drift shells and that it is important to include shell splitting effects in

order to understand particle behavior in this region. Pfitzer, et al., (1969) using data from the geosynchronous satellite ATS-1 and the elliptic orbit satellite OGO-3, first demonstrated experimentally the importance of shell splitting. It was shown that at synchronous orbit particles passing through a given point and having different pitch angles will follow drift shells that may separate by as much as one R_E . (See Figure 22)

3.1 Generalization to the Distorted Field

The first step in generalizing the (B, L) coordinate system is to modify the magnetic field code to combine an accurate expansion for the internal field sources with an expansion for the external field sources. The currently available (B, L) program uses the 1960 Jensen and Cain expansion. We have selected IGS 75 (Barraclough et al. 1975), a more up-to-date and accurate version of the internal field code and have combined it with the external field expansion discussed in the Section 2.0. The internal magnetic field code is in spherical geographic coordinates and the external code in cartesian solar magnetic coordinates and therefore several coordinate transformation (see Appendix B) were developed in order to combine the fields. This total magnetic field is then used for all (B, L) calculations.

Several methods of extending (B, L) to the distorted field case are possible. No matter how distorted the field, it is always possible to map directional particle fluxes, $F(\alpha)$, by either using the adiabatic invariants (B_{mir} , I) directly to organize the data or by defining a new L (L^*) which is a function of the pitch angle of the measured particle as well as its location. This coordinate system would most accurately organize directional particle data.

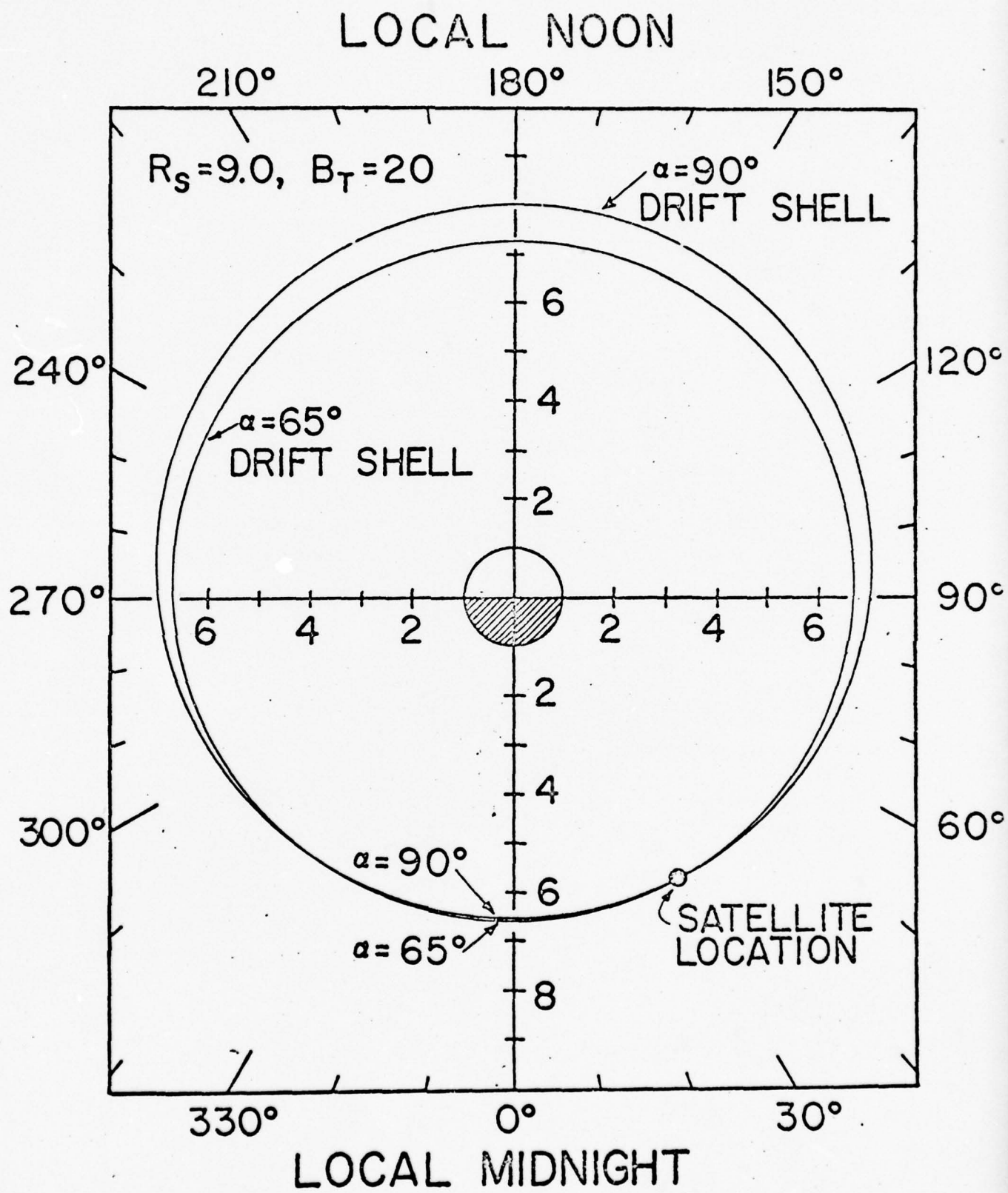


FIGURE 22 -Equatorial intersection of drift shells (using the Mead-Williams magnetic field model) for particles having pitch angles of $\alpha=65^\circ$ and $\alpha=90^\circ$ at the location of the satellite are shown when the satellite is positioned at $6.6 R_E$, 0° latitude, and 30° local time; R_s and B_T are input parameter to the Mead-Williams model (from Pfitzer, et al., 1969).

If, however, only omnidirectional data with unspecified pitch angle distributions are available, very little can be done to improve (B, L) beyond the inclusion of the external field sources in the calculation of L . However, when the pitch angle distribution is known, then (B, L) can be modified to represent the average shell on which the observed particles move. In this study we have used this third approach. We have modified L and defined an \bar{L} which represents the average L value when the particle flux is known to be isotropic.

McIlwain's program for calculating (B, L) evaluates the second invariant by integrating from the location of the satellite (i.e., B_{mir} in Equation (3) is set to the value of B at the location of the measurement) to the conjugate point. This gives a value of I which is identically accurate for particles having a pitch angle of $\alpha = 90^\circ$ and thus represents one extreme of the pitch angle distribution. All other particles with different pitch angles will drift on shells either outside or inside the $\alpha = 90^\circ$ shell. By modifying the B_{mir} used to determine I to represent a particle that drifts on a shell near the center of the drift shell distribution we can define a \bar{B}_{mir} and then determine the average second invariant, \bar{I} , for the isotropic flux case.

A modified (B, \bar{L}) thus replaces the (B, L) system where \bar{L} can be obtained from the following procedure:

- 1) Determine \bar{B}_{mir} . A number of drift shells were computed for isotropic particle distribution in the combined external plus internal field and the following algorithm was empirically developed for \bar{B}_{mir} .

$$\bar{B}_{\text{mir}} = B_{\text{mir}} \text{ if } B_{\text{mir}} > 3 \cdot B_{\text{mir}}$$

where B_{mir} is the minimum B along the field line.

If $B_{\text{mir}} < 3 \cdot B_{\text{mir}}$, then

$$\bar{B}_{\text{mir}} = B_{\text{mir}} \quad \text{if } EL < 3$$

where

$$EL = \left(\frac{0.311653}{B_{\text{mir}}} \right)^{1/3}$$

$$\bar{B}_{\text{mir}} = C \cdot B_{\text{mir}} \leq 3 \cdot B_{\text{mir}} \quad \text{if } EL \geq 3$$

where

$$C = 1.3 \text{ if } EL \geq 5$$

$$C = 1 + 0.15 (EL - 3) \text{ if } EL < 5$$

2) Determine \bar{T} using the equation

$$\bar{T} = \int_A^{A'} \left(1 - \frac{B(s)}{\bar{B}_{\text{mir}}} \right)^{1/2} ds \quad (3.7)$$

where A and A' are the points on the field line where $B(s) = \bar{B}_{\text{mir}}$.

3) Substitute \bar{B}_{mir} and \bar{T} into

$$\ln \left(\frac{\bar{T}^3 \bar{B}_{\text{mir}}}{M} - 1 \right) = \sum_{n=0}^{n=6} a_n \left[\ln \left(\frac{\bar{T}^3 \bar{B}_{\text{mir}}}{M} \right) \right]^n \quad (3.8)$$

where M is the dipole moment and a_n are the coefficients of McIlwain's expansion.

The above procedure has the property that as drift shell splitting becomes small, \bar{L} approaches L . When drift shell splitting becomes important \bar{L} will represent the average drift shell more accurately than L . The procedure is only slightly more complicated than the present (B, L) procedure and the only difference in computer time results from evaluating I over a slightly longer path and from having a more complicated expansion for the magnetic field. Since \bar{L} is determined for an isotropic particle distribution, it will be less accurate for other pitch angle distributions. Also, since \bar{L} represents an average drift shell, exceedingly strong (e.g., discontinuous) radial gradients in the particle distribution cannot be mapped accurately with \bar{L} . For the highly anisotropic cases and for strong radial gradients only directional measurements can be mapped and \bar{L} is not the most useful approach, instead L^* which is a modification of L that takes into account the pitch angle of the measurement must be used.

3.2 Tilt Effects in B, \bar{L}

In the previous paragraphs we have discussed our extension of the McIlwain (B, L) coordinate system to a highly distorted field. Since the dipole of the earth is inclined to the rotation axis, the tilt angle, μ , changes slowly. This causes the magnetic field at large geocentric distances $> 5R_e$ to vary periodically with a frequency that is slow compared to the time it takes all but the lowest energy particles to drift around the earth. Therefore, the particles adiabatic invariants remain constant during this change, and at the end of a day when a 24-hour cycle has been completed the particles (if no other disturbances have occurred) will be in their initial shell positions. Therefore even though the magnetic field is changing with time, \bar{L} (for a given particle

set) remains approximately fixed such that any particle whose adiabatic invariants remain constant will have the same label over the entire 24-hour period of changing tilt.

Since the magnetic field at a given location varies with the tilt, μ , the value of \bar{L} will move inward and outward over the 24-hour period. Thus, \bar{L} correctly labels the constant drift shells on which the particles move during the adiabatic field changes.

Appendix A describes the computer programs developed to evaluate \bar{L} , as well as all of the programs for determining the magnetic field at a given point in space. The user is given the option of calculating L as defined initially by McIlwain, calculating L using the external plus internal field or calculating \bar{L} using the external plus internal field.

Section 4

SUMMARY AND CONCLUSIONS

A new magnetospheric magnetic field model has been developed and described. It is valid throughout the inner magnetosphere and we believe it currently offers the best description of the total magnetospheric magnetic field during quiet magnetic conditions. It is valid for all angles of incidence of the solar wind on the earth's magnetic dipole axis. Its region of validity is out to a geocentric distance of 15 earth radii or to the magnetopause, whichever is smaller. The model is semiempirical. That is, it is based on both the several physical principles that govern our current understanding of the magnetospheric magnetic field, and on several data sets that describe quantitatively the structure of the magnetospheric magnetic field. The quantitative model representation was done by fitting both the spatial and the tilt angle coordinates simultaneously. The resulting four-dimensional model represents on average the magnetic field values input to the fitting routine to approximately 15 percent of their values with an average error over all three magnetic field components of 0.27 gammas.

The model has been tested in several ways and found to offer an accurate description of the field in the inner magnetosphere. The model has already been used to predict the earth intercept of field lines from various geosynchronous satellites. This information is of vital interest to satellite experimental groups wishing to coordinate their work with ground based and balloon experiments. The primary reason for developing the model was to combine it with adiabatic invariant theory to offer a more accurate means for organizing charged particle data out to and beyond geosynchronous orbit. This has resulted in the development

of a new "coordinate system," the (B, \bar{L}) coordinates, which will be useful for such particle mapping exercises.

Because this magnetic field model is in some sense time-variant (as the tilt angle changes the magnetic field changes through the day), there is associated with it an induced electric field. Although this induced electric field was anticipated and vector potential representation of the magnetic field components were obtained in order to easily calculate this induced electric field, it was not the principle purpose of the contract research and therefore has not been studied in detail. It is believed, however, that this electric field may exert considerable influence on the magnetospheric plasma and its study may shed light on many important problems in magnetospheric physics.

The magnetic field model has also been used together with Lorenz force calculations to study the cutoff in magnetic latitude of the region of penetration of solar cosmic ray particles. With the introduction of this model there is no longer any discrepancy between model calculations and observations. Prior to the recent earlier work of Olson and Pfitzer (1974) the "cutoff problem" was considered to be one of the key problems in cosmic ray physics and several theories were promulgated to explain the difference in the observed and calculated cutoff latitudes. It therefore may be said that use of this model has led to the solution of this classical cosmic ray physics problem.

Complete listings of the model magnetic field and the new (B, \bar{L}) coordinate system routines are given in Appendix A. It is again called to the reader's attention that this document is meant to be only what it says, an annual

report. The final descriptions of the magnetic field model and its testing and uses will eventually be provided by journal articles which will be submitted shortly. Also, the listings provided in the appendices should be considered provisional. A final authoritative description of the model and the (B , \bar{L}) coordinate system will be available after some final inputs are obtained from DoD personnel.

Section 5
APPENDIX A -
COMPUTER CODES

The complete computer program developed under this contract effort consists of a set of nine separate routines. These routines may be combined in several different ways depending on user needs. The four most important configurations are shown in Table A-1. The program listing which is included in this appendix is typical for configuration 1. A test deck which exercises all of the subroutines is supplied with configuration 1. This test program can be used to verify correct operation of the code on the user's computer. All subroutines have been written in ANSI standard FORTRAN IV.

A definition of each subroutine, the calling sequences, restrictions and limitations are contained in the COMMENT cards associated with each routine.

5.1 Subroutine Description

A brief description of each subroutine follows:

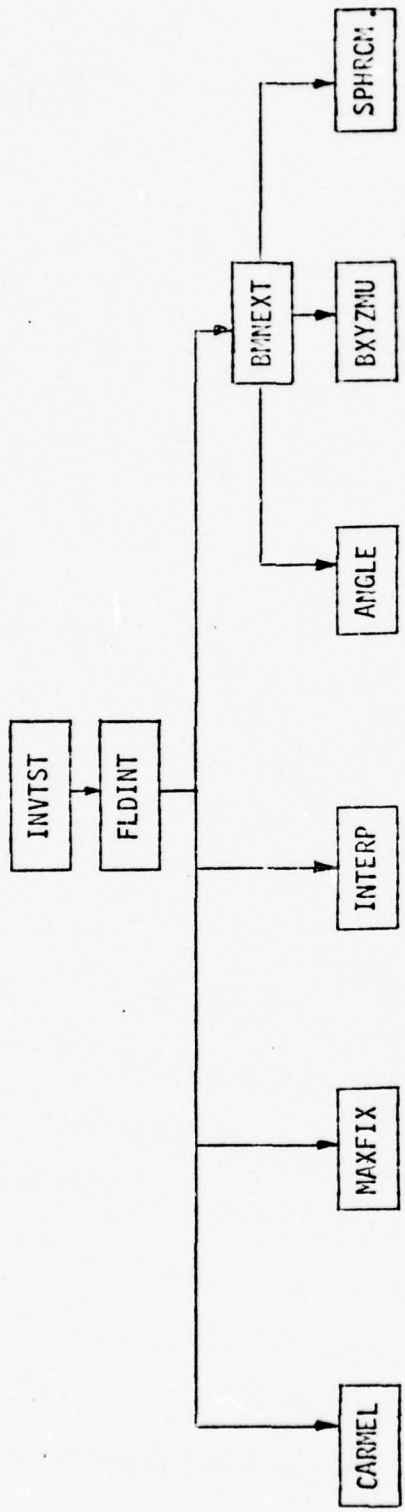
INVTST is a test program designed to exercise the subroutines. It permits the user to verify the correct operation of the program on his computer.

FLDINT is the field line integration routine which calculates L or \bar{L} depending on the option selected. It requires all other subroutines for correct operation.

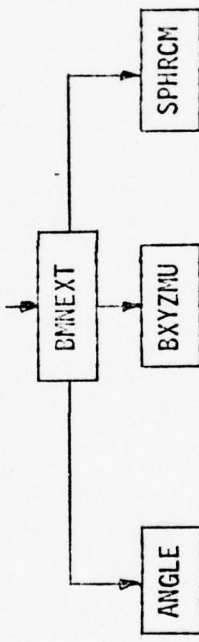
BMNEXT determines the total magnetic field at a point by combining an internal magnetic field code given in geographic spherical coordinates with an external magnetic field code given in cartesian solar magnetic

Table A-1
PROGRAM STRUCTURES

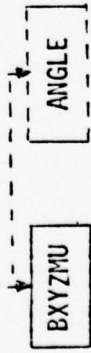
1. Deck structure for determining \bar{L}



2. Deck structure for determining the total magnetic field (internal plus external)



3. Deck structure for determining external field only



4. Deck structure for determining internal field only



coordinates. BMNEXT requires the internal field routine SPHRCM, the external field routine BXYZMU, and the tilt angle routine ANGLE.

BMNEXT is a generalized total field routine and can provide input and output in either spherical or cartesian geographic coordinates.

BXYZMU is the tilt dependent external magnetic field subroutine. It supplies the magnetic field contribution from the external current sources (ring, tail, and magnetopause) as a function of position and the tilt of the dipole axis. Input and output are in solar magnetic coordinates. This routine is completely self-contained and requires no other routines for its operation. However, subroutine ANGLE may be used to determine the tilt angle, μ , as a function of time.

SPHRCM is a modification of J. C. Cain's (USGS) fast SPHRC routines. They have been shortened from a fourteenth order expansion to a ninth order expansion and combined into a single subroutine. A smooth truncation scheme has been added such that for large distances fewer terms are used. The terms are turned off gradually. The version used for this study contains the IGS 75 (Barracough, et al., 1975) coefficients through $n = 9$. SPHRCM may be used independent of all other routines.

ANGLE is a subroutine which calculates the position of the sun in the celestial sphere and determines the tilt angle, μ , as well as the rotation sines and cosines for transforming from geomagnetic to solar magnetic coordinates. ANGLE is self-contained and may be used independent of all other routines. Derivations of these angles are given in Appendix B.

INTERP is a parabolic interpolation routine which fits a parabola through three points and evaluates the function at a specified location. It is an independent routine.

MAXFIX determines \bar{B}_{mir} given B_{mir} and B_{min} . The algorithm for \bar{B}_{mir} is given in Section 3.2.

CARMEL is a copy of C. E. McIlwain's (University of California, San Diego) code for determining L. Given B_{mir} and I, CARMEL calculates L; or given \bar{B}_{mir} and \bar{I} , CARMEL determines \bar{L} . CARMEL may be used independent of all other routines.

5.2 Sample Output Description

The test program (INVTST) produces a sample output used by calling the field line integration routine (FLDINT) at various locations and times (see Section 5.4). L is determined for three separate cases: (1) Internal field only (L INT), (2) internal plus the external field (L INT+EXT), and (3) \bar{L} which uses internal plus the external field (L AVE).

The definition of the column headings for the sample output are given below:

LAT The geographic latitude in degrees.

LONG The geographic east longitude in degrees.

R The geocentric radial distances. R = 1.0 is 6371.2 km.

DAYOFYR The day of the year (1-366). January 1 is DAYOFYR = 1.

L The value of L or \bar{L} .

BMIN The minimum value of the magnetic field along the field line.

MAGLONG The magnetic longitude in degrees measured eastward of the meridian through the dipole and the geographic pole ($\sim 69^\circ$ W longitude).

MAGLAT The magnetic latitude in degrees. $+90^\circ$ magnetic latitude is at 11.7° North and 69° West geographic.

CPTIME Central processor execution time in seconds on a CDC 6600 for the determination of a single value of L. Because of the uncertainties involved in measuring such short times, the times may be in error by as much as ±0.002 second. These times are useful in informing the user of the relative computer times required for the three L options.

5.3 Program Listing

```
PROGRAM INVST(INPUT,OUTPUT,TAPE6=OUTPUT)
DIMENSION IAR(3)
DATA IAR/ 10H L INT      ,10H L INT+EXT,10H L AVE   /
LN=100
DO 1 ID=1,90,89
DA=ID
DO 1 IU=1,19,6
UT=IU-1
LN=100
DO 1 IL=1,31,30
FLAT=IL-1
DO 1 ILG=1,181,90
XLONG=ILG-1
DO 1 IR=2,8,3
R=IR
DO 1 IC=1,3
CALL SECOND(TA)
CALL FLDINT(FLAT,XLONG,R,1975.,DA,UT,IC-2,EL,BM,XMLONG,XMLAT)
CALL SECOND(TB)
TC=TB-TA
LN=LN+1
IF (LN.LT.58) GO TO 10
LN=0
PRINT 11
11  FORMAT(1H1,15X,*LAT      LONG      R      DAYOFYR      TI
*ME      L      BMIN      MAGLONG      MAGLAT      CPTIME*,*
*)
12  FORMAT(A10,10F12.5)
10  PRINT 12,IAR(IC),FLAT,XLONG,R,DA,UT,EL,BM,XMLONG,XMLAT,TC
1  CONTINUE
END
```

```

SUBROUTINE FLDINT(XLAT,XLONG,R,YR,DAY,TIME,JSWTCH,EL,BBMIN,XMLONG,
*XMLAT)

C
C FLDINT CALCULATES THE SECOND ADIABATIC INVARIANT BY INTEGRATING ALONG
C MAGNETIC LINES OF FORCE
C IT CAN CALCULATE EITHER THE OLD INTERNAL FIELD ONLY L, L MODIFIED
C BY THE EXTERNAL FIELD, OR AN AVERAGE L BASED ON ISOTROPIC PARTICLES
C CALLING SEQUENCE - INPUT PARAMETER
C   XLAT  GEOCENTRIC LATITUDE INDEGREES
C   XLONG GEOCENTRIC LONGITUDE EAST OF GREENWICH IN DEGREES
C   R    GEOCENTRIC DISTANCE FROM THE EARTHS CENTER IN UNITS OF
C        EARTH RADII, RE. RE=6371.2 KM
C   YR   THE YEAR - USED BY SOME MAIN FIELD ROUTINES TO SET THE
C        COEFFICIENTS (E.G. JULY 15, 1964=1964.54)
C        NOTE*** YR SHOULD BE CHANGED ONLY EVERY FEW DAYS OR MONTHS.
C        NEW FIELD COEFFICIENTS MUST BE COMPUTED FOR EVERY CHANGE
C        IN YR, THIS COULD CAUSE A LARGE INCREASE IN COMPUTER TIME.
C        THE EARTHS FIELD CHANGES ONLY ABOUT .001 GAUSS/YEAR AT THE
C        EARTHS SURFACE.
C   DAY   THE DAY OF YEAR (1.-366.). DAY IS USED BY THE DIPOLE TILT
C        ROUTINE.
C        DAY MUST BE A WHOLE NUMBER AND DAY 1 IS JANUARY 1
C   TIME  UNIVERSAL TIME IN HOURS (0.000-24.0000)
C   JSWTCH =-1 COMPUTE L USING INTERNAL FIELD ONLY
C           = 0 COMPUTE L USING INTERNAL + EXTERNAL FIELD
C           =+1 COMPUTE AVERAGE L USING INTERNAL + EXTERNAL FIELD
C
C OUTPUT PARAMETERS
C   EL    THE L VALUE DETERMINED AS REQUESTED BY JSWTCH
C   BBMIN THE MINIMUM VALUE OF B ALONG THE FIELD LINE IN GAUSS
C   XMLONG THE MAGNETIC LONGITUDE MEASURED EAST OF THE MERIDIAN
C           CONNECTING THE TWO POLES (APP.EAST OF 69W GEOGRAPHIC)
C   XMLAT THE MAGNETIC LATITUDE
C
C ****NOTE****
C SINCE THIS ROUTINE USES AN ACTUAL MAGNETOSPHERIC MAGNETIC FIELD,
C THE FIELD LINES ARE NOT ALL CLOSED. THUS L IS DEFINED ONLY IN THE
C INNER MAGNETOSPHERE. AN ATTEMPT TO CALCULATED L OUTSIDE OF THIS
C REGION WILL SET L EQUAL TO 100. (EL=100.)
C BBMIN WILL BE SET TO THE LOCAL VALUE OF B.
C ****
COMMON/BXYZCM/YEAR,DAVYR,UT,XMLG,KODE,JSW,INITL,XMLT
DIMENSION X(3),XL(3),Q(3),QL(3),B(3),BL(3),SS(3),RR(3),BB(100,4),
*S(100),SDS(100),BINTL(3),XX(3)
DIMENSION SXJ(100)
DATA P29,OPT/.29289322,1.70710678/
DATA PICON/.01745329252/
C SET UP INITIAL CONDITIONS
YEAR=YR
UT=TIME
DAVYR=DAY
KODE=1
JSW=JSWTCH
COSINE=COS(XLAT*PICON)
XX(1)=R*COSINE*COS(XLONG*PICON)
XX(2)=R*COSINE*SIN(XLONG*PICON)
XX(3)=R*SIN(XLAT*PICON)
INITL=0.

```

```

N=2
CALL BMNEXT(XX,B,BB(2,1))
IF(XMLG.LT.0.) XMLG=XMLG+360.
XMLAT=XMLT
XMLONG=XMLG
C EXIT IF OVER THE POLAR CAP OR DISTANCE IS TOO LARGE OR FIELD IS TOO
C WEAK.
IF(ABS(XMLT).GT.75..OR.R.GT.12..OR.BB(2,1).LT.0.00025) GO TO 330
INITL=1
NBMIN=2
MAXFLG=0
XJ=0
ISW=0
IPASS=0
EL=0
DO 10 I=1,3
BINTL(I)=B(I)
X(I)=XX(I)
10 Q(I)=0.
S(2)=0.
C SET UP ERROR CONSTRAINTS
ERRR=.005
ERR=ERRR/10.
SER=SQRT((X(1)**2+X(2)**2+X(3)**2)*ERR )
FER=ERR**0.25
DEL=-2.5*FER
DS=SER
BMAX=BB(2,1)
BMIN=BMAX
C STEP ONCE IN THE INCREASING FIELD STRENGTH DIRECTION AND SET STEP TO
C INTEGRATE IN DECREASING FIELD DIRECTION
IF(XMLT.GT.0.)GO TO 30
20 DEL=-DEL
DS=-DS
30 DO 35 I=1,3
35 XL(I)=X(I)+DS*B(I)/BB(2,1)
CALL BMNEXT(XL,BL,BB(1,1))
IF(BB(1,1).LT.BB(2,1)) GO TO 20
C DETERMINE CURVATURE AND DETERMINE STEP SIZE
S(1)=DS
40 CURV=0.
CURVMN=ABS(DEL)/(1.5*(X(1)**2+X(2)**2+X(3)**2)**(.75)*FER)
DO 50 I=1,3
50 CURV=CURV+((B(I)/BB(N,1)-BL(I)/BB(N-1,1))/DS)**2
CURV=SQRT(CURV)
CURV=AMAX1(CURV,CURVMN)
C DEL/CURV
DS=SIGN(AMINI(ABS(DS),2.8),DS)
C SAVE LAST STEP
60 DO 65 I=1,3
XL(I)=X(I)
QL(I)=Q(I)
65 BL(I)=B(I)
C BEGIN GILLS METHOD OF RUNGE KUTTA INTEGRATION
66 P5DS=.5*DS
P29DS=P29*DS
OP7DS=OP7*DS

```

```

SDS(N)=DS
DO 70 I=1,3
SS(I)=P5DS*B(I)/BB(N,1)
RR(I)=SS(I)-Q(I)
X(I)=X(I)+RR(I)
70 Q(I)=Q(I)+3.*RR(I)-SS(I)
CALL BMNEXT(X,B,dB(N,2))
DO 71 I=1,3
SS(I)=P29DS*B(I)/BB(N,2)
RR(I)=SS(I)-P29*Q(I)
X(I)=X(I)+RR(I)
71 Q(I)=Q(I)+3.*RR(I)-SS(I)
CALL BMNEXT(X,B,BB(N,3))
DO 72 I=1,3
SS(I)=OP7DS*B(I)/BB(N,3)
RR(I)=SS(I)-OP7*Q(I)
X(I)=X(I)+RR(I)
72 Q(I)=Q(I)+3.*RR(I)-SS(I)
CALL BMNEXT(X,B,BB(N,4))
DO 73 I=1,3
SS(I)=P5DS*B(I)/BB(N,4)
RR(I)=(SS(I)-Q(I))/3.
X(I)=X(I)+RR(I)
73 Q(I)=Q(I)+3.*RR(I)-SS(I)
N=N+1
S(N)=S(N-1)+DS
CALL BMNEXT(X,B,BB(N,1))
C IF N IS TOO BIG STOP CALCULATION
IF(N.GE.100) GO TO 300
C IF DISTANCE TOO LARGE OR FIELD TOO SMALL EXIT
IF(X(1)**2+X(2)**2+X(3)**2.GT.144..OR.BB(N,1).LT.0.00025)GO TO 330
IF(ISW)200,100,150
100 IF(BB(N,1).GE.BMIN)GO TO 110
BMIN=BB(N,1)
NBMIN=N
110 IF(BB(N,1).LT.BMAX) GO TO 40
C IF BMAX IS EXCEEDED STOP INTEGRATION
IF(MAXFLG.EQ.0) GO TO 190
120 M=1
125 CALL INTERP(BB(N-2,1),S(N-2),BMAX,SF, 1)
N=N-M
C CHECK TO SEE THAT LAST STEP IS CLOSE TO BMAX
IF(ABS(SF-S(N)).LT.SER) GO TO 160
DS=.97*(SF-S(N))
ISW=1
130 IF(M.EQ.0) GO TO 60
DO 140 I=1,3
X(I)=XL(I)
Q(I)=QL(I)
140 B(I)=BL(I)
GO TO 66
150 IF(BB(N,1).GT.BMAX) GO TO 120
M=0
GO TO 125
160 IF(N-3)180,170,200
170 IF(IPASS.NE.0) GO TO 200
C TOO FEW POINTS TO FIND L GET ONE MORE

```

```

ISW=-1
DS=0.5*(S(N-1)-S(N))
GO TO 130
180 IF(IPASS.EQ.0) GO TO 185
182 SXJ(3)=SXJ(2)
SXJ(2)=SXJ(1)
SXJ(1)=SXJ(4)
BB(3,1)=BB(2,1)
BB(2,1)=BB(1,1)
BB(1,1)=BB(4,1)
N=3
GO TO 215
C CALCULATE L FROM BMIN IF POINT IS NEAR BMIN OR IF INTEGRATION FAILS
185 XJ=0.
EL=(0.311653/BBMIN)**(1./3.)
RETURN
190 MAXFLG=1
CALL INTERP(BB(NBMIN-1,1),S(NBMIN-1),DUMMY,BBMIN,-1)
CALL MAXFIX(BMAX,BBMIN)
GO TO 110
C
C FIELD LINE INTEGRATION COMPLETE CALCULATE INVARIANT
200 XA=0
QA=0
SDSV=SDS(2)
SXJ(2)=0.
NN=N-1
DO 210 K=2,NN
DS=SDS(K)
P5DS=.5*DS
P29DS=P29*DS
OPTDS=OPT*DS
FACTOR=0.
IF(BB(K,1).LT.BMAX)FACTOR=SQRT(1.-BB(K,1)/BMAX)
SA=P5DS*FACTOR
RA=SA-QA
XA=XA+RA
QA=QA+3.*RA-SA
FACTOR=0.
IF(BB(K,2).LT.BMAX)FACTOR=SQRT(1.-BB(K,2)/BMAX)
SA=P29DS*FACTOR
RA=SA-P29*QA
XA=XA+RA
QA=QA+3.*RA-SA
FACTOR=0.
IF(BB(K,3).LT.BMAX)FACTOR=SQRT(1.-BB(K,3)/BMAX)
SA=OPTDS*FACTOR
RA=SA-OPT*QA
XA=XA+RA
QA=QA+3.*RA-SA
FACTOR=0.
IF(BB(K,4).LT.BMAX)FACTOR=SQRT(1.-BB(K,4)/BMAX)
SA=P5DS*FACTOR
RA=(SA-QA)/3.
XA=XA+RA
QA=QA+3.*RA-SA
SXJ(K+1)=XA

```

```

210  CONTINUE
C  INTERPOLATE TO IMPROVE INVARIANT VALUE
215  CALL INTERP(BB(N-2,1),SXJ(N-2),BMAX,XXJ, N)
      XJ=XJ+ABS(XXJ)
C  IF 2ND PASS OR BMAX WAS NOT CHANGED STOP INTEGRATION
IF(IPASS.NE.0) GO TO 230
IF(ABS(BB(2,1)-BMAX)/BMAX.LT.ERR) GO TO 230
IPASS=1
SXJ(1)=SXJ(3)
BB(1,1)=BB(3,1)
S(1)=S(3)
CALL INTERP(BB(2,1),S(2),BMAX,SF,2)
IF(ABS(SF).LT.SER) GO TO 182
DEL=-DEL
DS=-SDSV
DO 220 I=1,3
X(I)=XX(I)
Q(I)=0
220  B(I)=BINTL(I)
N=2
ISW=0
GO TO 60
C  CALL MCILWAINS L EXPANSION
230  CALL CARMEL(BMAX,XJ,EL)
      RETURN
300  WRITE(6,310)
310  FORMAT(20H FIELD LINE TOO LONG)
C  IF EL CANNOT BE CALCULATED SET BBMIN TO LAST VALID VALUE OF B
C  AND SET EL TO 100.
330  BBMIN=SQRT(BINTL(1)**2+BINTL(2)**2+BINTL(3)**2)
      EL=100.
      RETURN
      END

```

```

        SUBROUTINE BMNEXT(XX,B,BMAG)
C SUBROUTINE FOR MAGNETIC FIELD MAIN PLUS EXTERNAL
C VERSION 9/1/76
C DETERMINES THE VECTOR MAGNETIC FIELD IN GEOGRAPHIC COORDINATES
C USING A SPHERICAL COORDINATE EXPANSION OF THE EARTHS FIELD AND A
C CARTESIAN COORDINATE EXPANSION OF THE BOUNDARY, TAIL AND RING
C CURRENT FIELDS IN SOLAR MAGNETIC COORDINATES
C
C INPUT AND OUTPUT ARE VIA THE ARGUMENT LIST AS WELL AS THRU A COMMON
C BLOCK BXXYZCM. UT, KODE, DAYYR, XMLG, XMLT, JSW, AND INITL ARE
C TRANSMITTED THROUGH COMMON.
C
C COMMON BLOCK ARGUMENTS
C KODE=1 SPECIFIES THAT INPUT AND OUTPUT ARE TO BE IN CARTESIAN COORDS
C KODE=2 SPECIFIES THAT INPUT AND OUTPUT ARE TO BE IN SPHERICAL COORDS
C UT IS THE UNIVERSAL TIME IN HOURS (0.-24.)
C DAYYR IS THE DAY OF YEAR IN DAYS -- IT IS ONLY USED IF A TILTED
C MAGNETOSHERIC EXTERNAL FIELD IS USED
C THIS DECK IS SUPPLIED WITH A TILT DEPENDENT VERSION OF THE
C EXTERNAL FIELD.
C JSW LESS THAN ZERO -- GET INTERNAL FIELD ONLY
C IF GREATER THAN ZERO GET INTERNAL PLUS EXTERNAL MAGNETIC FIELD
C INITL IF EQUAL TO ZERO SET UP THE VALUES FOR XMLT AND XMLG
C IF NOT EQUAL TO ZERO DO NOT CHANGE THE VALUES OF XMLG AND XMLT
C XMLG THE MAGNETIC LONGITUDE IN DEGREES.
C 69 DEGREES WEST GEOGRAPHIC IS ZERO MAGNETIC LONGITUDE
C XMLT THE MAGNETIC LATITUDE IN DEGREES.
C
C ARGUMENT LIST
C XX IS A THREE DIMENSION INPUT ARRAY CONTAINING THE POSITION IN
C GEOGRAPHIC COORDINATES
C IF KODE = 1
C     XX(1)=X, XX(2)=Y, XX(3)=Z. X,Y,Z ARE IN EARTH RADII Z IS THE
C     GEOGRAPHIC N. POLE X IS IN THE MERIDIAN OF GREENWICH Y=X CROSS Z
C IF KODE = 2
C     XX(1)=R, XX(2)=COLATITUDE IN DEGREES, XX(3)=LONGITUDE IN DEGREES
C     R IS IN EARTH RADII, LONGITUDE IS 0-360 + IS EAST OF GREENWICH
C     B IS A THREE DIMENSIONED OUTPUT ARRAY CONTAINING VECTOR FIELD
C     IF KODE = 1
C         B(1)=BX, B(2)=BY, B(3)=BZ B IS CARTISIAN AND IN GAUSS
C     IF KODE = 2
C         B(1)=BR (OUTWARD), B(2)=BTHETA (SOUTH), B(3)=BPHI (EAST) IN GAUSS
C     BMAG IS THE MAGNITIDUE OF THE FIELD IN GAUSS
C FOR FURTHER INFORMATION CALL OR WRITE K.A. PFITZER AT MCDONNELL
C DOUGLAS IN HUNTINGTON BEACH CALIFORNIA (714) 896-3231
C DIMENSION X(3),B(3),XX(3)
C COMMON/BXYZCM/YEAR,DAYYR,UT,XMLG,KODE,JSW,INITL,XMLT
C COMMON /GCOM/ ST,CT,SP,CP,AOR,BT,BP,BR,NMAX
C DATA PICON/57.29577951/,SIND,COSD/.2027872954,.9792228106/,
C *S69,C69/.9335804265,.3583679495/,UTLST,DAYLST/2*123456./
C IF EITHER TIME OF DAY OR DAY OF YEAR HAS CHANGED -- UPDATE THE TILT
C IF(UT.EQ.UTLST.AND.DAYYR.EQ.DAYLST) GO TO 1
C UTLST=UT
C DAYLST=DAYYR
C CALL ANGLE (TILT,SPS,CPS)
C IF(KODE.GT.1) GO TO 3
C CARTESIAN ENTRY

```

```

X(1)=XX(1)
X(2)=XX(2)
X(3)=XX(3)
R2=X(1)**2+X(2)**2
R=SQRT(X(3)**2+R2)
R2=SQRT(R2)
CT=X(3)/R
ST=R2/R
CP=X(1)/R2
SP=X(2)/R2
GO TO 5
C SPHERICAL ENTRY
3   R=XX(1)
    THETAG=XX(2)/PICON
    PHIG=XX(3)/PICON
    CT=COS(THETAG)
    ST=SIN(THETAG)
    CP=COS(PHIG)
    SP=SIN(PHIG)
    X(1)=R*ST*CP
    X(2)=R*ST*SP
    X(3)=R*CT
C ROTATE THE X-AXIS INTO THE DIPOLE LONG -69
5   BX=0.
    BY=0.
    BZ=0.
    IF(JSW.LT.0.AND.INITL.NE.0) GO TO 9
7   XPP=X(1)*C69-X(2)*S69
    YPP= X(1)*S69+X(2)*C69
C ROTATE THE Z-AXIS INTO THE DIPOLE AXIS (11.8)
    ZP=XPP*SIND+X(3)*COSD
    XP=XPP*COSD-X(3)*SIND
    YP=YPP
    IF(INITL.NE.0) GO TO 6
C IF INITL IS ZERO SET UP XMLG AND XMLT
    XMLG=0.
    IF(YP.NE.0..OR.XP.NE.0.) XMLG=PICON*ATAN2(YP,XP)
    XMLT=90.-ACOS(ZP/R)*PICON
    IF(JSW.LT.0) GO TO 9
C ROTATE X-AXIS BACK TOWARD THE SUN APPROXIMATELY -(180+UT-69)
6   X(1)=XP*CPS-YP*SPS
    X(2)=XP*SPS+YP*CPS
    X(3)=ZP
C GET THE EXTERNAL CONTRIBUTION
    CALL BXYZMU(X,B,TILT)
C ROTATE THE X-AXIS TO THE DIPOLE LONG APPROXIMATELY (180+UT-69)
    BMX=B(1)*CPS+B(2)*SPS
    BMY=-B(1)*SPS+B(2)*CPS
    BMZ=B(3)
C ROTATE THE Z-AXIS BACK TO GEOGRAPHIC THE Z-AXIS (-11.8)
    BGMX=BMX*COSD+BMZ*SIND
    BGMY=BMY
    BGMZ=-BMX*SIND+BMZ*COSD
C ROTATE X-AXIS BACK TOWARD THE GREENWICH MERIDIAN
    BX=BGMX*C69+BGMY*S69
    BY=-BGMX*S69+BGMY*C69
    BZ=BGMZ

```

```

C GET MAIN FIELD
9  CONTINUE
    AOR=1./R
    CALL SPHRCM
C COMBINE MAIN FIELD AND EXTERNAL FIELD
    IF(KODE.GT.1) GO TO 10
C CONVERT COMPONENTS TO CARTESIAN COORDS (X TOWARD GREENWICH MERIDIAN)
    B(1)=(BX+CP*(ST*BR+CT*BT)-SP*BP)*0.00001
    B(2)=(BY+SP*(ST*BR+CT*BT)+CP*BP)*0.00001
    B(3)=(BZ+CT*BR-ST*BT)*0.00001
    GO TO 20
C CONVERT TO SPHERICAL COORDINATES
10   B(1)=(BR+(BX*CP+BY*SP)*ST+BZ*CT)*0.00001
    B(2)=(BT+(BX*CP+BY*SP)*CT-BZ*ST)*0.00001
    B(3)=(BP+BY*CP-BX*SP)*0.00001
20   BMAG=SQRT(B(1)**2+B(2)**2+B(3)**2)
    RETURN
    END

```

SUBROUTINE BXYSMU(XX,BF,TILT)

C
C VERSION 11/01/76
C THIS SUBROUTINE COMPUTES THE MAGNETIC FIELD FROM SOURCES EXTERNAL
C TO THE EARTH. NO INTERNAL FIELD IS INCLUDED IN THIS ROUTINE.
C IT INCLUDES THE FIELD CONTRIBUTIONS FROM THE MAGNETOPAUSE CURRENTS,
C AND CURRENTS DISTRIBUTED THROUGHOUT THE MAGNETOSPHERE (THE TAIL AND
C RING CURRENTS). IT IS VALID FOR ALL TILTS OF THE EARTH'S DIPOLE
C AXIS AND IS VALID DURING QUIET MAGNETIC CONDITIONS.
C A GENERALIZED ORTHONORMAL LEAST SQUARES PROGRAM WAS USED TO FIT THE
C COEFFICIENTS OF A POWER SERIES (INCLUDING EXPONENTIAL TERMS) THROUGH
C FOURTH ORDER IN SPACE AND SECOND ORDER IN TILT.
C THIS EXPANSION HAS BEEN OPTIMIZED FOR THE NEAR EARTH REGION AND
C IS VALID TO 15 EARTH RADII. OUTSIDE OF THIS REGION THE FIELD
C DIVERGES RAPIDLY AND A TEMPLATE SETS THE FIELD TO ZERO.
C IN ORDER TO IMPROVE COMPUTATIONAL SPEED THE FIELD IS SET TO ZERO
C BELOW 2 EARTH RADII. (IN THIS REGION THE MAIN FIELD DOMINATES AND
C THE VARIATIONS EXPRESSED BY THIS EXPANSION ARE NOT SUFICIENTLY
C ACCURATE TO PREDICT VARIATION ON THE EARTH'S SURFACE).
C CALLING SEQUENCE*****
C INPUT PARAMETERS
C XX IS A 3 DIMENSIONED ARRAY GIVING THE POSITION OF THE POINT
C WHERE THE FIELD IS TO BE CALCULATED. XX(1), XX(2), AND XX(3)
C ARE RESPECTIVELY X, Y, AND Z EXPRESSED IN
C EARTH RADII IN SOLAR MAGNETIC COORDINATES. Z IS ALONG THE
C NORTH DIPOLE AXIS, X IS PERPENDICULAR TO Z AND IN THE PLANE
C CONTAINING THE Z AXIS AND THE SUN-EARTH LINE, Y IS PERP. TO X
C AND Z FORMING A RIGHT HANDED COORDINATE SYSTEM. X IS POSITIVE
C IN THE SOLAR DIRECTION.
C TILT IS THE TILT OF THE DIPOLE AXIS IN DEGREES. IT IS THE
C COMPLIMENT OF THE ANGLE BETWEEN THE NORTH DIPOLE AXIS AND
C THE SOLAR DIRECTION (PSI). TILT=90-PSI.
C OUTPUT PARAMETERS
C BF IS THE 3 DIMENSIONED ARRAY CONTAINING THE COMPONENTS OF THE
C FIELD IN SOLAR MAGNETIC COORDINATES. BF(1), BF(2), AND BF(3)
C ARE THE BX,BY, AND BZ COMPONENTS IN GAMMA.
C
DIMENSION BF(3),XX(3),AA(64),BB(64),CC(44),DD(44),EE(64),FF(64),
*A(32),B(32),C(22),D(22),E(32),F(32),TT(4),ITA(32),ITB(22),ITC(32)
DATA (ITA(I),I=1,32) /2,1,2,1,2,2,1,2,1,2,1,2,1,2,2,1,2,2,1,
*2,1,2,1,2,2,2,1/
DATA (ITB(I),I=1,22) /2,1,2,1,2,2,1,2,2,2,1,2,1,2,1,2,2,2,1,2/
DATA (ITC(I),I=1,32) /1,2,1,2,1,1,2,1,2,1,2,1,2,1,1,2,1,1,2,1,1,2/
*1,2,1,2,1,2,1,1,1,2/
DATA (AA(I),I=1,64)/-2.26836E-02,-1.01863E-04, 3.42986E+00, TOTAL
*-3.12195E-04, 9.50629E-03,-2.91512E-06,-1.57317E-03, 8.62856E-08, TOTAL
*-4.26478E-05, 1.62924E-08,-1.27549E-04, 1.90732E-06,-1.65983E-02, TOTAL
* 8.46680E-09,-5.55850E-05, 1.37404E-08, 9.91815E-05, 1.59296E-08, TOTAL
* 4.52864E-07,-7.17669E-09, 4.98627E-05, 3.33662E-10,-5.97620E-02, TOTAL
* 1.60669E-05,-2.29457E-01,-1.43777E-04, 1.09403E-03,-9.15606E-07, TOTAL
* 1.60658E-03,-4.01198E-07,-3.15064E-06, 2.03125E-09, 4.92887E-04, TOTAL
*-1.80676E-07,-1.12022E-03, 5.98568E-07,-5.90009E-06, 5.16504E-09, TOTAL
*-1.48737E-06, 4.83477E-10,-7.44379E-04, 3.82472E-06, 7.41737E-04, TOTAL
*-1.31468E-05,-1.24729E-04, 1.92930E-08,-1.91764E-04,-5.30371E-08, TOTAL
* 1.38186E-05,-2.81594E-08, 7.46386E-06, 2.64404E-08, 2.45049E-04, TOTAL
*-1.81802E-07,-1.00278E-03, 1.98742E-06,-1.16425E-05, 1.17556E-08, TOTAL
*-2.46079E-06,-3.45831E-10, 1.02440E-05,-1.90716E-08,-4.00855E-05, TOTAL

* 1.25818E-07/
 DATA (BB(I), I=1, 64) / 9.47753E-02, 1.45981E-04, -1.82933E+00, TOTAL
 * 5.54882E-04, 5.03665E-03, -2.07698E-06, 1.10959E-01, -3.45837E-05, TOTAL
 * -4.40075E-05, 5.06464E-07, -1.20112E-03, 3.64911E-06, 1.49849E-01, TOTAL
 * -7.44429E-05, 2.46382E-04, 9.65870E-07, -9.54881E-04, 2.43647E-07, TOTAL
 * 3.06520E-04, 3.07836E-07, 6.48301E-03, 1.26251E-06, -7.09548E-03, TOTAL
 * -1.55596E-05, 3.06465E+00, -7.84893E-05, 4.95145E-03, 3.71921E-06, TOTAL
 * -1.52002E-01, 6.81988E-06, -8.55686E-05, -9.01230E-08, -3.71458E-04, TOTAL
 * 1.30476E-07, -1.82971E-01, 1.51390E-05, -1.45912E-04, -2.22778E-07, TOTAL
 * 6.49278E-05, -3.72758E-08, -1.59932E-03, 8.04921E-06, 5.38012E-01, TOTAL
 * -1.43182E-04, 1.50000E-04, 5.88020E-07, -1.59000E-02, 1.60744E-06, TOTAL
 * 3.17837E-04, 1.78959E-07, -8.93794E-03, 6.37549E-06, 1.27887E-03, TOTAL
 * -2.45878E-07, -1.93210E-01, 6.91233E-06, -2.80637E-04, -2.57073E-07, TOTAL
 * 5.78343E-05, 4.52128E-10, 1.89621E-04, -4.84911E-08, -1.50058E-02, TOTAL
 * 6.21772E-06/
 DATA (CC(I), I=1, 44) / -1.88177E-02, -1.92493E-06, -2.89064E-01, TOTAL
 * -8.49439E-05, -4.76380E-04, -4.52998E-08, 1.61086E-03, 3.18728E-07, TOTAL
 * 1.29159E-06, 5.52259E-10, 3.95543E-05, 5.61209E-08, 1.38287E-03, TOTAL
 * 5.74237E-07, 1.86489E-06, 7.10175E-10, 1.45243E-07, -2.97591E-10, TOTAL
 * -2.43029E-03, -6.70000E-07, -2.30624E-02, -6.22193E-06, -2.40815E-05, TOTAL
 * 2.01689E-08, 1.76721E-04, 3.78689E-08, 9.88496E-06, 7.33820E-09, TOTAL
 * 7.32126E-05, 8.43986E-08, 8.82449E-06, -6.11708E-08, 1.78881E-04, TOTAL
 * 8.62589E-07, 3.43724E-06, 2.53783E-09, -2.04239E-07, 8.16641E-10, TOTAL
 * 1.68075E-05, 7.62815E-09, 2.26026E-04, 3.66341E-08, 3.44637E-07, TOTAL
 * 2.25531E-10/
 DATA (DD(I), I=1, 44) / 2.50143E-03, 1.01200E-06, 3.23821E+00, TOTAL
 * 1.08589E-05, -3.39199E-05, -5.27052E-07, -9.46161E-02, -1.95413E-09, TOTAL
 * -4.23614E-06, 1.43153E-08, -2.62948E-04, 1.05138E-07, -2.15784E-01, TOTAL
 * -2.20717E-07, -2.65687E-05, 1.26370E-08, 5.88917E-07, -1.13658E-08, TOTAL
 * 1.64385E-03, 1.44263E-06, -1.66045E-01, -1.46096E-05, 1.22811E-04, TOTAL
 * 3.43922E-08, 9.66760E-05, -6.32150E-07, -4.97400E-05, -2.78578E-08, TOTAL
 * 1.77366E-02, 2.05401E-07, -1.91756E-03, -9.49392E-07, -1.99488E-01, TOTAL
 * -2.07170E-06, -5.40443E-05, 1.59289E-08, 7.30914E-05, 3.38786E-08, TOTAL
 * -1.59537E-04, -1.65504E-07, 1.90940E-02, 2.03238E-06, 1.01148E-04, TOTAL
 * 5.20815E-08/
 DATA (EE(I), I=1, 64) / -2.77924E+01, -1.01457E-03, 9.21436E-02, TOTAL
 * -8.52177E-06, 5.19106E-01, 8.28881E-05, -5.59651E-04, 1.16736E-07, TOTAL
 * -2.11206E-03, -5.35469E-07, 4.41990E-01, -1.33679E-05, -7.18642E-04, TOTAL
 * 6.17358E-08, -3.51990E-03, -5.29070E-07, 1.88443E-06, -6.60696E-10, TOTAL
 * -1.34708E-03, 1.02160E-07, 1.58219E-06, 2.05040E-10, 1.18039E+00, TOTAL
 * 1.58903E-04, 1.86944E-02, -4.46477E-06, 5.49869E-02, 4.94690E-06, TOTAL
 * -1.18335E-04, 6.95684E-09, -2.73839E-04, -9.17883E-08, 2.79126E-02, TOTAL
 * -1.02567E-05, -1.25427E-04, 3.07143E-08, -5.31826E-04, -2.98476E-08, TOTAL
 * -4.89899E-05, 4.91480E-08, 3.85563E-01, 4.16966E-05, 6.74744E-04, TOTAL
 * -2.08736E-07, -3.42654E-03, -3.13957E-06, -6.31361E-06, -2.92981E-09, TOTAL
 * -2.63883E-03, -1.32235E-07, -6.19406E-06, 3.54334E-09, 6.65986E-03, TOTAL
 * -5.81949E-06, -1.88809E-04, 3.62055E-08, -4.64380E-04, -2.21159E-07, TOTAL
 * -1.77496E-04, 4.95560E-08, -3.18867E-04, -3.17697E-07, -1.05815E-05, TOTAL
 * 2.22220E-09/
 DATA (FF(I), I=1, 64) / -5.07092E+00, 4.71960E-03, -3.79851E-03, TOTAL
 * -3.67309E-06, -6.02439E-01, 1.08490E-04, 5.09287E-04, 5.62210E-07, TOTAL
 * 7.05718E-02, 5.13160E-06, -2.85571E+00, -4.31728E-05, 1.03185E-03, TOTAL
 * 1.05332E-07, 1.04106E-02, 1.60749E-05, 4.18031E-05, 3.32759E-08, TOTAL
 * 1.20113E-01, 1.40486E-05, -3.37993E-05, 5.48340E-09, 9.10815E-02, TOTAL
 * -4.00608E-04, 3.75393E-03, -4.69939E-07, -2.48561E-02, 1.31836E-04, TOTAL
 * -2.67755E-04, -7.60285E-08, 3.04443E-03, -3.28956E-06, 5.82367E-01, TOTAL
 * 5.39496E-06, -6.15261E-04, 4.05316E-08, 1.13546E-02, -4.26493E-06, TOTAL

```

*-2.72007E-02, 5.72523E-08,-2.98576E+00, 3.07325E-05, 1.51645E-03, TOTAL
* 1.25098E-06, 4.07213E-02, 1.05964E-05, 1.04232E-04, 1.77381E-08, TOTAL
* 1.92781E-01, 2.15734E-05,-1.65741E-05,-1.88683E-09, 2.44803E-01, TOTAL
* 1.51316E-05,-3.01157E-04, 8.47006E-08, 1.86971E-02,-6.94074E-06, TOTAL
* 9.13198E-03,-2.38052E-07, 1.28552E-01, 6.92595E-06,-8.36792E-05, TOTAL
*-6.10021E-08/
      DATA TILTTL/99./

```

C

```

X=XX(1)
Y=XX(2)
Z=XX(3)
Y2=Y**2
Z2=Z**2
R2=X**2+Y2+Z2
BX=0.
BY=0.
BZ=0.

```

C TEST FOR LOCATION OF INPUT POSITION

C IF THE LOCATION IS OUTSIDE THE REGION OF SERIES CONVERGENCE SET
C THE MAGNETIC FIELD TO ZERO AND PRINT AN ERROR MESSAGE

CON=1.

```

IF(R2.GT.225.) GO TO 50
IF(R2.LT.4.)GO TO 40

```

C TAPER THE FIELD LINEARLY TO ZERO IF INSIDE R = 2.5.

```

IF(R2.LT.6.25) CON=CON*(R2-4.0)/2.25
IF(TILTTL.EQ.TILT)GO TO 6
TILTTL=TILT

```

C IF THE TILT HAS CHANGED UPDATE THE COEFFICIENTS.

TT(1)=1

TT(2)=TILTTL

TT(3)=TILTTL**2

TT(4)=TILT*T(3)

DO 1 I=1,32

J=(I-1)*2+1

K=ITA(I)

A(I)=AA(J)*TT(K)+AA(J+1)*TT(K+2)

B(I)=BB(J)*TT(K)+BB(J+1)*TT(K+2)

K=ITC(I)

E(I)=EE(J)*TT(K)+EE(J+1)*TT(K+2)

F(I)=FF(J)*TT(K)+FF(J+1)*TT(K+2)

DO 2 I=1,22

J=(I-1)*2+1

K=ITB(I)

C(I)=CC(J)*TT(K)+CC(J+1)*TT(K+2)

2 D(I)=DD(J)*TT(K)+DD(J+1)*TT(K+2)

C CALCULATED THE FIELD FROM THE POLYNOMIAL EXPANSION

6 EXPR=EXP(-0.06*R2)

II=1

JJ=1

KK=1

XB=1.

DO 30 I=1,5

YEXB=XB

DO 20 J=1,3

IF(I+2+J.GT. 8) GO TO 30

ZEXXB=YEXB

IJK=I+2+J+1

```

K=0
10  BZ=BZ+( E(KK)+F(KK)*EXPR )*ZEYEXB
    KK=KK+1
    BX=BX+( A(II)+B(II)*EXPR )*ZEYEXB
    II=II+1
    IF( IJK .GT. 8 ) GO TO 20
    BY=BY+( C(JJ)+D(JJ)*EXPR )*ZEYEXB*Y
    JJ=JJ+1
15  ZEYEXB=ZEYEXB*Z
    IJK=IJK+1
    K=K+1
    IF( IJK.LE.9 .AND. K.LE.4 ) GO TO 10
20  YEXB=YEXB*Y2
30  XB=XB*X
40  BF(1)=BX*CON
    BF(2)=BY*CON
    BF(3)=BZ*CON
    RETURN
C   ERROR EXIT
50  WRITE(6,60) XX
60  FORMAT(4H X= ,E10.3,4H Y= ,E10.3,4H Z= ,E10.3,76H IS OUTSIDE THE
     *VALID REGION--POWER SERIES DIVERGES BFIELD IS SET TO ZERO  )
     GO TO 40
END

```



```

DATA GTT/0.,-.35,.15,.35,0.,.51,-.51,0.,0.,0.,.25,0.,0.,0.,.47,.71
*,-.38,0.,0.,-.59,0.,-.07,.31,0.,.54,-.9,0.,0.,0.,-.2,0.,0.,0.,.
*15,.24,-.55,0.,0.,0.,-.83,0.,0.,-.06,.06,0.,0.,0.,0.,.71,-.38,0
*,0.,-.04,0.,-.1,0.,0.,0.,0.,.5,0.,0.,0.,0.,0.,0.,0.,0.,0.,0.,0.,0.,0
*,0.,0.,0.,0.,0.,0.,0.,0.,0.,0.,0.,0.,0.,0.,0.,0.,0.,0.,0.,0.,0.,0.,0
*,0.,0.,0.,0./

C SET UP INITIAL CONSTANTS DURING FIRST CALL
IF(IFIRST.NE.0) GO TO 199
IFIRST=1
FM(1)=0
DO 6 N=2,10
FM(N)=N-1
FN(N)=N
DO 6 M=1,N
6 CONST(N,M)=FLOAT((N-2)**2-(M-1)**2)/FLOAT((2*N-3)*(2*N-5))
C SET UP THE COEFFICIENTS
C IF YEAR HAS CHANGED BY MORE THAN .1YEAR UPDATE THE COEFFICINTS.
199 IF(ABS(YRLAST-YEAR).LT.0.1) GO TO 230
IF(YEAR.GE.TF.AND.YEAR.LE.TL) GO TO 210
WRITE(6,200) YEAR
200 FORMAT(10H0**WARNING,F7.1,23H IS OUTSIDE TIME LIMITS)
210 T=YEAR-TZERO
DO 220 N=1,NMAX
DO 220 M=1,NMAX
220 G(N,M)=GO(N,M)+T*(GT(N,M)+T*GTT(N,M))
YRLAST=YEAR
C
230 AR=AOR*AOR*AOR
AR=AOR*AOR*AOR
C2=G(2,2)*CPH+G(1,2)*SPH
BR=-(AR+AR)*(G(2,1)*CT+C2*ST)
BT=AR*(C2*CT-G(2,1)*ST)
BP=AR*(G(1,2)*CPH-G(2,2)*SPH)
IF (NMAX.LE.2) RETURN
R=1./AOR
IF(R.GT.CONA(2)) RETURN
CON=0.
SP2=SPH
CP2=CPH
P21=CT
P22=ST
DP21=-ST
DP22=CT
N=3
SP3=(SP2+SP2)*CP2
CP3=(CP2+SP2)*(CP2-SP2)
P31=CT*P21-CONST(3,1)
P32=CT*P22
P33=ST*P22
DP31=-P32-P32
DP32=CT*DP22-P33
DP33=-DP31
C2=G(3,2)*CP2+G(1,3)*SP2
C3=G(3,3)*CP3+G(2,3)*SP3
AR=AOR*AR
XR=BR-FN(3)*AR*(G(3,1)*P31+C2*P32+C3*P33)
XT=BT+AR*(G(3,1)*DP31+C2*DP32+C3*DP33)

```

1-00006
1-00007
1-00008
1-00009
1-00010
1-00011
1-00012
1-00013
1-00014
1-00015
1-00016
1-00017
1-00019
1-00020
1-00021
1-00022
1-00023
1-00024
1-00025
1-00026
1-00027
1-00028
1-00029
1-00030
1-00031

```

XP=BP-AR*(FM(2)*(G(3,2)*SP2-G(1,3)*CP2)*P21+FM(3)*(G(3,3)*SP3-G(2,1-00032
+3)*CP3)*P22) 1-00033
BP=BP*ST 1-00035
XP=XP*ST 1-00035
IF(NMAX.LE.3) GO TO 21
IF(R.GT.CONA(3)) GO TO 20
N=4
SP4=SPH*CP3+CPH*SP3 1-00037
CP4=CPH*CP3-SPH*SP3 1-00038
P41=CT*P31-CONST(4,1)*P21 1-00039
DP41=CT*DP31-ST*P31-CONST(4,1)*DP21 1-00040
P42=CT*P32-CONST(4,2)*P22 1-00041
DP42=CT*DP32-ST*P32-CONST(4,2)*DP22 1-00042
P43=CT*P33 1-00043
DP43=CT*DP33-ST*P33 1-00044
P44=ST*P33 1-00045
DP44=FM(4)*P43 1-00046
C2=G(4,2)*CP2+G(1,4)*SP2 1-00047
C3=G(4,3)*CP3+G(2,4)*SP3 1-00048
C4=G(4,4)*CP4+G(3,4)*SP4 1-00049
AR=AOR*AR 1-00050
BR=XR-FN(4)*AR*(G(4,1)*P41+C2*P42+C3*P43+C4*P44) 1-00051
BT=XT+AR*(G(4,1)*DP41+C2*DP42+C3*DP43+C4*DP44) 1-00052
BP=XP-AR*(FM(2)*(G(4,2)*SP2-G(1,4)*CP2)*P42+FM(3)*(G(4,3)*SP3-G(2,1-00053
+4)*CP3)*P43+FM(4)*(G(4,4)*SP4-G(3,4)*CP4)*P44) 1-00054
IF(NMAX.LE.4) GO TO 11
IF(R.GT.CONA(4)) GO TO 10
N=5
SP5=(SP3+SP3)*CP3 1-00057
CP5=(CP3+SP3)*(CP3-SP3) 1-00058
P51=CT*P41-CONST(5,1)*P31 1-00059
DP51=CT*DP41-ST*P41-CONST(5,1)*DP31 1-00060
P52=CT*P42-CONST(5,2)*P32 1-00061
DP52=CT*DP42-ST*P42-CONST(5,2)*DP32 1-00062
P53=CT*P43-CONST(5,3)*P33 1-00063
DP53=CT*DP43-ST*P43-CONST(5,3)*DP33 1-00064
P54=CT*P44 1-00065
DP54=CT*DP44-ST*P44 1-00066
P55=ST*P44 1-00067
DP55=FM(5)*P54 1-00068
C2=G(5,2)*CP2+G(1,5)*SP2 1-00069
C3=G(5,3)*CP3+G(2,5)*SP3 1-00070
C4=G(5,4)*CP4+G(3,5)*SP4 1-00071
C5=G(5,5)*CP5+G(4,5)*SP5 1-00072
AR=AOR*AR 1-00073
XR=BR-FN(5)*AR*(G(5,1)*P51+C2*P52+C3*P53+C4*P54+C5*P55) 1-00074
XT=BT+AR*(G(5,1)*DP51+C2*DP52+C3*DP53+C4*DP54+C5*DP55) 1-00075
XP=BP-AR*(FM(2)*(G(5,2)*SP2-G(1,5)*CP2)*P52+FM(3)*(G(5,3)*SP3-G(2,1-00076
+5)*CP3)*P53+FM(4)*(G(5,4)*SP4-G(3,5)*CP4)*P54+FM(5)*(G(5,5)*SP5-G(1-00077
+4,5)*CP5)*P55) 1-00078
IF(NMAX.LE.5) GO TO 21
IF(R.GT.CONA(5)) GO TO 20
N=6
SP6=SPH*CP5+CPH*SP5 1-00081
CP6=CPH*CP5-SPH*SP5 1-00082
P61=CT*P51-CONST(6,1)*P41 1-00083
DP61=CT*DP51-ST*P51-CONST(6,1)*DP41 1-00084

```

```

P62=CT*P52-CONST(6,2)*P42 1-00085
DP62=CT*DP52-ST*P52-CONST(6,2)*DP42 1-00086
P63=CT*P53-CONST(6,3)*P43 1-00087
DP63=CT*DP53-ST*P53-CONST(6,3)*DP43 1-00088
P64=CT*P54-CONST(6,4)*P44 1-00089
DP64=CT*DP54-ST*P54-CONST(6,4)*DP44 1-00090
P65=CT*P55 1-00091
DP65=CT*DP55-ST*P55 1-00092
P66=ST*P55 1-00093
DP66=FM(6)*P65 1-00094
C2=G(6,2)*CP2+G(1,6)*SP2 1-00095
C3=G(6,3)*CP3+G(2,6)*SP3 1-00096
C4=G(6,4)*CP4+G(3,6)*SP4 1-00097
C5=G(6,5)*CP5+G(4,6)*SP5 1-00098
C6=G(6,6)*CP6+G(5,6)*SP6 1-00099
AR=AOR*AR 1-00100
BR=XR-FN(6)*AR*(G(6,1)*P61+C2*P62+C3*P63+C4*P64+C5*P65+C6*P66) 1-00101
BT=XT+AR*(G(6,1)*DP61+C2*DP62+C3*DP63+C4*DP64+C5*DP65+C6*DP66) 1-00102
BP=XP-AR*(FM(2)*(G(6,2)*SP2-G(1,6)*CP2)*P62+FM(3)*(G(6,3)*SP3-G(2,1-00103
+6)*CP3)*P63+FM(4)*(G(6,4)*SP4-G(3,6)*CP4)*P64+FM(5)*(G(6,5)*SP5-G(1-00104
+4,6)*CP5)*P65+FM(6)*(G(6,6)*SP6-G(5,6)*CP6)*P66) 1-00105
IF(NMAX.LE.6) GO TO 11
IF(R.GT.CONA(6)) GO TO 10
N=7
SP7=(SP4+SP4)*CP4 1-00108
CP7=(CP4+SP4)*(CP4-SP4) 1-00109
P71=CT*P61-CONST(7,1)*P51 1-00110
DP71=CT*DP61-ST*P61-CONST(7,1)*DP51 1-00111
P72=CT*P62-CONST(7,2)*P52 1-00112
DP72=CT*DP62-ST*P62-CONST(7,2)*DP52 1-00113
P73=CT*P63-CONST(7,3)*P53 1-00114
DP73=CT*DP63-ST*P63-CONST(7,3)*DP53 1-00115
P74=CT*P64-CONST(7,4)*P54 1-00116
DP74=CT*DP64-ST*P64-CONST(7,4)*DP54 1-00117
P75=CT*P65-CONST(7,5)*P55 1-00118
DP75=CT*DP65-ST*P65-CONST(7,5)*DP55 1-00119
P76=CT*P66 1-00120
DP76=CT*DP66-ST*P66 1-00121
P77=ST*P66 1-00122
DP77=FM(7)*P76 1-00123
C2=G(7,2)*CP2+G(1,7)*SP2 1-00124
C3=G(7,3)*CP3+G(2,7)*SP3 1-00125
C4=G(7,4)*CP4+G(3,7)*SP4 1-00126
C5=G(7,5)*CP5+G(4,7)*SP5 1-00127
C6=G(7,6)*CP6+G(5,7)*SP6 1-00128
C7=G(7,7)*CP7+G(6,7)*SP7 1-00129
AR=AOR*AR 1-00130
XR=BR-FN(7)*AR*(G(7,1)*P71+C2*P72+C3*P73+C4*P74+C5*P75+C6*P76+C7*P1-00131
+77) 1-00132
XT=BT+AR*(G(7,1)*DP71+C2*DP72+C3*DP73+C4*DP74+C5*DP75+C6*DP76+C7*D1-00133
+P77) 1-00134
XP=BP-AR*(FM(2)*(G(7,2)*SP2-G(1,7)*CP2)*P72+FM(3)*(G(7,3)*SP3-G(2,1-00135
+7)*CP3)*P73+FM(4)*(G(7,4)*SP4-G(3,7)*CP4)*P74+FM(5)*(G(7,5)*SP5-G(1-00136
+4,7)*CP5)*P75+FM(6)*(G(7,6)*SP6-G(5,7)*CP6)*P76+FM(7)*(G(7,7)*SP7-1-00137
+G(6,7)*CP7)*P77) 1-00138
IF(NMAX.LE.7) GO TO 21
IF(R.GT.CONA(7)) GO TO 20

```

N=8
 SP8=SPH*CP7+CPH*SP7 1-00141
 CP8=CPH*CP7-SPH*SP7 1-00142
 P81=CT*P71-CONST(8,1)*P61 1-00143
 DP81=CT*DP71-ST*P71-CONST(8,1)*DP61 1-00144
 P82=CT*P72-CONST(8,2)*P62 1-00145
 DP82=CT*DP72-ST*P72-CONST(8,2)*DP62 1-00146
 P83=CT*P73-CONST(8,3)*P63 1-00147
 DP83=CT*DP73-ST*P73-CONST(8,3)*DP63 1-00148
 F84=CT*P74-CONST(8,4)*P64 1-00149
 DP84=CT*DP74-ST*P74-CONST(8,4)*DP64 1-00150
 P85=CT*P75-CONST(8,5)*P65 1-00151
 DP85=CT*DP75-ST*,75-CONST(8,5)*DP65 1-00152
 P86=CT*P76-CONST(8,6)*P66 1-00153
 DP86=CT*DP76-ST*P76-CONST(8,6)*DP66 1-00154
 P87=CT*P77 1-00155
 DP87=CT*DP77-ST*P77 1-00156
 P88=ST*P77 1-00157
 DP88=FM(8)*P87 1-00158
 C2=G(8,2)*CP2+G(1,8)*SP2 1-00159
 C3=G(8,3)*CP3+G(2,8)*SP3 1-00160
 C4=G(8,4)*CP4+G(3,8)*SP4 1-00161
 C5=G(8,5)*CP5+G(4,8)*SP5 1-00162
 C6=G(8,6)*CP6+G(5,8)*SP6 1-00163
 C7=G(8,7)*CP7+G(6,8)*SP7 1-00164
 C8=G(8,8)*CP8+G(7,8)*SP8 1-00165
 AR=AOR*AR 1-00166
 BR=XR-FN(8)*AR*(G(8,1)*P81+C2*P82+C3*P83+C4*P84+C5*P85+C6*P86+C7*P1-00167
 +87+C8*P88) 1-00168
 BT=XT+AR*(G(8,1)*DP81+C2*DP82+C3*DP83+C4*DP84+C5*DP85+C6*DP86+C7*D1-00169
 +P87+C8*DP88) 1-00170
 BP=XP-AR*(FM(2)*(G(8,2)*SP2-G(1,8)*CP2)*P82+FM(3)*(G(8,3)*SP3-G(2,1-00171
 +8)*CP3)*P83+FM(4)*(G(8,4)*SP4-G(3,8)*CP4)*P84+FM(5)*(G(8,5)*SP5-G(1-00172
 +4,8)*CP5)*P85+FM(6)*(G(8,6)*SP6-G(5,8)*CP6)*P86+FM(7)*(G(8,7)*SP7-1-00173
 +G(6,8)*CP7)*P87+FM(8)*(G(8,8)*SP8-G(7,8)*CP8)*P88) 1-00174
 IF(NMAX.LE.8) GO TO 11
 IF(R.GT.CONA(8)) GO TO 10
N=9
 SP9=(SP5+SP5)*CP5 1-00177
 CP9=(CP5+SP5)*(CP5-SP5) 1-00178
 P91=CT*P81-CONST(9,1)*P71 1-00179
 DP91=CT*DP81-ST*P81-CONST(9,1)*DP71 1-00180
 P92=CT*P82-CONST(9,2)*P72 1-00181
 DP92=CT*DP82-ST*P82-CONST(9,2)*DP72 1-00182
 P93=CT*P83-CONST(9,3)*P73 1-00183
 DP93=CT*DP83-ST*P83-CONST(9,3)*DP73 1-00184
 P94=CT*P84-CONST(9,4)*P74 1-00185
 DP94=CT*DP84-ST*P84-CONST(9,4)*DP74 1-00186
 P95=CT*P85-CONST(9,5)*P75 1-00187
 DP95=CT*DP85-ST*P85-CONST(9,5)*DP75 1-00188
 P96=CT*P86-CONST(9,6)*P76 1-00189
 DP96=CT*DP86-ST*P86-CONST(9,6)*DP76 1-00190
 P97=CT*P87-CONST(9,7)*P77 1-00191
 DP97=CT*DP87-ST*P87-CONST(9,7)*DP77 1-00192
 P98=CT*P88 1-00193
 DP98=CT*DP88-ST*P88 1-00194
 P99=ST*P88 1-00195

```

DP99=FM(9)*P98 1-00196
C2=G(9,2)*CP2+G(1,9)*SP2 1-00197
C3=G(9,3)*CP3+G(2,9)*SP3 1-00198
C4=G(9,4)*CP4+G(3,9)*SP4 1-00199
C5=G(9,5)*CP5+G(4,9)*SP5 1-00200
C6=G(9,6)*CP6+G(5,9)*SP6 1-00201
C7=G(9,7)*CP7+G(6,9)*SP7 1-00202
C8=G(9,8)*CP8+G(7,9)*SP8 1-00203
C9=G(9,9)*CP9+G(8,9)*SP9 1-00204
AR=AOR*AR 1-00205
XR=BR-FN(9)*AR*(G(9,1)*P91+C2*P92+C3*P93+C4*P94+C5*P95+C6*P96+C7*P1-00206
+97+C8*P98+C9*P99) 1-00207
XT=BT+AR*(G(9,1)*DP91+C2*DP92+C3*DP93+C4*DP94+C5*DP95+C6*DP96+C7*DP1-00208
+P97+C8*DP98+C9*DP99) 1-00209
XP=BP-AR*(FM(2)*(G(9,2)*SP2-G(1,9)*CP2)*P92+FM(3)*(G(4,3)*SP3-G(2,1-00210
+9)*CP3)*P93+FM(4)*(G(9,4)*SP4-G(3,9)*CP4)*P94+FM(5)*(G(9,5)*SP5-G(1-00211
+4,9)*CP5)*P95+FM(6)*(G(9,6)*SP6-G(5,9)*CP6)*P96+FM(7)*(G(9,7)*SP7-1-00212
+G(6,9)*CP7)*P97+FM(8)*(G(9,8)*SP8-G(7,9)*CP8)*P98+FM(9)*(G(9,9)*SP1-00213
+9-G(8,9)*CP9)*P99) 1-00214
IF(NMAX.LE.9) GO TO 21
IF(R.GT.CONA(9)) GO TO 20
N=10
SP10=SPH*CP9+CPH*SP9 1-00217
CP10=CPH*CP9-SPH*SP9 1-00218
P101=CT*P91-CONST(10,1)*P81 1-00219
DP101=CT*DP91-ST*P91-CONST(10,1)*DP81 1-00220
P102=CT*P92-CONST(10,2)*P82 1-00221
DP102=CT*DP92-ST*P92-CONST(10,2)*DP82 1-00222
P103=CT*P93-CONST(10,3)*P83 1-00223
DP103=CT*DP93-ST*P93-CONST(10,3)*DP83 1-00224
P104=CT*P94-CONST(10,4)*P84 1-00225
DP104=CT*DP94-ST*P94-CONST(10,4)*DP84 1-00226
P105=CT*P95-CONST(10,5)*P85 1-00227
DP105=CT*DP95-ST*P95-CONST(10,5)*DP85 1-00228
P106=CT*P96-CONST(10,6)*P86 1-00229
DP106=CT*DP96-ST*P96-CONST(10,6)*DP86 1-00230
P107=CT*P97-CONST(10,7)*P87 1-00231
DP107=CT*DP97-ST*P97-CONST(10,7)*DP87 1-00232
P108=CT*P98-CONST(10,8)*P88 1-00233
DP108=CT*DP98-ST*P98-CONST(10,8)*DP88 1-00234
P109=CT*P99 1-00235
DP109=CT*DP99-ST*P99 1-00236
P1010=ST*P99 1-00237
DP1010=FM(10)*P109 1-00238
C2=G(10,2)*CP2+G(1,10)*SP2 1-00239
C3=G(10,3)*CP3+G(2,10)*SP3 1-00240
C4=G(10,4)*CP4+G(3,10)*SP4 1-00241
C5=G(10,5)*CP5+G(4,10)*SP5 1-00242
C6=G(10,6)*CP6+G(5,10)*SP6 1-00243
C7=G(10,7)*CP7+G(6,10)*SP7 1-00244
C8=G(10,8)*CP8+G(7,10)*SP8 1-00245
C9=G(10,9)*CP9+G(8,10)*SP9 1-00246
C10=G(10,10)*CP10+G(9,10)*SP10 1-00247
AR=AOR*AR 1-00248
BR=XR-FN(10)*AR*(G(10,1)*P101+C2*P102+C3*P103+C4*P104+C5*P105+C6*P1-00249
+106+C7*P107+C8*P108+C9*P109+C10*P1010) 1-00250
BT=XT+AR*(G(10,1)*DP101+C2*DP102+C3*DP103+C4*DP104+C5*DP105+C6*DP11-00251

```

```

+06+C7*DP107+C8*DP108+C9*DP109+C10*DP1010) 1-00252
BP=XP-AR*(FM(2)*(G(10,2)*SP2-G(1,10)*CP2)*P102+FM(3)*(G(10,3)*SP3-1-00253
+G(2,10)*CP3)*P103+FM(4)*(G(10,4)*SP4-G(3,10)*CP4)*P104+FM(5)*(G(101-00254
+,5)*SP5-G(4,10)*CP5)*P105+FM(6)*(G(10,6)*SP6-G(5,1)*CP6)*P106+FM(1-00255
+7)*(G(10,7)*SP7-G(6,10)*CP7)*P107+FM(8)*(G(10,8)*SP8-G(7,10)*CP8)*1-00256
+P108+FM(9)*(G(10,9)*SP9-G(8,10)*CP9)*P109+FM(10)*(G(10,10)*SP10-G(1-00257
+9,10)*CP10)*P1010) 1-00258
1 BP=BP/ST 1-00474
IF(NMAX.LE.10) RETURN
WRITE (6,2) NMAX
STOP
C 1-00476
2 FORMAT(57HO ERROR, THIS SPHRC ONLY FOR NMAX=<10, CALL WAS FOR NMAX
*=,15)
C MAKE A SMOOTH FIT BETWEEN TRUNCATED TERMS.
10 CON=(R-CONA(N))/(CONA(N-1)-CONA(N))
11 BR=BR+(XR-BR)*CON
BT=BT+(XT-BT)*CON
BP=(BP+(XP-BP)*CON)/ST
RETURN
20 CON=(R-CONA(N))/(CONA(N-1)-CONA(N))
21 BR=BR+(BR-XR)*CON
BT=BT+(BT-XT)*CON
BP=(XP+(BP-XP)*CON)/ST
RETURN
END 1-00477
1-00478
1-00479

```

```

SUBROUTINE ANGLE(TILT,SINPHE,COSPHE)
C THIS ROUTINE CALCULATES THE ANGLE BETWEEN THE DIPOLE AXIS AND THE
C SUN-EARTH LINE AS WELL AS THE ROTATION SINES AND COSINES TO CONVERT
C FROM GEOMAGNETIC TO SOLAR MAGNETIC COORDINATES.
C INPUT PARAMETERS ARE VIA COMMON/BXYZCM/
C DAYYR IS THE DAY OF YEAR (1-366.). IT MUST BE A WHOLE NUMBER.
C DAY 1 IS JANUARY 1
C UT IS THE UNIVERSAL TIME IN HOURS (0.-24.)
C OUTPUT PARAMETERS ARE VIA THE PARAMETER LIST IN THE ARGUMENTS
C TILT IS 90-PSI. WHERE PSI IS THE ANGLE BETWEEN THE DIPOLE AXIS
C AND THE SOLAR DIRECTION.
C SINPHE SIN(BETA)
C COSPHE COS(BETA) BETA IS THE ROTATION ANGLE FROM GEOMAGNETIC
C TO SOLAR MAGNETIC COORDINATES
COMMON/BXYZCM/YEAR,DAYYR,UT,XMLG,KODE,JSW,INITL,XMLT
DATA IFIRST/0/
C THE FIRST TIME THROUGH THE SUBROUTINE SET UP FIXED CONSTANTS.
IF(IFIRST.NE.0) GO TO 10
IFIRST=1
PI2=ATAN2(0.,-1.)/2.
CON=90./PI2
SALF=SIN(11.7/CON)
CALF=COS(11.7/CON)
SGAM=SIN(23.5/CON)
CGAM=COS(23.5/CON)
SASG=SALF*SGAM
SACG=SALF*CGAM
CASG=CALF*SGAM
CACG=CALF*CGAM
W=PI2/6.*(1.+1./365.256)
C MAIN ENTRY SET UP SINES AND COSINES
10 WT=(UT-16.6+(DAYYR-172.)*24.)*W
CWT=-WT/365.256
SSMLT=SIN(WT)
CSMLT=COS(WT)
SBWT=SIN(CWT)
CBWT=COS(CWT)
SMLSWT=SSMLT*SBWT
SMLCWT=SSMLT*CBWT
CMLSWT=CSMLT*SBWT
CMLCWT=CSMLT*CBWT
C COMPONENTS OF THE DIPOLE AXIS ARE IN ECLIPTIC COORDINATES
ZX=CASG*CBWT+SACG*CMLCWT-SALF*SMLSWT
ZY=CASG*SBWT+SACG*CMLCWT+CALF*SMLCWT
ZZ=CACG-SASG*CSMLT
PSI=ACOS(ZX)
OSP=1./(SIN(PSI))
TILT=CON*(PI2-PSI)
C COMPONENTS OF GEOMAGNETIC X AXIS IN ECLIPTIC COORDINATES
XX=CACG*CMLCWT-SASG*CBWT-CALF*SMLSWT
XY=CACG*CMLCWT-SASG*SBWT+CALF*SMLCWT
XZ=-CASG*CSMLT-SACG
SINPHE=(XY*ZZ-XZ*ZY)*OSP
COSPHE=(XX*(ZZ*ZZ+ZY*ZY)-ZX*(XY*ZY+XZ*ZZ))*OSP
RETURN
END

```

```

SUBROUTINE INTERP(BB,CC,D,E,J)
C
C   INTERPOLATION ROUTINE
C   GIVEN A SET OF THREE POINTS BB(3) AND CC(3), WITH CC THE INDEPENDENT
C   VARIABLES X AND BB THE DEPENDENT VARIABLE Y, INTERP FINDS THE SOLUTION
C   TO THE THREE LINEAR EQUATION EXPRESSING Y AS A SECOND ORDER
C   POLYNOMIAL OF X.
C   IF J LESS THAN ZERO, SET D TO THE MINIMUM VALUE OF THE DEPENDENT
C   VARIABLE
C   IF J GREATER THAN ZERO SET D TO THE VALUE OF THE INDEPENDENT
C   VARIABLE SUCH THAT THE DEPENDENT VARIABLE Y EQUALS E.
C   SINCE THERE ARE TWO ROOTS TO THE EQUATION CHOOSE THE ONE
C   CLOSEST TO CC(K), WHERE K=3 IF J=1, K=2 IF J=4, K=1 IF J=2.
C
C   DIMENSION BB(3),CC(3)
Y1=ALOG(BB(1))
Y2=ALOG(BB(2))
Y3=ALOG(BB(3))
X2=CC(2)-CC(1)
X3=CC(3)-CC(1)
DD=(X3-X2)*X2*X3
A=(X3*(Y1-Y2)+X2*(Y3-Y1))/DD
B=(X3**2*(Y2-Y1)-X2**2*(Y3-Y1))/DD
IF(J.LT.0)GO TO 100
C=Y1-ALOG(D)
DIS=B**2-4.*A*C
IF(DIS.LE.0.)STOP
DIS=SQRT(DIS)
SA=(-B+DIS)/(2.*A)+CC(1)
SB=(-B-DIS)/(2.*A)+CC(1)
E=SA
K=3
IF(J.EQ.4) K=2
IF(J.EQ.2) K=1
IF(ABS(SB-CC(K)).LT.ABS(SA-CC(K)))E=SB
RETURN
100 X=-B/(2.*A)
E=EXP(A*X**2+B*X+Y1)
RETURN
END

```

```
SUBROUTINE MAXFIX(BMAX,BMIN)
C
C MAXFIX MODIFIES BMAX SUCH THAT THE COMPUTED L BETTER FITS THE
C DRIFT SHELLS OF ISOTROPIC PARTICLE DISTRIBUTIONS.
C
C     COMMON/BXYZCM/YEAR,DAYYR,UT,XMLG,KODE,JSW,INITL,XMLT
C     IF JSW LESS THAN OR EQUAL TO ZERO, AVERAGE L SHELLS ARE NOT WANTED.
C         IF(JSW.LE.0)RETURN
C     IF BMAX IS GREATER THAN 3*BMIN NO MODIFICATION IS REQUIRED, DRIFT
C     SHELLS ARE ALREADY CLOSE TO AVERAGE AND NO FURTHER CHANGE WILL OCCUR.
C         IF(BMAX.GT.3.*BMIN) RETURN
C     CALCULATE PRELIMINARY VALUE OF L -- IF L LESS THAN 3, AVERAGE
C     SHELL DOES NOT CHANGE.
C         EL=(0.311653/BMIN)**(1./3.)
C         IF(EL.LT.3.) RETURN
C         CON=1.3
C         IF(EL.LT.5.) CON=1.+0.15*(EL-3.)
C         BMAX=AMINI(3.*BMIN,CON*BMAX)
C         RETURN
C     END
```

```

      SUBROUTINE CARMEL (B,XI,VL)
C      COMPUTE L
      IF(XI-1.0E-36)14,14,15
14    VL=(0.311653/B)**(1./3.)
      RETURN
15    XX=3.0*ALOG(XI)
      XX=XX+ALOG(B/0.311653)
      IF(XX+22.)1,1,8
8     IF(XX+3.)2,2,9
9     IF(XX-3.)3,3,10
10    IF(XX-11.7)4,4,11
11    IF(XX-23.)5,5,6
1    GG=.333338*XX+.30062102
      GO TO 7
2    GG=((((-8.1537735E-14*XX+8.3232531E-13)*XX+1.0066362E-9)*XX+
      18.1048663E-8)*XX+3.2916354E-6)*XX+8.2711096E-5)*XX+1.3714667E-3)*
      2XX+.015017245)*XX+.43432642)*XX+.62337691
      GO TO 7
3    GG=(((((2.6047023E-10*XX+2.3028767E-9)*XX-2.1997983E-8)*XX-
      15.3977642E-7)*XX-3.3408822E-6)*XX+3.8379917E-5)*XX+1.1784234E-3)*
      2XX+1.4492441E-2)*XX+.43352788)*XX+.6228644
      GO TO 7
4    GG=(((((6.3271665E-10*XX-3.958306E-8)*XX+9.9766148E-07)*XX-
      11.2531932E-5)*XX+7.9451313E-5)*XX-3.2077032E-4)*XX+2.1680398E-3)*
      2XX+1.2817956E-2)*XX+.43510529)*XX+.6222355
      GO TO 7
5    GG=((((2.8212095E-8*XX-3.8049276E-6)*XX+2.170224E-4)*XX-6.7310339
      1E-3)*XX+.12038224)*XX-.18461796)*XX+2.0007187
      GO TO 7
6    GG=XX-3.0460681
7    VL=((1.0+EXP(GG))*0.311653)/B)**(1./3.)
      END COMPUTE L
      RETURN
      END

```

CARMLO00
CARMLO01
CARMLO02
CARMLO082
CARMLO02
CARMLO03
CARMLO04
CARMLO05
CARMLO06
CARMLO07
CARMLO08
CARMLO09
CARMLO10
CARMLO11
CARMLO12
CARMLO13
CARMLO14
CARMLO15
CARMLO16
CARMLO17
CARMLO18
CARMLO19
CARMLO20
CARMLO21
CARMLO22
CARMLO23
CARMLO24
CARMLO25
CARMLO26
CARMLO27
CARMLO28
CARMLO29

5.4 Sample Program Output

	LAT	LONG	R	DAYOFYR	TIME	L	BMIN	MAGLONG	MAGLAT	OPTIME
L INT	0.00000	0.00000	2.00000	1.00000	0.00000	2.06360	.03546	69.39934	4.16750	.01000
L INT+EXT	0.00000	0.00000	2.00000	1.00000	0.00000	2.06360	.03546	69.39934	4.16750	.01000
L AVE	0.00000	0.00000	2.00000	1.00000	0.00000	2.06360	.03546	69.39934	4.16750	.01200
L INT	0.00000	0.00000	5.00000	1.00000	0.00000	5.09586	.00236	69.39934	4.16750	.00700
L INT+EXT	0.00000	0.00000	5.00000	1.00000	0.00000	5.09586	.00236	69.39934	4.16750	.01900
L AVE	0.00000	0.00000	5.00000	1.00000	0.00000	5.09586	.00236	69.39934	4.16750	.02000
L INT	0.00000	0.00000	8.00000	1.00000	0.00000	8.10661	.00059	69.39934	4.16750	.00700
L INT+EXT	0.00000	0.00000	8.00000	1.00000	0.00000	8.10661	.00059	69.39934	4.16750	.00700
L AVE	0.00000	0.00000	8.00000	1.00000	0.00000	8.10661	.00059	69.39934	4.16750	.00700
L INT	0.00000	0.00000	8.00000	1.00000	0.00000	8.73789	.00047	69.39934	4.16750	.03400
L INT+EXT	0.00000	0.00000	8.00000	1.00000	0.00000	8.41144	.00047	69.39934	4.16750	.03400
L AVE	0.00000	0.00000	8.00000	1.00000	0.00000	8.41144	.00047	69.39934	4.16750	.03400
L INT	0.00000	90.00000	2.00000	1.00000	0.00000	1.99736	.03885	158.59438	-10.91300	.02100
L INT+EXT	0.00000	90.00000	2.00000	1.00000	0.00000	1.99736	.03885	158.59438	-10.91300	.03400
L AVE	0.00000	90.00000	2.00000	1.00000	0.00000	1.99736	.03885	158.59438	-10.91300	.03300
L INT	0.00000	90.00000	5.00000	1.00000	0.00000	5.13274	.00230	158.59438	-10.91300	.00800
L INT+EXT	0.00000	90.00000	5.00000	1.00000	0.00000	5.13274	.00230	158.59438	-10.91300	.02300
L AVE	0.00000	90.00000	5.00000	1.00000	0.00000	5.13274	.00230	158.59438	-10.91300	.04000
L INT	0.00000	90.00000	5.00000	1.00000	0.00000	5.2452	.00210	158.59438	-10.91300	.00600
L INT+EXT	0.00000	90.00000	5.00000	1.00000	0.00000	5.2452	.00210	158.59438	-10.91300	.02500
L AVE	0.00000	90.00000	5.00000	1.00000	0.00000	5.2452	.00210	158.59438	-10.91300	.02700
L INT	0.00000	90.00000	8.00000	1.00000	0.00000	8.27007	.00052	158.59438	-10.91300	.04500
L INT+EXT	0.00000	90.00000	8.00000	1.00000	0.00000	8.21934	.00052	158.59438	-10.91300	.01600
L AVE	0.00000	90.00000	8.00000	1.00000	0.00000	8.21934	.00052	158.59438	-10.91300	.02200
L INT	0.00000	180.00000	2.00000	1.00000	0.00000	1.97879	.04018	249.39934	-4.16750	.04000
L INT+EXT	0.00000	180.00000	2.00000	1.00000	0.00000	1.97879	.04017	249.39934	-4.16750	.04000
L AVE	0.00000	180.00000	2.00000	1.00000	0.00000	1.97879	.04017	249.39934	-4.16750	.04000
L INT	0.00000	180.00000	2.00000	1.00000	0.00000	1.97879	.04017	249.39934	-4.16750	.04000
L INT+EXT	0.00000	180.00000	5.00000	1.00000	0.00000	4.99826	.00249	249.39934	-4.16750	.04000
L AVE	0.00000	180.00000	5.00000	1.00000	0.00000	5.02867	.00245	249.39934	-4.16750	.04000
L INT	0.00000	180.00000	5.00000	1.00000	0.00000	5.03043	.00245	249.39934	-4.16750	.04000
L INT+EXT	0.00000	180.00000	5.00000	1.00000	0.00000	5.03043	.00245	249.39934	-4.16750	.04000
L AVE	0.00000	180.00000	8.00000	1.00000	0.00000	8.03880	.00060	249.39934	-4.16750	.04000
L INT	0.00000	180.00000	8.00000	1.00000	0.00000	7.61944	.00073	249.39934	-4.16750	.04000
L INT+EXT	0.00000	180.00000	8.00000	1.00000	0.00000	7.78912	.00073	249.39934	-4.16750	.04000
L AVE	0.00000	180.00000	8.00000	1.00000	0.00000	7.65158	.01648	75.93790	33.54197	.03700
L INT	0.00000	180.00000	2.00000	1.00000	0.00000	2.66668	.01585	75.93790	33.54197	.01800
L INT+EXT	0.00000	180.00000	2.00000	1.00000	0.00000	2.66668	.01585	75.93790	33.54197	.01800
L AVE	0.00000	180.00000	2.00000	1.00000	0.00000	2.66668	.01585	75.93790	33.54197	.01800
L INT	0.00000	180.00000	5.00000	1.00000	0.00000	7.00276	.00090	75.93790	33.54197	.01500
L INT+EXT	0.00000	180.00000	5.00000	1.00000	0.00000	7.58319	.00049	75.93790	33.54197	.04800
L AVE	0.00000	180.00000	5.00000	1.00000	0.00000	7.58319	.00049	75.93790	33.54197	.04800
L INT	0.00000	30.00000	0.00000	1.00000	0.00000	100.00000	.00081	100.00000	33.54197	.00500
L INT+EXT	0.00000	30.00000	0.00000	1.00000	0.00000	100.00000	.00097	100.00000	33.54197	.00600
L AVE	0.00000	30.00000	0.00000	1.00000	0.00000	7.00276	.00090	75.93790	33.54197	.02200
L INT	0.00000	30.00000	5.00000	1.00000	0.00000	2.46411	.02723	160.83745	19.00538	.03400
L INT+EXT	0.00000	30.00000	5.00000	1.00000	0.00000	2.46408	.02697	160.83745	19.00538	.05000
L AVE	0.00000	30.00000	5.00000	1.00000	0.00000	2.46408	.02697	160.83745	19.00538	.05000
L INT	0.00000	30.00000	8.00000	1.00000	0.00000	5.63305	.00173	160.83745	19.00538	.01400
L INT+EXT	0.00000	30.00000	8.00000	1.00000	0.00000	5.73189	.00155	160.83745	19.00538	.01200
L AVE	0.00000	30.00000	8.00000	1.00000	0.00000	5.73189	.00155	160.83745	19.00538	.01200
L INT	0.00000	30.00000	90.00000	2.00000	1.00000	5.00000	.00000	2.46411	160.83745	.04900
L INT+EXT	0.00000	30.00000	90.00000	2.00000	1.00000	9.00933	.00042	160.83745	19.00538	.05000
L AVE	0.00000	30.00000	90.00000	2.00000	1.00000	8.81557	.00042	160.83745	19.00538	.05000
L INT	0.00000	30.00000	90.00000	5.00000	1.00000	8.79354	.001327	160.83745	19.00538	.04500
L INT+EXT	0.00000	30.00000	90.00000	5.00000	1.00000	8.79354	.001327	160.83745	19.00538	.04500
L AVE	0.00000	30.00000	90.00000	5.00000	1.00000	8.79354	.001327	160.83745	19.00538	.04500
L INT	0.00000	180.00000	2.00000	1.00000	0.00000	2.00000	.00000	2.39559	.02235	.05000
L INT+EXT	0.00000	180.00000	2.00000	1.00000	0.00000	2.00000	.00000	2.39559	.02235	.05000
L AVE	0.00000	180.00000	2.00000	1.00000	0.00000	2.00000	.00000	2.39559	.02235	.05000
L INT	0.00000	180.00000	5.00000	1.00000	0.00000	6.05104	.00140	160.83745	19.00538	.01600
L INT+EXT	0.00000	180.00000	5.00000	1.00000	0.00000	6.01327	.00149	160.83745	19.00538	.01600
L AVE	0.00000	180.00000	5.00000	1.00000	0.00000	6.01327	.00149	160.83745	19.00538	.01600
L INT	0.00000	180.00000	8.00000	1.00000	0.00000	8.00020	.00033	243.37551	25.25674	.01400
L INT+EXT	0.00000	180.00000	8.00000	1.00000	0.00000	8.36184	.00058	243.37551	25.25674	.03200
L AVE	0.00000	180.00000	8.00000	1.00000	0.00000	8.61843	.00058	243.37551	25.25674	.04600
L INT	0.00000	180.00000	8.00000	1.00000	0.00000	8.61843	.00058	243.37551	25.25674	.04600

CPTIME		MAGLAT		MAGLNG		BMIN		TIME		DAYOFYR		R		LONG		LAT	
-																	
INT	INT+EXT	0.00000	0.00000	2.00000	1.00000	6.00000	2.06360	6.00000	2.06360	6.00000	2.06360	0.03546	69.39934	4.16750	.00900	.01200	
AVE		0.00000	0.00000	2.00000	1.00000	6.00000	2.06360	6.00000	2.06360	6.00000	2.06360	.03546	69.39934	4.16750	.01100	.01100	
INT	INT+EXT	0.00000	0.00000	5.00000	1.00000	6.00000	5.09586	6.00000	5.09586	6.00000	5.09586	.00236	69.39934	4.16750	.00600	.00600	
AVE		0.00000	0.00000	5.00000	1.00000	6.00000	5.09586	6.00000	5.09586	6.00000	5.09586	.00236	69.39934	4.16750	.01600	.01600	
INT	INT+EXT	0.00000	0.00000	5.00000	1.00000	6.00000	5.21900	6.00000	5.21900	6.00000	5.21900	.00220	69.39934	4.16750	.03900	.03900	
AVE		0.00000	0.00000	5.00000	1.00000	6.00000	5.16506	6.00000	5.16506	6.00000	5.16506	.00220	69.39934	4.16750	.00600	.00600	
INT	INT+EXT	0.00000	0.00000	8.00000	1.00000	6.00000	8.10661	6.00000	8.10661	6.00000	8.10661	.00059	69.39934	4.16750	.00600	.00600	
AVE		0.00000	0.00000	8.00000	1.00000	6.00000	8.06429	6.00000	8.06429	6.00000	8.06429	.00059	69.39934	4.16750	.00700	.00700	
INT	INT+EXT	0.00000	0.00000	8.00000	1.00000	6.00000	7.98042	6.00000	7.98042	6.00000	7.98042	.00059	69.39934	4.16750	.03200	.03200	
AVE		0.00000	0.00000	8.00000	1.00000	6.00000	7.99936	6.00000	7.99936	6.00000	7.99936	.03885	158.59438	-10.91300	.02200	.02200	
INT	INT+EXT	0.00000	0.00000	90.00000	1.00000	6.00000	1.00000	6.00000	1.00000	6.00000	1.00000	.00055	158.59438	-10.91300	.03300	.03300	
AVE		0.00000	0.00000	90.00000	1.00000	6.00000	1.00000	6.00000	1.00000	6.00000	1.00000	.00055	158.59438	-10.91300	.03100	.03100	
INT	INT+EXT	0.00000	0.00000	90.00000	1.00000	6.00000	1.00000	6.00000	1.00000	6.00000	1.00000	.00066	158.59438	-10.91300	.02700	.02700	
AVE		0.00000	0.00000	90.00000	1.00000	6.00000	1.00000	6.00000	1.00000	6.00000	1.00000	.00066	158.59438	-10.91300	.04100	.04100	
INT	INT+EXT	0.00000	0.00000	90.00000	1.00000	6.00000	1.00000	6.00000	1.00000	6.00000	1.00000	.00230	158.59438	-10.91300	.01700	.01700	
AVE		0.00000	0.00000	90.00000	1.00000	6.00000	1.00000	6.00000	1.00000	6.00000	1.00000	.00228	158.59438	-10.91300	.03900	.03900	
INT	INT+EXT	0.00000	0.00000	90.00000	1.00000	6.00000	1.00000	6.00000	1.00000	6.00000	1.00000	.00055	158.59438	-10.91300	.00800	.00800	
AVE		0.00000	0.00000	90.00000	1.00000	6.00000	1.00000	6.00000	1.00000	6.00000	1.00000	.00055	158.59438	-10.91300	.02700	.02700	
INT	INT+EXT	0.00000	0.00000	90.00000	1.00000	6.00000	1.00000	6.00000	1.00000	6.00000	1.00000	.000231	158.59438	-10.91300	.04000	.04000	
AVE		0.00000	0.00000	90.00000	1.00000	6.00000	1.00000	6.00000	1.00000	6.00000	1.00000	.00018	249.39934	-4.16750	.01700	.01700	
INT	INT+EXT	0.00000	0.00000	180.00000	1.00000	6.00000	1.97863	6.00000	1.97863	6.00000	1.97863	.04017	249.39934	-4.16750	.02200	.02200	
AVE		0.00000	0.00000	180.00000	1.00000	6.00000	1.97863	6.00000	1.97863	6.00000	1.97863	.04017	249.39934	-4.16750	.03900	.03900	
INT	INT+EXT	0.00000	0.00000	180.00000	1.00000	6.00000	4.98826	6.00000	4.98826	6.00000	4.98826	.00249	249.39934	-4.16750	.00600	.00600	
AVE		0.00000	0.00000	180.00000	1.00000	6.00000	4.98826	6.00000	4.98826	6.00000	4.98826	.00231	249.39934	-4.16750	.01800	.01800	
INT	INT+EXT	0.00000	0.00000	180.00000	1.00000	6.00000	5.13274	6.00000	5.13274	6.00000	5.13274	.00231	158.59438	-10.91300	.04000	.04000	
AVE		0.00000	0.00000	180.00000	1.00000	6.00000	5.15716	6.00000	5.15716	6.00000	5.15716	.00228	158.59438	-10.91300	.03900	.03900	
INT	INT+EXT	0.00000	0.00000	180.00000	1.00000	6.00000	5.16324	6.00000	5.16324	6.00000	5.16324	.00226	158.59438	-10.91300	.03300	.03300	
AVE		0.00000	0.00000	180.00000	1.00000	6.00000	8.27531	6.00000	8.27531	6.00000	8.27531	.00055	158.59438	-10.91300	.03100	.03100	
INT	INT+EXT	0.00000	0.00000	180.00000	1.00000	6.00000	1.93958	6.00000	1.93958	6.00000	1.93958	.00055	158.59438	-10.91300	.02700	.02700	
AVE		0.00000	0.00000	180.00000	1.00000	6.00000	8.09308	6.00000	8.09308	6.00000	8.09308	.00080	158.59438	-10.91300	.00800	.00800	
INT	INT+EXT	0.00000	0.00000	180.00000	1.00000	6.00000	1.97859	6.00000	1.97859	6.00000	1.97859	.00060	249.39934	-4.16750	.01700	.01700	
AVE		0.00000	0.00000	180.00000	1.00000	6.00000	8.03880	6.00000	8.03880	6.00000	8.03880	.00060	249.39934	-4.16750	.00500	.00500	
INT	INT+EXT	0.00000	0.00000	180.00000	1.00000	6.00000	7.82546	6.00000	7.82546	6.00000	7.82546	.00059	249.39934	-4.16750	.01800	.01800	
AVE		0.00000	0.00000	180.00000	1.00000	6.00000	7.95843	6.00000	7.95843	6.00000	7.95843	.00059	249.39934	-4.16750	.03700	.03700	
INT	INT+EXT	0.00000	0.00000	180.00000	1.00000	6.00000	2.65758	6.00000	2.65758	6.00000	2.65758	.01648	75.93790	33.54197	.03700	.03700	
AVE		0.00000	0.00000	180.00000	1.00000	6.00000	2.66645	6.00000	2.66645	6.00000	2.66645	.01595	75.93790	33.54197	.06100	.06100	
INT	INT+EXT	0.00000	0.00000	180.00000	1.00000	6.00000	2.66645	6.00000	2.66645	6.00000	2.66645	.01595	75.93790	33.54197	.06400	.06400	
AVE		0.00000	0.00000	180.00000	1.00000	6.00000	7.00276	6.00000	7.00276	6.00000	7.00276	.00090	75.93790	33.54197	.01500	.01500	
INT	INT+EXT	0.00000	0.00000	180.00000	1.00000	6.00000	7.25837	6.00000	7.25837	6.00000	7.25837	.00076	75.93790	33.54197	.04800	.04800	
AVE		0.00000	0.00000	180.00000	1.00000	6.00000	7.25837	6.00000	7.25837	6.00000	7.25837	.00076	75.93790	33.54197	.03700	.03700	
INT	INT+EXT	0.00000	0.00000	180.00000	1.00000	6.00000	10.00000	6.00000	10.00000	6.00000	10.00000	.00081	75.93790	33.54197	.04700	.04700	
AVE		0.00000	0.00000	180.00000	1.00000	6.00000	10.74265	6.00000	10.74265	6.00000	10.74265	.00028	75.93790	33.54197	.04700	.04700	
INT	INT+EXT	0.00000	0.00000	180.00000	1.00000	6.00000	10.74265	6.00000	10.74265	6.00000	10.74265	.00028	75.93790	33.54197	.04800	.04800	
AVE		0.00000	0.00000	180.00000	1.00000	6.00000	2.47483	6.00000	2.47483	6.00000	2.47483	.02702	160.83745	19.00538	.05700	.05700	
INT	INT+EXT	0.00000	0.00000	180.00000	1.00000	6.00000	5.63305	6.00000	5.63305	6.00000	5.63305	.00173	160.83745	19.00538	.05300	.05300	
AVE		0.00000	0.00000	180.00000	1.00000	6.00000	5.60336	6.00000	5.60336	6.00000	5.60336	.00180	160.83745	19.00538	.05400	.05400	
INT	INT+EXT	0.00000	0.00000	180.00000	1.00000	6.00000	5.61378	6.00000	5.61378	6.00000	5.61378	.00180	160.83745	19.00538	.05500	.05500	
AVE		0.00000	0.00000	180.00000	1.00000	6.00000	9.00933	6.00000	9.00933	6.00000	9.00933	.00042	160.83745	19.00538	.05600	.05600	
INT	INT+EXT	0.00000	0.00000	180.00000	1.00000	6.00000	7.92390	6.00000	7.92390	6.00000	7.92390	.00044	160.83745	19.00538	.05700	.05700	
AVE		0.00000	0.00000	180.00000	1.00000	6.00000	8.10539	6.00000	8.10539	6.00000	8.10539	.00064	160.83745	19.00538	.04500	.04500	
INT	INT+EXT	0.00000	0.00000	180.00000	1.00000	6.00000	2.39208	6.00000	2.39208	6.00000	2.39208	.02249	243.37551	25.25674	.05800	.05800	
AVE		0.00000	0.00000	180.00000	1.00000	6.00000	2.39208	6.00000	2.39208	6.00000	2.39208	.02249	243.37551	25.25674	.01100	.01100	
INT	INT+EXT	0.00000	0.00000	180.00000	1.00000	6.00000	2.39600	6.00000	2.39600	6.00000	2.39600	.02240	243.37551	25.25674	.03700	.03700	
AVE		0.00000	0.00000	180.00000	1.00000	6.00000	2.39600	6.00000	2.39600	6.00000	2.39600	.02240	243.37551	25.25674	.05200	.05200	
INT	INT+EXT	0.00000	0.00000	180.00000	1.00000	6.00000	6.05104	6.00000	6.05104	6.00000	6.05104	.00140	243.37551	25.25674	.01400	.01400	
AVE		0.00000	0.00000	180.00000	1.00000	6.00000	6.17007	6.00000	6.17007	6.00000	6.17007	.00123	243.37551	25.25674	.04400	.04400	
INT	INT+EXT	0.00000	0.00000	180.00000	1.00000	6.00000	6.17007	6.00000	6.17007	6.00000	6.17007	.00133	243.37551	25.25674	.05800	.05800	
AVE		0.00000	0.00000	180.00000	1.00000	6.00000	9.80020	6.00000	9.80020	6.00000	9.80020	.00035	243.37551	25.25674	.01100	.01100	
INT	INT+EXT	0.00000	0.00000	180.00000	1.00000	6.00000	9.45842	6.00000	9.45842	6.00000	9.45842	.00035	243.37551	25.25674	.03700	.03700	
AVE		0.00000	0.00000	180.00000	1.00000	6.00000	9.48028	6.00000	9.48028	6.00000	9.48028	.00035	243.37551	25.25674	.05200	.05200	

LAT	LONG	R	DAYOFYR	TIME	L	BMIN	MAGLNG	MAGLAT	CPTIME
L INT	0.00000	2.00000	1.00000	18.00000	2.06360	.03546	69.39934	4.16750	.00900
L INT+EXT	0.00000	2.00000	1.00000	18.00000	2.06360	.03546	69.39934	4.16750	.01200
L AVE	0.00000	2.00000	1.00000	18.00000	2.06360	.03546	69.39934	4.16750	.01100
L INT	0.00000	5.00000	1.00000	18.00000	5.09586	.00226	69.39934	4.16750	.00400
L INT+EXT	0.00000	5.00000	1.00000	18.00000	5.22862	.00218	69.39934	4.16750	.01700
L AVE	0.00000	5.00000	1.00000	18.00000	5.17447	.00218	69.39934	4.16750	.03700
L INT	0.00000	8.00000	1.00000	18.00000	8.10661	.00059	69.39934	4.16750	.00500
L INT+EXT	0.00000	8.00000	1.00000	18.00000	8.03121	.00000	69.39934	4.16750	.01600
L AVE	0.00000	8.00000	1.00000	18.00000	7.91239	.00040	69.39934	4.16750	.03700
L INT	0.00000	2.00000	1.00000	18.00000	1.99936	.03885	158.59438	-10.91300	.02100
L INT+EXT	0.00000	2.00000	1.00000	18.00000	1.99936	.03880	158.59438	-10.91300	.03300
L AVE	0.00000	2.00000	1.00000	18.00000	1.99937	.03880	158.59438	-10.91300	.03500
L INT	0.00000	5.00000	1.00000	18.00000	5.13274	.00020	158.59438	-10.91300	.00800
L INT+EXT	0.00000	5.00000	1.00000	18.00000	5.35685	.00192	158.59438	-10.91300	.03300
L AVE	0.00000	5.00000	1.00000	18.00000	5.28296	.00112	158.59438	-10.91300	.03900
L INT	0.00000	8.00000	1.00000	18.00000	8.27531	.00055	158.59438	-10.91300	.00700
L INT+EXT	0.00000	8.00000	1.00000	18.00000	8.81132	.00035	158.59438	-10.91300	.03200
L AVE	0.00000	8.00000	1.00000	18.00000	8.60384	.00035	158.59438	-10.91300	.03900
L INT	0.00000	2.00000	1.00000	18.00000	1.97859	.04018	249.39934	-4.16750	.01800
L INT+EXT	0.00000	2.00000	1.00000	18.00000	1.97863	.04017	249.39934	-4.16750	.02100
L AVE	0.00000	2.00000	1.00000	18.00000	1.97863	.04017	249.39934	-4.16750	.02200
L INT	0.00000	5.00000	1.00000	18.00000	5.19826	.00249	249.39934	-4.16750	.00700
L INT+EXT	0.00000	5.00000	1.00000	18.00000	5.11149	.00231	249.39934	-4.16750	.01800
L AVE	0.00000	5.00000	1.00000	18.00000	5.01316	.00231	249.39934	-4.16750	.03800
L INT	0.00000	8.00000	1.00000	18.00000	8.03880	.00060	249.39934	-4.16750	.00500
L INT+EXT	0.00000	8.00000	1.00000	18.00000	7.98841	.00061	249.39934	-4.16750	.01500
L AVE	0.00000	8.00000	1.00000	18.00000	7.92465	.00061	249.39934	-4.16750	.03600
L INT	0.00000	18.00000	1.00000	18.00000	4.93826	.00249	249.39934	-4.16750	.00700
L INT+EXT	0.00000	18.00000	1.00000	18.00000	5.11149	.00231	249.39934	-4.16750	.01800
L AVE	0.00000	18.00000	1.00000	18.00000	5.01316	.00231	249.39934	-4.16750	.03800
L INT	0.00000	18.00000	1.00000	18.00000	8.03880	.00060	249.39934	-4.16750	.00500
L INT+EXT	0.00000	18.00000	1.00000	18.00000	7.98841	.00061	249.39934	-4.16750	.01500
L AVE	0.00000	18.00000	1.00000	18.00000	7.92465	.00061	249.39934	-4.16750	.03600
L INT	30.00000	2.00000	1.00000	18.00000	2.65158	.01648	75.93790	33.54197	.03700
L INT+EXT	30.00000	2.00000	1.00000	18.00000	2.66759	.01589	75.93790	33.54197	.05700
L AVE	30.00000	2.00000	1.00000	18.00000	2.66759	.01589	75.93790	33.54197	.05900
L INT	30.00000	5.00000	1.00000	18.00000	5.66759	.00090	75.93790	33.54197	.01300
L INT+EXT	30.00000	5.00000	1.00000	18.00000	5.01276	.00092	75.93790	33.54197	.01300
L AVE	30.00000	5.00000	1.00000	18.00000	7.33623	.00072	75.93790	33.54197	.04800
L INT	30.00000	8.00000	1.00000	18.00000	7.33623	.00072	75.93790	33.54197	.04600
L INT+EXT	30.00000	8.00000	1.00000	18.00000	100.00000	.00081	75.93790	33.54197	.05700
L AVE	30.00000	8.00000	1.00000	18.00000	100.00000	.00092	75.93790	33.54197	.05900
L INT	30.00000	5.00000	1.00000	18.00000	100.00000	.00092	75.93790	33.54197	.01300
L INT+EXT	30.00000	5.00000	1.00000	18.00000	100.00000	.00132	160.83745	19.00538	.04000
L AVE	30.00000	5.00000	1.00000	18.00000	2.24611	.02723	160.83745	19.00538	.03200
L INT	30.00000	2.00000	1.00000	18.00000	1.00000	.00042	160.83745	19.00538	.05100
L INT+EXT	30.00000	2.00000	1.00000	18.00000	2.24683	.02693	160.83745	19.00538	.06000
L AVE	30.00000	2.00000	1.00000	18.00000	2.24683	.02693	160.83745	19.00538	.06200
L INT	30.00000	90.00000	1.00000	18.00000	5.63305	.00173	160.83745	19.00538	.01500
L INT+EXT	30.00000	90.00000	1.00000	18.00000	5.84268	.00132	160.83745	19.00538	.04000
L AVE	30.00000	90.00000	1.00000	18.00000	1.79332	.00132	160.83745	19.00538	.05200
L INT	30.00000	90.00000	1.00000	18.00000	9.00933	.00042	160.83745	19.00538	.01000
L INT+EXT	30.00000	90.00000	1.00000	18.00000	100.00000	.00074	160.83745	19.00538	.01400
L AVE	30.00000	90.00000	1.00000	18.00000	100.00000	.00074	160.83745	19.00538	.01200
L INT	30.00000	180.00000	1.00000	18.00000	2.39208	.02269	243.37551	25.25674	.03600
L INT+EXT	30.00000	180.00000	1.00000	18.00000	2.39654	.02225	243.37551	25.25674	.05900
L AVE	30.00000	180.00000	1.00000	18.00000	2.39654	.02225	243.37551	25.25674	.06100
L INT	30.00000	180.00000	5.00000	18.00000	6.05104	.00140	243.37551	25.25674	.04400
L INT+EXT	30.00000	180.00000	5.00000	18.00000	6.21749	.00119	243.37551	25.25674	.05200
L AVE	30.00000	180.00000	5.00000	18.00000	6.21906	.00119	243.37551	25.25674	.01200
L INT	30.00000	180.00000	8.00000	18.00000	9.80020	.00033	243.37551	25.25674	.04300
L INT+EXT	30.00000	180.00000	8.00000	18.00000	9.80592	.00028	243.37551	25.25674	.04000
L AVE	30.00000	180.00000	8.00000	18.00000	9.80592	.00028	243.37551	25.25674	.04300

LAT	LONG	A	DAYOFYR	TIME	L	BMIN	MAGLNG	MAGLAT	CPTIME
L INT	0.00000	0.00000	90.00000	12.00000	2.06360	.03546	69.39934	4.16750	.00900
L INT+EXT	0.00000	0.00000	90.00000	12.00000	2.06360	.03546	69.39934	4.16750	.01100
L AVE	0.00000	0.00000	90.00000	12.00000	2.06360	.03546	69.39934	4.16750	.01000
L INT	0.00000	0.00000	90.00000	12.00000	0.0986	.00236	69.39934	4.16750	.00600
L INT+EXT	0.00000	0.00000	90.00000	12.00000	5.12775	.00232	69.39934	4.16750	.01700
L AVE	0.00000	0.00000	90.00000	12.00000	5.12866	.00232	69.39934	4.16750	.03700
L INT	0.00000	0.00000	90.00000	12.00000	8.10661	.00059	69.39934	4.16750	.00500
L INT+EXT	0.00000	0.00000	90.00000	12.00000	7.4587	.00076	69.39934	4.16750	.01700
L AVE	0.00000	0.00000	90.00000	12.00000	7.78143	.00076	69.39934	4.16750	.03800
L INT	0.00000	0.00000	90.00000	12.00000	1.99836	.03885	158.59438	-10.91300	.02200
L INT+EXT	0.00000	0.00000	90.00000	12.00000	1.99962	.03881	158.59438	-10.91300	.03500
L AVE	0.00000	0.00000	90.00000	12.00000	1.99962	.03881	158.59438	-10.91300	.03200
L INT	0.00000	0.00000	90.00000	12.00000	5.13274	.00231	158.59438	-10.91300	.00800
L INT+EXT	0.00000	0.00000	90.00000	12.00000	5.24939	.00211	158.59438	-10.91300	.00200
L AVE	0.00000	0.00000	90.00000	12.00000	5.20810	.00211	158.59438	-10.91300	.04000
L INT	0.00000	0.00000	90.00000	12.00000	8.27531	.00055	158.59438	-10.91300	.00700
L INT+EXT	0.00000	0.00000	90.00000	12.00000	8.16418	.00056	158.59438	-10.91300	.02300
L AVE	0.00000	0.00000	90.00000	12.00000	8.12917	.00056	158.59438	-10.91300	.03800
L INT	0.00000	0.00000	90.00000	12.00000	1.9859	.04018	249.39934	-4.16750	.01600
L INT+EXT	0.00000	0.00000	90.00000	12.00000	1.97863	.04017	249.39934	-4.16750	.02400
L AVE	0.00000	0.00000	90.00000	12.00000	1.97863	.04017	249.39934	-4.16750	.02300
L INT	0.00000	0.00000	90.00000	12.00000	4.99826	.00249	249.39934	-4.16750	.00700
L INT+EXT	0.00000	0.00000	90.00000	12.00000	5.21829	.00056	249.39934	-4.16750	.02200
L AVE	0.00000	0.00000	90.00000	12.00000	5.12672	.00217	249.39934	-4.16750	.04000
L INT	0.00000	0.00000	90.00000	12.00000	8.0380	.00060	249.39934	-4.16750	.00500
L INT+EXT	0.00000	0.00000	90.00000	12.00000	8.65484	.00047	249.39934	-4.16750	.02200
L AVE	0.00000	0.00000	90.00000	12.00000	8.31204	.00047	249.39934	-4.16750	.04000
L INT	30.00000	0.00000	90.00000	12.00000	2.65158	.01648	75.93790	33.54197	.03800
L INT+EXT	30.00000	0.00000	90.00000	12.00000	5.226519	.01600	75.93790	33.54197	.06500
L AVE	30.00000	0.00000	90.00000	12.00000	2.665159	.01600	75.93790	33.54197	.06100
L INT	30.00000	0.00000	90.00000	12.00000	7.00276	.00090	75.93790	33.54197	.01500
L INT+EXT	30.00000	0.00000	90.00000	12.00000	6.932348	.00106	75.93790	33.54197	.05000
L AVE	30.00000	0.00000	90.00000	12.00000	6.932248	.00106	75.93790	33.54197	.04700
L INT	30.00000	0.00000	90.00000	12.00000	100.00000	.00081	75.93790	33.54197	.00400
L INT+EXT	30.00000	0.00000	90.00000	12.00000	9.55651	.00057	75.93790	33.54197	.04100
L AVE	30.00000	0.00000	90.00000	12.00000	9.92910	.00057	75.93790	33.54197	.05400
L INT	30.00000	0.00000	90.00000	12.00000	6.02723	.02723	160.83745	19.00538	.03200
L INT+EXT	30.00000	0.00000	90.00000	12.00000	2.24611	.02695	160.83745	19.00538	.05500
L AVE	30.00000	0.00000	90.00000	12.00000	2.24829	.02695	160.83745	19.00538	.05400
L INT	30.00000	0.00000	90.00000	12.00000	5.63305	.00173	160.83745	19.00538	.01400
L INT+EXT	30.00000	0.00000	90.00000	12.00000	2.39208	.02269	243.37551	25.25674	.03400
L AVE	30.00000	0.00000	90.00000	12.00000	2.39757	.02217	243.37551	25.25674	.05900
L INT	30.00000	0.00000	90.00000	12.00000	5.73593	.0153	160.83745	19.00538	.05000
L INT+EXT	30.00000	0.00000	90.00000	12.00000	2.39157	.00042	160.83745	19.00538	.01000
L AVE	30.00000	0.00000	90.00000	12.00000	8.91473	.00042	160.83745	19.00538	.03400
L INT	30.00000	0.00000	90.00000	12.00000	8.92316	.00042	160.83745	19.00538	.04700
L INT+EXT	30.00000	0.00000	90.00000	12.00000	2.39208	.02269	243.37551	25.25674	.04400
L AVE	30.00000	0.00000	90.00000	12.00000	6.44519	.00090	243.37551	25.25674	.01200
L INT	30.00000	0.00000	90.00000	12.00000	9.80020	.00033	243.37551	25.25674	.01300
L INT+EXT	30.00000	0.00000	90.00000	12.00000	100.00000	.00095	243.37551	25.25674	.01300
L AVE	30.00000	0.00000	90.00000	12.00000	100.00000	.00095	243.37551	25.25674	.01300

LAT	LONG	R	DAYOFYR	TIME	L	BMIN	MAGLONG	MAGLAT	CPTIME
L INT	0.00000	0.0.00000	90.00000	18.00000	2.06360	.03546	69.39934	4.16750	.00900
L INT+EXT	0.00000	0.0.00000	90.00000	18.00000	2.06360	.03546	69.39934	4.16750	.01200
L AVE	0.00000	0.0.00000	90.00000	18.00000	2.06360	.03546	69.39934	4.16750	.01100
L INT	0.00000	0.0.00000	90.00000	18.00000	5.09586	.00236	69.39934	4.16750	.00600
L INT+EXT	0.00000	0.0.00000	90.00000	18.00000	5.09586	.00218	69.39934	4.16750	.01700
L AVE	0.00000	0.0.00000	90.00000	18.00000	5.22918	.00218	69.39934	4.16750	.03900
L INT	0.00000	0.0.00000	90.00000	18.00000	5.17552	.00218	69.39934	4.16750	.00600
L INT+EXT	0.00000	0.0.00000	90.00000	18.00000	8.10661	.00059	69.39934	4.16750	.01700
L AVE	0.00000	0.0.00000	90.00000	18.00000	8.06091	.00059	69.39934	4.16750	.03700
L INT	0.00000	0.0.00000	90.00000	18.00000	7.9458	.00059	69.39934	4.16750	.02000
L INT+EXT	0.00000	0.0.00000	90.00000	18.00000	7.9458	.00059	158.59438	-10.91300	.03300
L AVE	0.00000	0.0.00000	90.00000	18.00000	7.9458	.00059	158.59438	-10.91300	.03300
L INT	0.00000	0.0.00000	90.00000	18.00000	5.13274	.00230	158.59438	-10.91300	.00900
L INT+EXT	0.00000	0.0.00000	90.00000	18.00000	5.33900	.00195	158.59438	-10.91300	.02400
L AVE	0.00000	0.0.00000	90.00000	18.00000	5.25750	.00195	158.59438	-10.91300	.03800
L INT	0.00000	0.0.00000	90.00000	18.00000	90.00000	.00055	158.59438	-10.91300	.00700
L INT+EXT	0.00000	0.0.00000	90.00000	18.00000	90.00000	.00041	158.59438	-10.91300	.03000
L AVE	0.00000	0.0.00000	90.00000	18.00000	8.48077	.00041	158.59438	-10.91300	.04800
L INT	0.00000	0.0.00000	90.00000	18.00000	1.97859	.00418	249.39934	-4.16750	.01700
L INT+EXT	0.00000	0.0.00000	90.00000	18.00000	1.97863	.00417	249.39934	-4.16750	.02200
L AVE	0.00000	0.0.00000	90.00000	18.00000	1.97863	.00417	249.39934	-4.16750	.02300
L INT	0.00000	0.0.00000	90.00000	18.00000	8.27531	.00055	158.59438	-10.91300	.00700
L INT+EXT	0.00000	0.0.00000	90.00000	18.00000	8.73936	.00041	158.59438	-10.91300	.03300
L AVE	0.00000	0.0.00000	90.00000	18.00000	8.73936	.00041	158.59438	-10.91300	.04800
L INT	0.00000	0.0.00000	90.00000	18.00000	5.11361	.00232	249.39934	-4.16750	.01700
L INT+EXT	0.00000	0.0.00000	90.00000	18.00000	5.06811	.00232	249.39934	-4.16750	.03800
L AVE	0.00000	0.0.00000	90.00000	18.00000	8.03880	.00060	249.39934	-4.16750	.04000
L INT	0.00000	0.0.00000	90.00000	18.00000	7.95092	.00062	249.39934	-4.16750	.01900
L INT+EXT	0.00000	0.0.00000	90.00000	18.00000	7.89363	.00062	249.39934	-4.16750	.03800
L AVE	0.00000	0.0.00000	90.00000	18.00000	2.65758	.00249	75.93790	33.54197	.00700
L INT	0.00000	0.0.00000	90.00000	18.00000	6.66783	.01648	75.93790	33.54197	.02400
L INT+EXT	0.00000	0.0.00000	90.00000	18.00000	6.66783	.01648	75.93790	33.54197	.04800
L AVE	0.00000	0.0.00000	90.00000	18.00000	2.66783	.01589	75.93790	33.54197	.06000
L INT	0.00000	0.0.00000	90.00000	18.00000	7.00276	.00098	75.93790	33.54197	.01600
L INT+EXT	0.00000	0.0.00000	90.00000	18.00000	7.34356	.00071	75.93790	33.54197	.05000
L AVE	0.00000	0.0.00000	90.00000	18.00000	7.34356	.00071	75.93790	33.54197	.03800
L INT	0.00000	0.0.00000	90.00000	18.00000	1.00	.00081	75.93790	33.54197	.06300
L INT+EXT	0.00000	0.0.00000	90.00000	18.00000	1.00	.00098	75.93790	33.54197	.01100
L AVE	0.00000	0.0.00000	90.00000	18.00000	1.00	.00098	75.93790	33.54197	.01300
L INT	0.00000	0.0.00000	90.00000	18.00000	5.85796	.00127	160.83745	19.00538	.03200
L INT+EXT	0.00000	0.0.00000	90.00000	18.00000	2.44880	.00269	160.83745	19.00538	.05400
L AVE	0.00000	0.0.00000	90.00000	18.00000	2.44880	.00269	160.83745	19.00538	.01100
L INT	0.00000	0.0.00000	90.00000	18.00000	5.63305	.00113	160.83745	19.00538	.01300
L INT+EXT	0.00000	0.0.00000	90.00000	18.00000	1.00	.00127	160.83745	19.00538	.03400
L AVE	0.00000	0.0.00000	90.00000	18.00000	2.31208	.00226	243.37551	25.25674	.05700
L INT	0.00000	0.0.00000	90.00000	18.00000	5.85796	.00127	160.83745	19.00538	.05400
L INT+EXT	0.00000	0.0.00000	90.00000	18.00000	2.31208	.00226	243.37551	25.25674	.01100
L AVE	0.00000	0.0.00000	90.00000	18.00000	2.31208	.00226	243.37551	25.25674	.04300
L INT	0.00000	0.0.00000	90.00000	18.00000	1.00	.00042	160.83745	19.00538	.01400
L INT+EXT	0.00000	0.0.00000	90.00000	18.00000	6.05104	.00083	160.83745	19.00538	.02202
L AVE	0.00000	0.0.00000	90.00000	18.00000	1.00	.00119	160.83745	19.00538	.01200
L INT	0.00000	0.0.00000	90.00000	18.00000	6.22262	.00119	243.37551	25.25674	.03400
L INT+EXT	0.00000	0.0.00000	90.00000	18.00000	2.39662	.00226	243.37551	25.25674	.05700
L AVE	0.00000	0.0.00000	90.00000	18.00000	2.39662	.00226	243.37551	25.25674	.01300
L INT	0.00000	0.0.00000	90.00000	18.00000	2.39662	.00226	243.37551	25.25674	.04200
L INT+EXT	0.00000	0.0.00000	90.00000	18.00000	9.84531	.00030	243.37551	25.25674	.01400
L AVE	0.00000	0.0.00000	90.00000	18.00000	9.84531	.00030	243.37551	25.25674	.01300

Section 6.0

APPENDIX B - COORDINATE TRANSFORMATIONS AND RELATED ANALYTIC DERIVATIONS

The magnetospheric magnetic field model described in Section 2 is represented in solar-magnetic coordinates. To use the model it is frequently necessary to express the components of the vector field in geographic or geomagnetic coordinates. Transformations between these coordinate systems are described below. Normally such transformations are time consuming and non analytic because of the earth's elliptical orbit around the sun. Here however the approximation of a circular orbit is made. This permits the transformations to be analytic and to require a minimum of computer time. The transformations are used in subroutines ANGLE and BMNEXT described in Appendix A.

6.1 Coordinate Transformations

Define α as the angle between the rotation and geomagnetic dipole axes, γ as the angle between the rotation axis and the perpendicular to the ecliptic plane. Two angular velocities are also defined, Ω as the velocity of the earth around the sun and ω as the earth's angular velocity about its rotation axis. Also the time, t , is measured from magnetic noon at summer solstice when the rotation and dipole axes and the sun-earth line are coplanar.

It is desired to add the external field (given in solar magnetic coordinates) vectorially to the internal field represented in geographic or geomagnetic coordinates. To do so the following three coordinate systems are defined.

- (1) the $X'Y'Z'$ - ecliptic coordinates with X' always toward the sun, Z' perpendicular to the ecliptic plane.
- (2) the X_G, Y_G, Z_G coordinates - with Z_G coincident with the geographic rotation axis. Time is measured such that at $t = 0$ the Y_G axis is in the ecliptic XZ plane as is Z_G . The angle γ between Z_G and Z is 23.5° .
- (3) the X_M, Y_M, Z_M coordinates - with Z_M coincident with the geomagnetic dipole axis. The angle α between Z_M and Z_G is 11.7° . At $t = 0$, X_M and Y_M are in the X_G, Z_G plane.

Note that Y' , Y_G , and Y_M are not usually coplanar.

The external field is given in 4 variables, the position X, Y, Z , and the "tilt" angle, μ , between the X' (ecliptic axis - toward the sun) and the solar magnetic Y axis - defined below.

Solar magnetic coordinates are defined in terms of the magnetic dipole axis and the sun earth line (the X' axis in solar ecliptic coordinates). The Y_{SM} axis is in the plane formed by the X' and Z_M ($\equiv Z_{SM}$) axes. The Y_{SM} axis then forms the orthogonal set.

Inputs to the transformations must include the position in geographic coordinates where \vec{B} is to be found, the universal time of day, t , and the day of the year, T .

In order to agree with these coordinate definitions t and T must be "corrected" - to magnetic moon summer solstice. T and t as discussed here are "corrected" - i.e., measured from magnetic moon at summer solstice.

Normally these transformations take much computer time and involve the equation of time which is not in closed form. However, great computational effort is avoided if it is assumed simply that the earth is in circular orbit around the sun. Then all transformations are analytic and require little computer time.

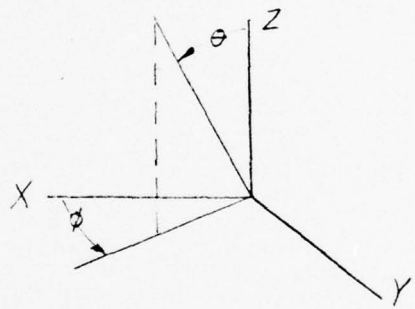
Given X, Y, Z in geographic coordinates, and t and T (T is an integer variable), the position must be transformed to solar magnetic coordinates and the tilt angle found.

$$X = r \sin \theta \cos \phi$$

$$Y = r \sin \theta \sin \phi$$

$$Z = r \cos \theta$$

where θ, ϕ are geographic latitude and east longitude (measured from Greenwich).



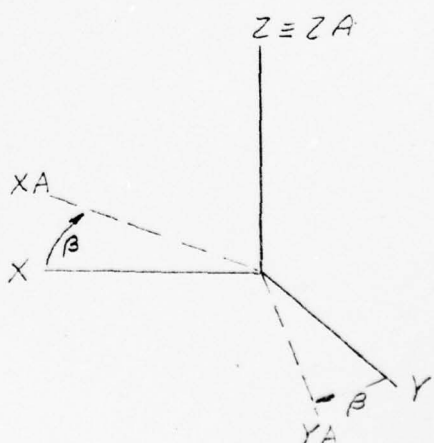
The transformation then proceeds as follows.

Rotate to the dipole longitude.

$$XA = X \cos \beta - Y \sin \beta$$

$$YA = Y \cos \beta + X \sin \beta$$

$$ZA \equiv Z$$



Rotate to the dipole axis about YA axis.

$$XB = XA \cos \alpha - ZA \sin \alpha$$

$$YB \equiv YA$$

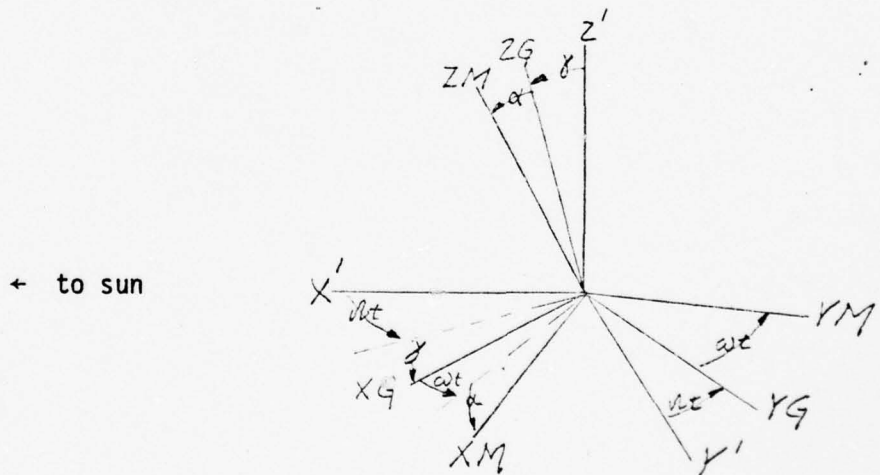
$$ZB = ZA \cos \alpha + XA \sin \alpha$$

X_B , Y_B , Z_B then give the position in geometric coordinates and the geomagnetic longitude of the point is

$$\phi_m \equiv \tan^{-1} \left(\frac{X_B}{Y_B} \right).$$

A final rotation about the magnetic axis is needed to transform to solar magnetic coordinates. To do this the tilt angle, μ , must be computed. This is best done by expressing \hat{M} , the unit vector along the magnetic dipole axis, in ecliptic coordinates

using the coordinates defined above.



In terms of unit vectors (their direction indicated by subscript), here the geomagnetic coordinates are to be expressed in terms of ecliptic coordinates. Thus

AD-A037 492

MCDONNELL DOUGLAS ASTRONAUTICS CO-WEST HUNTINGTON BEA--ETC F/G 4/1
MAGNETOSPHERIC MAGNETIC FIELD MODELING.(U)

JAN 77 W P OLSON, K A PFITZER

F44620-75-C-0033

UNCLASSIFIED

AFOSR-TR-77-0156

NL

2 OF 2
AD
AO37492



END

DATE
FILMED
4 - 7 -

$$\hat{j}_{YM} = \hat{j}_{ZG} \cos \omega t - \hat{i}_{ZG} \sin \omega t$$

$$\hat{M}_{ZM} = \hat{k}_{ZG} \cos \alpha + \hat{i}_{XG} \cos \omega t \sin \alpha + \hat{j}_{YG} \sin \omega t \sin \alpha$$

$$\hat{r}_{XM} = \hat{i}_{XG} \cos \omega t \cos \alpha + \hat{j}_{YG} \sin \omega t \cos \alpha - \hat{k}_{ZG} \sin \alpha$$

Then, in ecliptic coordinates (\hat{i}' , \hat{j}' , \hat{k}')

$$\hat{i}_{XG} = -\hat{k}' \sin \gamma + \hat{i}' \cos \Omega t \cos \gamma + \hat{j}' \sin \Omega t \cos \gamma$$

$$\hat{j}_{YG} = \hat{j}' \cos \Omega t - \hat{i}' \sin \Omega t$$

$$\hat{k}_{ZG} = \hat{k}' \cos \gamma + \hat{i}' \sin \gamma \cos \Omega t + \hat{j}' \sin \gamma \sin \Omega t$$

Then, the angle, ζ , between the earth sun line and the dipole axis (the complement of the tilt angle, μ) is given by

$$\cos \zeta = \hat{M}_{ZM} \cdot \hat{i}' \text{ which by inspection is:}$$

$$\begin{aligned} \cos \zeta = & \cos \alpha \sin \gamma \cos \Omega t \\ & + \cos \omega t \sin \alpha \cos \Omega t \cos \gamma \\ & - \sin \omega t \sin \alpha \sin \Omega t \end{aligned}$$

$$\begin{aligned} \text{Thus } \zeta = & \cos^{-1} (\cos \alpha \sin \gamma \cos \Omega t \\ & + \sin \alpha (\cos \omega t \cos \Omega t \cos \gamma - \sin \omega t \sin \Omega t)) \end{aligned}$$

$$\text{and finally } \mu = \frac{\pi}{2} - \zeta.$$

It remains to find the rotation angle δ between the magnetic prime meridian at the equator, \hat{i}_{XB} , and the solar magnetic X axis (\hat{i}_{GM}). From μ and \hat{M}_{ZM} and \hat{i}' construct the \hat{j}_{SM} (solar magnetic axis). ($\hat{M}_{ZM} \equiv \hat{M}_{SM}$)

$$\hat{j}_{SM} = \frac{\hat{M}_{SM} \times \hat{i}''}{\sin \zeta} \quad \text{or}$$

$$\hat{j}_{SM} = \frac{1}{\sin \zeta}$$

$$\begin{pmatrix} \hat{i}' & \hat{j}' & \hat{k}' \\ M_X & M_Y & M_Z \\ 1 & 0 & 0 \end{pmatrix} =$$

$$\frac{1}{\sin \zeta} \left(M_Z \hat{j}' - M_Y \hat{k}' \right).$$

The angle, ϕ , between \hat{j}_{SM} and the \hat{j}_{YM} axis (in geomagnetic coordinates) is given by

$$\hat{j}_{SM} \cdot \hat{j}_{YM} = \frac{1}{\sin \zeta} M_Z GM_Y - M_Y GM_Z \equiv \cos \phi$$

where

$$M_Y = \cos \alpha \sin \gamma \sin \Omega t + \cos \omega t \sin \alpha \sin \Omega t \cos \gamma + \sin \omega t \sin \alpha \cos \Omega t$$

$$M_Z = \cos \alpha \cos \gamma - \cos \omega t \sin \alpha \sin \gamma$$

$$GM_Y = \cos \omega t \cos \Omega t - \sin \omega t \sin \Omega t \cos \gamma$$

$$GM_Z = \sin \omega t \sin \gamma$$

To determine ϕ (the angle between the solar-magnetic X axis and the geomagnetic X axis) over the full range of angles (θ to 2π radius) it is necessary on the computer to use the \tan^{-1} function in place of the \cos^{-1} function described above.

Thus \hat{i}_{GM} (described above as \hat{i}_{XM}) must be projected onto the solar magnetic \hat{i}_{SM} and \hat{j}_{SM} axis. Then,

$$\hat{i}_{GM} = \hat{i}_{SM} (\cos \omega t \cos \alpha \cos \Omega t \cos \gamma - \sin \omega t \cos \alpha \sin \Omega t \\ - \sin \alpha \sin \gamma \cos \Omega t) +$$

$$\hat{j}_{SM} (\cos \omega t \cos \alpha \sin \Omega t \cos \gamma + \sin \omega t \cos \alpha \cos \Omega t \\ - \sin \alpha \sin \gamma \sin \Omega t) +$$

$$\hat{k}_{SM} (-\cos \omega t \cos \alpha \sin \gamma - \sin \alpha \cos \gamma)$$

$$\text{Then } \hat{i}_{GM} \cdot \hat{i}_{SM} = \cos \omega t \cos \alpha \cos \Omega t \cos \gamma \\ - \sin \omega t \cos \alpha \sin \Omega t - \sin \alpha \sin \gamma \cos \Omega t$$

$$\hat{i}_{GM} \cdot \hat{j}_{SM} = \cos \omega t \cos \alpha \sin \Omega t \cos \gamma \\ + \sin \omega t \cos \alpha \cos \Omega t - \sin \alpha \sin \gamma \sin \Omega t$$

The angle ϕ is then given by

$$\phi = \tan^{-1} \frac{\hat{i}_{GM} \cdot \hat{j}_{SM}}{\hat{i}_{GM} \cdot \hat{i}_{SM}}$$

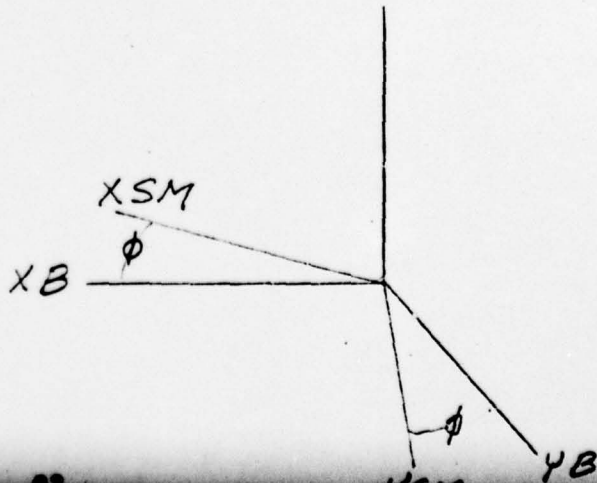
The transformation between geomagnetic and solar magnetic coordinates is then simply a rotation through the angle ϕ (as determined above).

$$ZB \equiv ZSM$$

$$XSM = XB \cos \phi - YB \sin \phi$$

$$YSM = YB \cos \phi + XB \sin \phi$$

$$ZSM \equiv ZB$$



Given the magnetic field in solar magnetic coordinates,

$$\vec{B} = B_X \hat{i}_{SM} + B_Y \hat{j}_{SM} + B_Z \hat{k}_{SM}$$

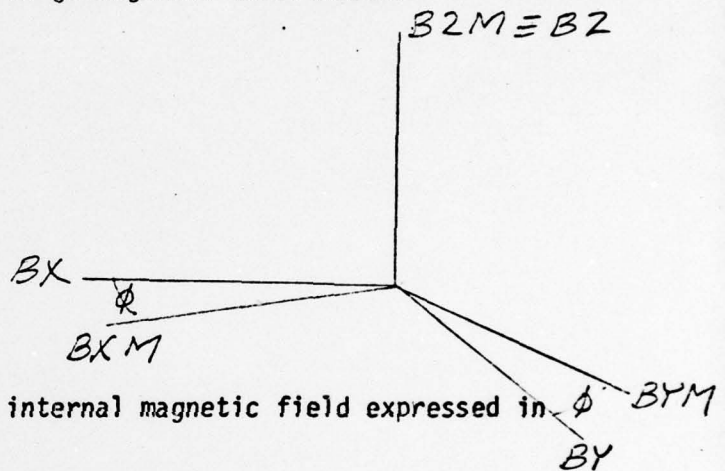
- (1) rotate back through the angle ϕ to geomagnetic coordinates.

$$B_{ZM} = B_Z$$

$$B_{XM} = B_X \cos \phi$$

$$+ B_Y \sin \phi$$

$$B_{YM} = B_Y \cos \phi - B_X \sin \phi$$



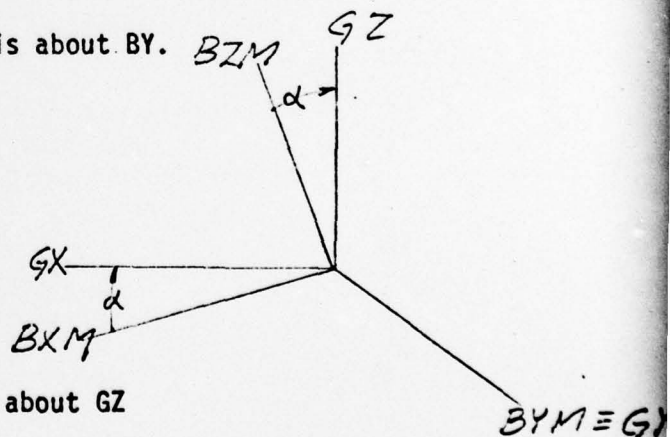
(These components can be added to an internal magnetic field expressed in geomagnetic coordinates.)

- (2) Rotate the magnetic into the dipole axis about BY .

$$G_X = B_{XM} \cos \alpha + B_{ZM} \sin \alpha$$

$$G_Y = B_{YM}$$

$$G_Z = B_{ZM} \cos \alpha - B_{XM} \sin \alpha$$

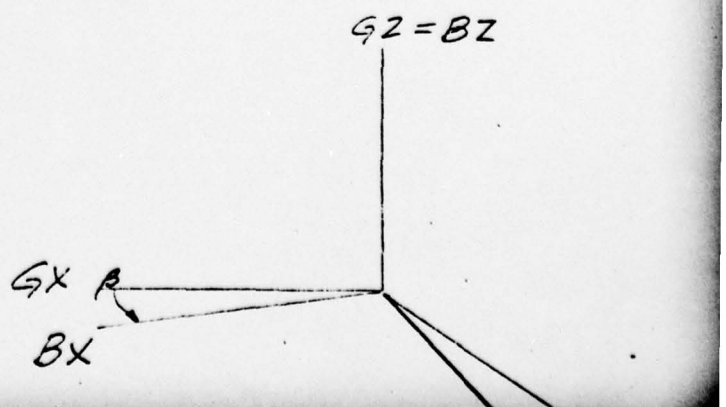


- (3) Rotate the longitude back to Greenwich about GZ

$$B_X = G_X \cos \beta + G_Y \sin \beta$$

$$B_Y = G_Y \cos \beta - G_X \sin \beta$$

$$B_Z = G_Z$$



These components can then be added to a main field representation given in geographic coordinates.

Note that the derivation of the analytic form of the tilt angle, μ , and of the rotation angle between solar magnetic and geomagnetic coordinates, ϕ , has also been given in the above transformations.

6.2 Time Derivation of the Tilt Angle

Since the induced electric field, \vec{E}_I , resulting from the daily variation in the tilt angle, μ , is given in terms of the magnetic vector potential, \vec{A} , ($\vec{E}_I = - \frac{\partial \vec{A}}{\partial t}$) it is necessary to compute the time variation in μ . This is because \vec{A} is given as a function of μ and not t . Thus

$$\vec{E}_I = - \left(\frac{\partial \vec{A}}{\partial \mu} \right) \left(\frac{\partial \mu}{\partial t} \right) . \text{ Then since}$$

$$\mu = \frac{\pi}{2} - \phi , \phi = \cos^{-1} (ZX) \text{ where}$$

$$ZX = \cos \alpha \sin \gamma \cos \Omega t + \cos \omega t \sin \alpha \cos \Omega t \cos \gamma \\ - \sin \omega t \sin \alpha \sin \Omega t .$$

It follows that

$$\frac{\partial \mu}{\partial t} = - \frac{\partial \phi}{\partial t} . \text{ Then, since generally}$$

$$\frac{d}{dx} (\cos^{-1} (y)) = - \frac{\frac{dy}{dx}}{\sqrt{1 - y^2}} .$$

or $\frac{\partial u}{\partial t} = \frac{\frac{\partial (ZX)}{\partial t}}{\sqrt{1 - (ZX)^2}}$. Finally

$$\begin{aligned}\frac{\partial (ZX)}{\partial t} &= -\Omega \cos \alpha \sin \gamma \sin \Omega t \\&\quad - \omega \sin \omega t \sin \alpha \cos \Omega t \cos \gamma \\&\quad - \Omega \cos \omega t \sin \alpha \sin \Omega t \cos \gamma \\&\quad - \omega \cos \omega t \sin \alpha \sin \Omega t \\&\quad - \Omega \sin \omega t \sin \alpha \cos \Omega t\end{aligned}$$

which can be used to find $\frac{\partial u}{\partial t}$ analytically.

Section 7
REFERENCES

Masley, A. J. Charged Particle Entry into the Earth's Magnetosphere and Propagation to the Polar Regions, Ph.D. Thesis, University of Melbourne, 1975.

McIlwain, C. E. Coordinates for Mapping the Distribution of Magnetically Trapped Particles, J. Geophys. Res., 66, 3681-3691, 1971.

Olson, W. P. A Model of the Magnetospheric Magnetic Field, J. Geophys. Res., 79, 3731, 1974.

Olson, W. P. and K. A. Pfitzer. A Quantitative Model of the Magnetospheric Magnetic Field, J. Geophys. Res., 79, 3739, 1974.

Pfitzer, K. A., T. W. Lezniak, and J. R. Winckler. Experimental Verification of Drift-Shell Splitting in the Distorted Magnetosphere, J. Geophys. Res., 74, 4687-4693, 1969.

Sugiura, M., B. G. Ledley, T. L. Skillman, and J. P. Heppner. Magnetospheric-Field Distortions Observed by OGO -3 and 5, J. Geophys. Res., 76, 7552, 1971.

Walker, R. J. An Evaluation of Recent Quantitative Magnetospheric Magnetic Field Models, Rev. Geophys. and Sp. Res., 14, 411-428, 1976.